Station Bulletin 677
May 1990

Model for Uptake of Organic Chemicals by Plants

Agricultural Experiment Station
Oregon State University

MODEL FOR UPTAKE OF ORGANIC CHEMICALS BY PLANTS

L. BOERSMA, F. T. LINDSTROM, C. MCFARLANE

AUTHORS: F. T. Lindstrom and L. Boersma, Department of Soil Science, Oregon State University; C. McFarlane, Research Scientist, Corvallis Environmental Research Laboratory, United States Environmental Protection Agency.

FOREWORD

The uptake, transport, and accumulation of organic and inorganic chemicals by plants are influenced by characteristics of the plant, properties of the chemical, properties of the soil, and by prevailing environmental conditions. Complex interrelationships exist between the physical, chemical, and physiological processes that occur in specific plant tissues and the response of these processes to environmental conditions, such as the daily cycle of radiation, evaporation, and air temperature. The uptake is further influenced by the availability of the chemical at the root surface, determined in turn by transport characteristics of the soil. Also important is the behavior of the chemical in the rhizosphere and the ease with which it moves across limiting membranes at the root surface.

This report describes the development of a predictive simulator for the uptake of xenobiotic chemicals by plants from the soil solution. The model is based on definition of the plant as a set of compartments separated from each other by thin membranes. Movement of water and solutes between compartments occurs by mass flow and diffusion. The compartments represent major pools for accumulation of water and solutes. Anatomical features of the compartments and the manner in which they are connected are described by a series of equations based on conservation of mass. Experimental data were used to calibrate and then validate the model.

ACKNOWLEDGMENTS

This publication reports results of studies supported, in part, by Research Grant CR 811940-01-0 "A Mathematical Model of the Bioaccumulation of Xenobiotic Organic Chemicals in Plants" from the Corvallis Environmental Research Laboratory of the United States Environmental Protection Agency to the Department of Soil Science at Oregon State University and by the Oregon Agricultural Experiment Station.

CONTENTS

CONTENTS (continued)

FIGURES

FIGURES (continued)

FIGURES (continued)

FIGURES (continued)

TABLES

TABLES (continued)

MATHEMATICAL MODEL OF PLANT UPTAKE OF ORGANIC CHEMICALS

SUMMARY

Uptake, in-plant transport, and local accumulation of organic chemicals by plants are influenced by plant characteristics, properties of the chemical and the soil, and by environmental conditions. Evaluations of plant contamination required by regulatory agencies cannot be made experimentally for the many thousands of xenobiotic chemicals in existence or being developed. A predictive simulator in the form of a mathematical model would provide a valuable tool for such evaluations. For this reason, a mathematical model (UTAB: Uptake, Translocation, Accumulation, Biodegradation) was formulated by defining a generic plant as a set of adjacent compartments representing the major pools involved in transport and accumulation of water and solutes. The model consists of one root compartment, three stem compartments, and three leaf compartments. Each compartment is subdivided into two transport compartments, one for xylem and one for phloem, and a storage compartment. In addition, two compartments model the root volume outside the Casparian strip, one for the apparent free space and one for the cell volume. Values for the anatomical dimensions of the compartments and for physical and chemical coefficients were chosen from the literature. The complete system of equations, which describes uptake and accumulation, consists of 24 differential equations which are solved in terms of the chemical mass in each compartment as a function of time. The solution procedure is also developed and presented.

For calibration purposes, concentrations measured in roots, stems, and leaves were compared with model predictions, while model parameters were changed until no further improvement in matching model predictions

with experimental results was obtained. This exercise revealed important plant behavior that was not accounted for in the original formulation of the model and, as such, showed the value of the model for elucidating plant response.

The model satisfactorily predicted the observed uptake and distribution patterns for bromacil in soybean plants, at the stage of growth and under the environmental conditions used in the experiments, involving a range of transpiration rates. This indicates that the model is flexible enough to provide an accurate representation of uptake and the influence of transpiration rate on the uptake and translocation of this chemical. Parameter values used in the model were selected from literature and experimental observation. They functioned well in these simulations and they are appropriately applied in the model. The chemical parameters for storage, mobilization, and diffusion when used in the model also yielded satisfactory results, suggesting that they are also appropriately applied. Finally, the calibration, although of limited scope, showed that the model equations yielded an accurate picture of the actual uptake patterns for bromacil in soybeans used in these experiments. The theoretical exercise of compiling the model is shown to be a constructive step in learning how to predict the fate of xenobiotic contamination in plants. The model shows excellent promise for future use. However, additional testing and validation are needed.

DEVELOPMENT OF THE MODEL

Introduction

The processes of plant uptake, translocation, accumulation, and biodegradation (UTAB) of xenobiotic chemicals are important in assessing the environmental risks involved in the use of those chemicals. Since it is impossible to study each chemical with each plant in each environment, a mathematical model for predicting environmental behavior would be a valuable tool for risk assessment. Such a model, when used to explain experimental results, would also help clarify physiological mechanisms and, when validated, would allow extrapolation of experimental results to hypothetical scenarios. This report is the description of a model developed for these purposes and application of the model to experimental results.

Whole plant experiments, which are necessary to evaluate UTAB, do not allow descrete examination of the apoplastic and symplastic regions, nor of the biological properties of individual plant parts such as membrane permeabilities. Means are required to quantify individual transport mechanisms indirectly by employing procedures which make it possible to extract this information from experimental results obtained with accepted whole plant experimental techniques. A mathematical model would serve this goal. At present, few models of xenobiotic mobility in plants exist (Boersma et al., 1988a,b). None are currently available in which all the major plant parts function simultaneously in an integrated manner and operate under accepted mechanistic rules at the macroscale.

A few mechanistic models of translocation have been formulated based on the Münch transport theory (Eschich et al., 1972; Christy and

Ferrier, 1973; Ferrier and Christy, 1975; Goeschl et al., 1976; Tyree et al., 1979; Weir, 1981). These models consider transport from a single source region to a single sink region and the equations are limited to processes which occur in the sieve tubes. These models have served as a valuable starting point for the model presented here. Our objective was to construct a model for the transport of a trace organic solute in a plant, based on principles of conservation of mass. The model is a first approximation of solute transport through a complex set of physiological compartments. Because of the large number of processes involved, simplifying assumptions had to be made. Only average Fickian membrane and xylem/phloem transport processes are included.

Structure of the Model

The model defines a plant as a set of compartments, each representing pertinent plant tissues (Figures 1 and 2). The compartments are separated by boundaries of specified thickness and area and distinguished by the physical and chemical properties that determine passage of water and solutes. Movement of water and solutes between compartments occurs by mass flow (advective flow) or diffusion and is restricted by tortuosity of the path, selective permeability (reflection), and partitioning with tissue components (sorption).

Formulation of the model was based on identification of appropriate compartments and determining their physical and chemical characteristics and the manner in which they are connected. The example considered here subdivides a soybean plant-soil system into the major pools: soil solution, root, stem, and leaf. Although the soybean was selected

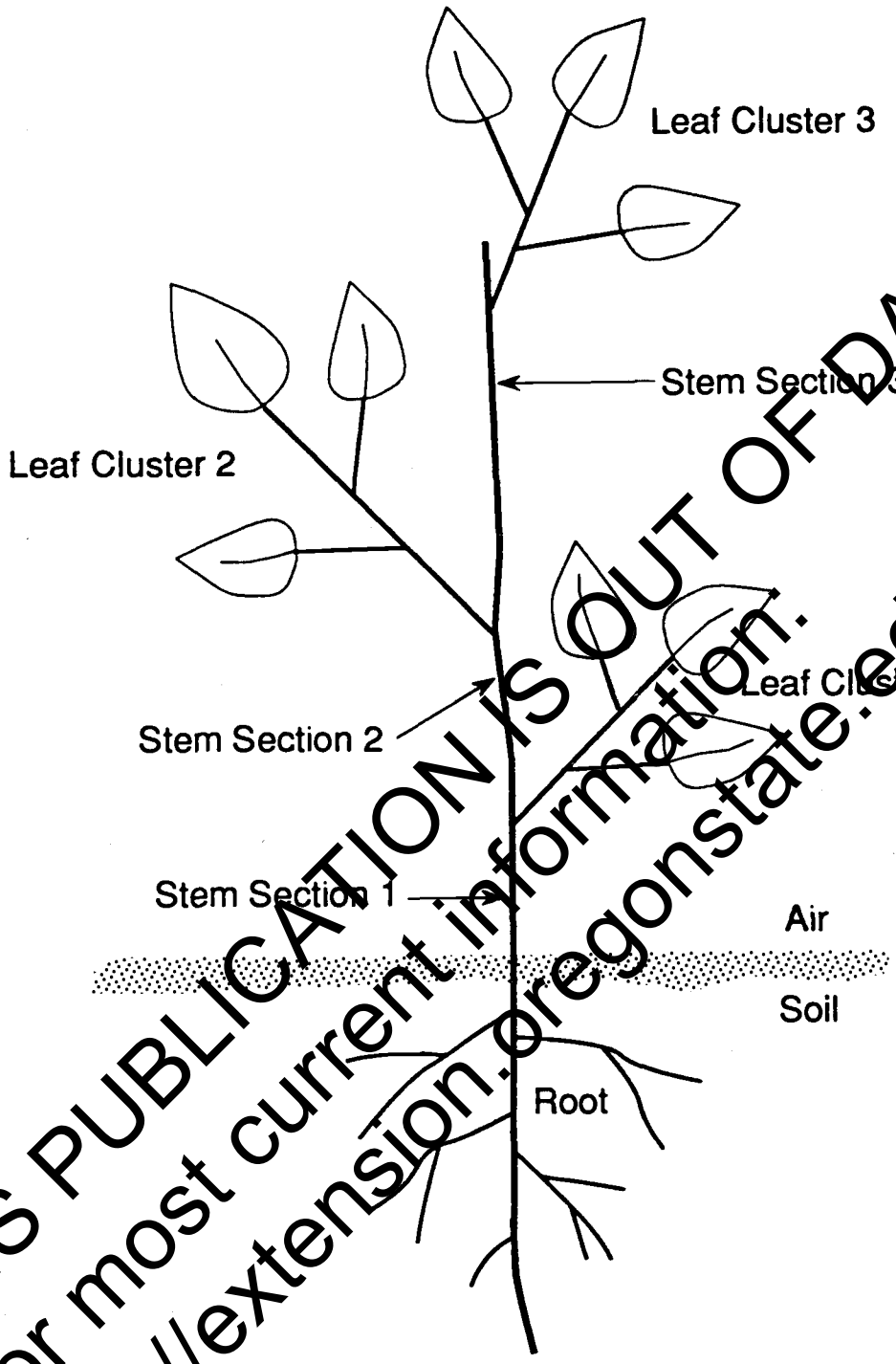

Figure 1. Schematic diagram of a generic plant, with three leaves showing the hierarchy of leaves on the stem and the numbering sequence used for model compartments.

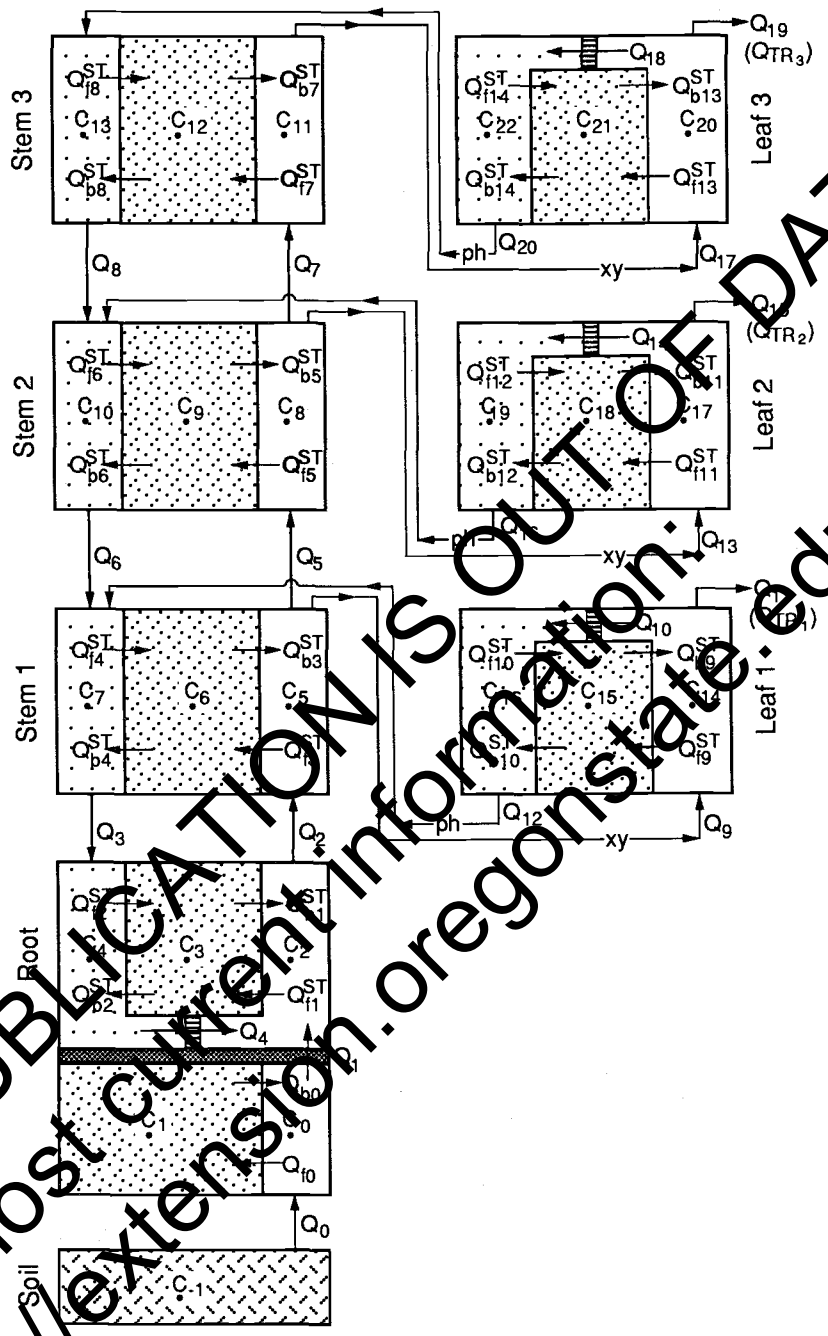

Figure 2. Conceptualization of the plant shown in Figure 1 in terms of compartments used for the mathematical model. Definitions of symbols are in Tables 1 and 2.

as the test species, a choice based on availability of experimental data, the model can be parameterized for most terrestrial vascular plants.

Major segments of the pathway of water and solute transport through the generic plant are identified in Figure 1 and the corresponding system of compartments is in Figure 2. Symbols are defined in Tables 1 and 2. The fluid flow rules are summarized in Table 3. Each compartment is considered to be a well-stirred tank with a uniform concentration. The compartments are separated by barriers for which chemical and physical characteristics differ with respect to the ease with which water and solutes can pass. Those differences are described in terms of their reflection coefficient, partition coefficient, and hydraulic conductivity. The properties of the compartments of concern are volume, area of contact between compartments, sorption coefficient, and coefficient for first-order loss processes.

Sequence of Compartments

Water fluxes in the model (Table 3) are driven by the water potential gradients created by evaporation from the substomatal cavity and propagated throughout the plant to the soil solution. Water moves along the transpiration stream via mass flow and to storage volumes in adjoining cells via diffusion. Water also moves through the phloem pathway driven by pressure gradients. Both pathways are accounted for in the model. Solutes follow the same paths and partition into storage compartments at rates determined by physical characteristics of the particular chemical.

Table 1. Notation used in the model.

A	Contact area between compartments (cm^2).
B	Sorption coefficient; describes the immobilization of the solute by reversible sorption to cell walls or large molecules in the compartment (dimensionless).
C	Concentration of solute in compartment ($\mu g/cm^3$)
D	Diffusion coefficient (cm^2/h)
Q_f^{ST}	Rate of storage (cm^3/h)
Q_b^{ST}	Rate of mobilization from storage (cm^3/h)
M	Mass of solute in compartment (μg)
V	Volume of compartment (cm^3)
Q	Water flow rate through xylem subcompartment (cm^3/h)
Δx	length of fluid flow path or membrane thickness connecting compartments (cm)
σ	Reflection coefficient for transport of chemical between compartments. The membrane is impermeable to the solute when the reflection coefficient has its maximum value of one. The membrane is nonselective; that is, it allows the solute to pass unimpeded with water when the reflection coefficient is equal to zero (dimensionless)
λ	Rate constant for first order loss processes in compartment; describes immobilization of solute by incorporation into structural material or loss of solute due to metabolism (1/h)

Table 2. Definitions of symbols and subscripts used to identify compartments, mass of chemical in compartments, and concentrations.

Compartment number	Compartment name	Mass in comp. (M_i)	Concentrations (C_i)
		μg	$\mu g/g$
-1	Soil	M_{-1}	C_{-1}
0	Root free volume	M_0	C_0
1	Root exterior cells	M_1	C_1
2	Root xylem lumen	M_2	C_2
3	Root storage	M_3	C_3
4	Root phloem lumen	M_4	C_4
5	Bottom stem xylem lumen	M_5	C_5
6	Bottom stem storage	M_6	C_6
7	Bottom stem phloem lumen	M_7	C_7
8	Mid stem xylem lumen	M_8	C_8
9	Mid stem storage	M_9	C_9
10	Mid stem phloem lumen	M_{10}	C_{10}
11	Top stem xylem lumen	M_{11}	M_{11}
12	Top stem storage	M_{12}	C_{12}
13	Top stem phloem lumen	M_{13}	C_{13}
14	Leaf 1 xylem lumen	M_{14}	C_{14}
15	Leaf 1 storage	M_{15}	C_{15}
16	Leaf 1 phloem lumen	M_{16}	C_{16}
17	Leaf 2 xylem lumen	M_{17}	C_{17}
18	Leaf 2 storage	M_{18}	C_{18}
19	Leaf 2 phloem lumen	M_{19}	C_{19}
20	Leaf 3 xylem lumen	M_{20}	C_{20}
21	Leaf 3 storage	M_{21}	C_{21}
22	Leaf 3 phloem lumen	M_{22}	C_{22}

Table 3. Fluid flow rules. Q_{11}, Q_{15}, and Q_{19} are specified transpiration rates (cm^3/h) where the fractions of total transpiration allocated to each leaf cluster are f_1 to Q_{11}, f_2 to Q_{15}, and f_3 to Q_{19}.

Flow rule	Region connected
$Q_1 = Q_{11} + Q_{15} + Q_{19}$	Soil-root xylem lumen
$Q_2 = (1 + f_1)Q_{11} + (1 + f_2)Q_{15} + (1 + f_3)Q_{19}$	Root xylem lumen-bottom stem xylem lumen
$Q_3 = f_1 Q_{11} + f_2 Q_{15} + f_3 Q_{19}$	Bottom stem phloem lumen-root phloem lumen
$Q_4 = Q_3$	Root phloem lumen-root xylem lumen
$Q_5 = (1 + f_2)Q_{15} + (1 + f_3)Q_{19}$	Bottom stem xylem lumen-mid stem xylem lumen
$Q_6 = f_2 Q_{15} + f_3 Q_{19}$	Mid stem phloem lumen-bottom stem phloem lumen
$Q_7 = (1 + f_3)Q_{19}$	Top stem xylem lumen-top stem xylem lumen
$Q_8 = f_3 Q_{19}$	Top stem phloem lumen-mid stem phloem lumen
$Q_9 = (1 + f_1)Q_{11}$	Bottom stem xylem lumen-leaf 1 xylem lumen
$Q_{10} = f_1 Q_{11}$	Leaf 1 xylem lumen-leaf 1 phloem
Q_{11} = specified ←	Leaf 1 transpiration rate (cm^3/h)
$Q_{12} = f_1 Q_{11}$	Leaf 1 phloem lumen-bottom stem phloem lumen
$Q_{13} = (1 + f_2)Q_{15}$	Mid stem xylem lumen-leaf 2 xylem lumen
$Q_{14} = f_2 Q_{15}$	Leaf 2 xylem lumen-leaf 2 phloem lumen
Q_{15} = specified ←	Leaf 2 transpiration rate (cm^3/h)
$Q_{16} = f_2 Q_{15}$	Leaf 2 phloem lumen-mid stem phloem lumen
$Q_{17} = (1 + f_3)Q_{19}$	Top stem xylem lumen-leaf 3 xylem lumen
$Q_{18} = f_3 Q_{19}$	Leaf 3 xylem lumen-leaf 3 phloem lumen
Q_{19} = specified ←	Leaf 3 transpiration rate (cm^3/h)
$Q_{20} = f_3 Q_{19}$	Leaf 3 phloem lumen-top stem phloem lumen

The open pathway for water and solute movement between the cortex cells of the root has been termed the "apparent free space" and is comprised of cellulose and open spaces which form a sponge-like material that provides structural support while allowing free water and solute movement. The apparent free space is typically about 7 percent of the tissue volume but because of its structure accounts for most of the water and solute movement from the rooting solution to the endodermis. The apparent free space is the first plant compartment in the model (0).

The next compartment (1) also lies outside the endodermis and consists primarily of the cortex cells, but also includes the epidermis and the root hairs. Solutes and water move into these cells and

migrate towards the endodermis via the symplasm. The cortex cells provide surfaces for adsorption and partitioning of the various organic chemicals with the lipoprotein membranes. They also provide a reactive environment where cytoplasmic enzymes catalyze some of the bonds of the xenobiotic chemicals of interest.

Analysis of experimental data, described later on in this paper, indicates the importance of these first two compartments in the uptake process. An extremely rapid uptake of bromacil by the roots occurred during the first hours of exposure. This was attributed to filling of the apparent free space by the bromacil containing solution as the transpiration stream was initiated. Furthermore, the apparent free space completely permeates the cortex, so that all cells are immediately bathed in the bromacil containing solution and diffusion and/or active transport into these cells can occur as soon as exposure is initiated.

Following the first two compartments are xylem, phloem, and storage compartments of roots, followed by the stem compartments and then the leaf compartments from where water and volatile pollutants pass to the atmosphere in the vapor phase. Solutes travel the same path as water, except they may sorb to various materials in the root, stem, and leaves, and they may partition between water and the cellulose lipids and proteins of the cell membranes. Many solutes do not evaporate in the stomatal cavity and are thus deposited or further translocated via the phloem to other areas in the plant.

In addition to the xylem pathway, water moves through the phloem. Connections between xylem and phloem in this model occur in the leaf compartments and in the root. Phloem also connects with the storage

compartments. Connection of leaf apoplast and leaf phloem was based on studies by Jachetta et al. (1986a,b). These connections allow water to pass from root phloem to root xylem and vice versa by either mass flow or diffusion between the two compartments.

Part of the volume of each compartment is available for storage of solute which passes through the xylem or phloem. Storage in stems was described by McCrady et al. (1987), storage in leaves by Jachetta et al. (1986a,b).

The mathematical description of rate of storage of chemical was based on the assumption that transport to and from storage involves several transport processes of which diffusion is the most important. Details of these processes are not currently known. We chose to represent the storage processes by first-order transport rates, which include diffusion-controlled processes but may also include mass flow.

Storage and mobilization coefficients were defined to lump together several transport processes occurring in plant structures of which geometric properties cannot easily be measured and where the relative contribution of each mechanism to the total process is not known. The diffusion component of the mass transport is

$$(\text{mass/unit time}) = D \cdot \frac{K\Delta C}{\Delta x} \cdot A \cdot (1 - \sigma) \qquad (1)$$

where D is the diffusion coefficient (cm^2/hr), K is the partition coefficient (dimensionless), A is the cross-sectional area (cm^2), ΔC is the concentration ($\mu g/cm^3$), Δx (cm) is the distance over which ΔC exists, and σ is the compound specific membrane reflection coefficient. When A and Δx are not known, this may be written as

$$= \left\{\frac{DKA}{\Delta x}\ (1 - \sigma)\right\} \Delta C. \qquad (2)$$

The quantity $(DKA/\Delta x)(1 - \sigma)$ is sometimes referred to as the permeability coefficient and has the units of cm^3/hr which is also the unit of the storage and mobilization coefficients used in our model. The storage and mobilization coefficients may thus be thought of as coefficients describing the effective diffusion process where the cross-sectional area and the diffusion distance are not known. According to this interpretation the storage and mobilization coefficients are proportional to the cross-sectional area of a storage compartment and inversely proportional to the thickness of the membrane across which transport occurs. The coefficients also are proportional to $(1 - \sigma)$. Values for the storage coefficients can only be obtained experimentally. These values are expected to vary with experimental conditions such as root temperature, water potential, rate of water flow, and properties of the chemical.

Mass Balance Equations

The mathematical model reported here is an adaptation of concepts presented in earlier reports (Boersma et al., 1988a,b). Development starts with the representation of a generic plant (Figure 1) by a system of compartments (Figure 2). Mathematical symbols in Figure 2 were defined in Tables 1 and 2. Numerical subscripts were used rather than mnemonic notations to avoid the confusion that such notations can lead to. Table 3 lists the fluid flow rules for the plant.

Development of the first five mass balance equations is now shown in detail. The remaining mass balance equations which were developed

in a similar manner are in Appendix 1. Figure 2 shows the numbering scheme of the compartments representing the various plant regions. The subscripts on the fluid flows can also be used as indicators for the intercompartmental parameter for chemical transport. In the mathematical model the term "mass transport" is used to describe the transport of chemical due to diffusion, advection, and/or active processes. This was done in accordance with concepts of transport modelling (Seagrave, 1971). The approach lumps diffusion, passive advection, and active first-order transport together in one general first-order term. Lack of knowledge generally precludes the separation of the active and passive processes, especially at the macroscale.

Soil Compartment

Beginning with the soil compartment (Figure 2) the first mass balance equation is

$$\frac{d[\epsilon_{-1} V_{-1}(1 + B_{-1} K_{-1}) C_{-1}]}{dt} = \text{instantaneous time rate of change of free phase plus reversibly bound chemical mass } (\mu g/h)$$

$$- \frac{D_0}{\Delta x_0} A_{-1}(C_{-1} - C_0) \quad \text{rate of diffusion of chemical mass across the soil/root interface } (\mu g/h)$$

$$- Q_0 C_{-1} \quad \text{rate of mass transport across the soil/root interface } (\mu g/h)$$

$$- \lambda_{-1} M_{-1} \quad \text{rate of irreversible first order loss processes operating in the soil compartment } (\mu g/h) \qquad (3)$$

where the subscript -1 identifies the soil compartment and 0 is the root free space.

The relationship between the concentration of chemical in the free phase and its mass in the soil compartment is

$$M_{-1} = \epsilon(1 + B_{-1})\, V_{-1}\, C_{-1} \qquad (\mu g) \qquad (4)$$

and similarly in the compartment simulating the free space of the cortex

$$M_0 = (1 + B_0)\, V_0\, C_0 \,. \qquad (\mu g) \qquad (5)$$

Solving equation (4) for C_{-1} in terms of M_{-1} and solving equation (5) for C_0 in terms of M_0 with subsequent substitution of C_{-1} and C_0 into equation (3) yields

$$\frac{dM_{-1}}{dt} = a_{-1,-1}\, M_{-1} + a_{-1,0}\, M_0 \,, \qquad (6)$$

which is the first mass balance equation. The matrix elements $a_{-1,-1}$ and $a_{-1,0}$ are defined by

$$a_{-1,-1} = -\left[\frac{\frac{D_D\, A_0}{\Delta x_0} + Q_{-1}}{\epsilon\, V_{-1}(1 + B_{-1})} + \lambda_{-1}\right] \qquad (1/h) \qquad (7)$$

$$a_{-1,0} = \frac{\frac{D_0\, A_0}{\Delta x_0}}{V_0(1 + B_0)} \qquad (1/h) \qquad (8)$$

where $a_{-1,-1}$ characterizes the total chemical transport from the soil compartment (compartment -1) to the root-free space and $a_{-1,0}$ characterizes diffusive transport from the root-free space back to the soil compartment.

Free Space of the Roots

The second mass balance equation defines the time rate of change of the chemical mass in the free space of the root cortex. The transport pathways into and out of this region are shown in Figure 2.

Compound is assumed to be brought into this region by advective flow due to the transpiration stream and by diffusion which occurs in response to gradients which exist between the soil solution, or nutrient solution, and the free space of the cortex. The compound may be either passively (diffusion) or actively taken up by the cells of the cortex which make up compartment 1. Forward and backward transport coefficients with dimensions of volume rate of flow (cm^3/h) define transport into and out of storage. If the uptake of compound by the exterior root cell stem compartment is by diffusion only, then Q_{10}^{ST} is the product of a membrane diffusion coefficient (cm^2/h) and an effective interfacial area (cm^2) divided by a characteristic membrane thickness (cm). The result may be multiplied by a partition coefficient and a transmission coefficient to allow gradients to exist across the cortex cells and free space at equilibrium conditions. Backward transport coefficients are similarly defined.

Putting the currently recognized process and transport rules together in a linear model obtains

$$\frac{dM_0}{dt} =$$ instantaneous time rate of change of free phase plus reversibly bound chemical mass in the free space of the cortex ($\mu g/h$)

$$\frac{D_0 A_0}{\Delta x_0}(C_{-1} - C_0)$$ rate of diffusion of chemical mass across the soil/ root interface ($\mu g/h$)

$$+ Q_0 C_{-1}$$ rate of mass transport across the soil/root interface ($\mu g/h$)

$$- Q_{10}^{ST} C_0$$ rate of first-order loss due to storage ($\mu g/h$)

$$+ Q_{b0}^{ST} C_1$$ rate of first-order gain due to mobilization from storage ($\mu g/h$)

$- Q_1(1 - \sigma_1)\, C_0$	rate of mass transport across the endodermis (μg/h)
$- \frac{D_1\, A_1}{\Delta x_1}\, (C_0 - C_2)$	rate of diffusion of chemical mass across the cortex/root xylem interface (μg/h)
$- \lambda_0\, M_0$.	rate of all other first-order irreversible processes in the free space of the cortex (μg/h) (9)

Define chemical masses in the compartments as follows:

$$M_1 = (1 + B_1)\, V_1\, C_1, \quad (\mu g) \qquad (10)$$

$$M_2 = (1 + B_2)\, V_2\, C_2, \quad (\mu g) \qquad (11)$$

Solving equations (10) and (11) for C in terms of M and substituting for C_{-1}, C_0, C_1, and C_2 into equation (9) yields the second mass balance equation

$$\frac{dM_0}{dt} = a_{0,-1}\, M_{-1} + a_{0,0}\, M_0 + a_{0,1}\, M_1 + a_{0,2}\, M_2 \quad , \quad (\mu g) \qquad (12)$$

where the "matrix elements" are defined by

$$a_{0,-1} = \frac{\frac{D_0\, A_0}{\Delta x_0} + Q_0}{(1 + B_{-1})\, V_{-1}} \quad , \qquad (1/h) \qquad (13)$$

$$a_{0,0} = -\left(\frac{\frac{D_0\, A_0}{\Delta x_0} + \frac{D_1\, A_1}{\Delta x_1} + Q_{fo}^{ST} + Q_1(1 - \sigma_1)}{(1 + B_0)\, V_0} + \lambda_0 \right) \quad , \qquad (1/h) \qquad (14)$$

$$a_{0,1} = \frac{Q_{BO}^{ST}}{(1 + B_1)\, V_1} \quad , \qquad (1/hr) \qquad (15)$$

$$a_{0,2} = \frac{\frac{D_1\, A_1}{\Delta x_1}}{(1 + B_2)\, V_2} \quad . \qquad (1/h) \qquad (16)$$

Storage Volume of Root Cortex

The third mass balance equation defines the time rate of change of chemical mass in the cells of the root cortex. Uptake of compound may be by diffusion and/or active mass transport. The balance equation is made up of three first-order processes:

$\frac{dM_1}{dt} =$	instantaneous time rate of change of free phase plus reversibly bound chemical mass in the root cortex storage compartment (μg/h)
$- Q_{f0}^{ST} C_0$	rate of first-order loss due to storage (μg/h)
$+ Q_{b0} C_1$	rate of first-order gain due to mobilization from storage (μg/h)
$- \lambda_1 M_1$	rate of all other first-order irreversible processes, including metabolism, in the cell volume of the cortex (μg/h)

(17)

Chemical masses in the compartments were defined earlier as follows:

$$M_0 = (1 + B_0)V_0C_0 \tag{5}$$

$$M_1 = (1 + B_1)B_1V_1 \tag{10}$$

Substitution for the two indicated concentrations yields

$$\frac{dM_1}{dt} = a_{1,0} M_0 + a_{1,1} M_1 \tag{18}$$

where the matrix elements are defined by

$$a_{1,0} = \frac{Q_{f0}^{ST}}{(1 + B_0) V_0} , \tag{19}$$

$$a_{1,1} = -\left(\frac{Q_{b0}^{ST}}{(1 + B_1) V_1} + \lambda_1 \right) . \tag{20}$$

Root Xylem Compartment

The fourth mass balance equation defines the time rate of change of mass in the compartment simulating the root xylem. The transport pathways and processes into and out of this compartment are shown in Figure 2. The flows are self explanatory.

The mass balance equation for the root xylem compartment is:

$$\frac{dM_2}{dt} =$$ instantaneous time rate of change of free phase plus reversibly bound chemical mass in the root xylem compartment (μg/h)

$$\frac{D_1 A_1}{\Delta x_1} (C_0 - C_2)$$ rate of diffusion of chemical mass across the root/xylem interface (μg/h)

$$+ Q_1(1 - \sigma_1)C_0$$ rate of mass transport from the cortex to the root xylem (μg/h)

$$+ \frac{D_4 A_4}{\Delta x_4} (C_4 - C_2)$$ rate of diffusion of chemical mass across the root phloem/root xylem interface (μg/h)

$$+ Q_4(1 - \sigma_4) C_4$$ rate of mass transport from root phloem to root xylem (μg/h)

$$- \frac{D_2 A_2}{\Delta x_2} (C_2 - C_3)$$ rate of diffusion of chemical mass across from root xylem adjacent stem xylem interface (μg/h)

$$- Q_2(1 - \sigma_2) C_2$$ rate of mass transport from root xylem to adjacent stem xylem (μg/h)

$$- Q_{fl}^{T} C_2$$ rate of first-order loss due to storage (μg/h)

$$+ Q_{fl}^{ST} C_3$$ rate of first-order gain due to mobilization from root storage (μg/h)

$$\lambda_2 M_2$$ rate of all other first-order irreversible processes in root xylem compartment (μg/h) (21)

Define masses in the three compartments as follows:

$$M_3 = (1 + B_3) V_3 C_3 , \quad (\mu g) \quad (22)$$

$$M_4 = (1 + B_4)\ V_4\ C_4\ , \qquad (\mu g) \qquad (23)$$

$$M_5 = (1 + B_5)\ V_5\ C_5\ . \qquad (\mu g) \qquad (24)$$

The fourth mass balance equation for the time rate of change of mass dM_2/dt is obtained by solving each of equations (22), (23), and (24) for its compartment concentration C_i in terms of its compartment mass M_i, substituting the result into equation (21), and collecting common terms. The result is:

$$\frac{dM_2}{dt} = a_{2,0}\ M_0 + a_{2,2}\ M_2 + a_{2,3}\ M_3 + a_{2,4}\ M_4 + a_{2,5}\ M_5\ , \qquad (25)$$

where

$$a_{2,0} = \frac{\frac{D_1\ A_1}{\Delta x_1} + Q_1(1 - \sigma_1)}{V_1(1 + B_1)}\ , \qquad (26)$$

$$a_{2,2} = -\left[\frac{\frac{D_1\ A_1}{\Delta x_1} + \frac{D_4\ A_4}{\Delta x_4} + \frac{D_2\ A_2}{\Delta x_2} + Q_2(1 - \sigma_2) + Q_{f1}^{ST}}{V_2(1 + B_2)} + \lambda_2\right]\ , \qquad (27)$$

$$a_{2,3} = \frac{Q_{b1}^{ST}}{V_3(1 + B_3)}\ , \qquad (28)$$

$$a_{2,4} = \frac{\frac{D_4\ A_4}{\Delta x_4} + Q_4(1 - \sigma_4)}{V_4(1 + B_4)}\ , \qquad (29)$$

$$a_{2,5} = \frac{\frac{D_2\ A_2}{\Delta x_2}}{V_5(1 + B_5)}\ . \qquad (30)$$

Root Storage Compartment

The equation for the time rate of change of mass in the root storage compartment yields the fifth mass balance equation:

$$\frac{dM_3}{dt} =$$ instantaneous time rate of change of free plus reversibly bound chemical mass in the root storage compartment ($\mu g/h$)

$$Q_{f1}^{ST} C_2$$ rate of first-order loss due to storage from root xylem to root storage compartment ($\mu g/h$)

$$- Q_{b1}^{ST} C_3$$ rate of first-order gain due to mobilization from root storage to root xylem compartment ($\mu g/h$)

$$+ Q_{f2}^{ST} C_4$$ rate of first-order loss due to storage from root phloem to root storage compartment ($\mu g/h$)

$$- Q_{b2}^{ST} C_3$$ rate of first-order gain due to mobilization from root storage to root phloem compartment ($\mu g/h$)

$$- \lambda_3 M_3 .$$ rate of all other first-order irreversible processes in root storage compartment ($\mu g/h$) (31)

M_2, M_3, and M_4 were defined by equations (11), (23), and (24). Solving each for concentrations C_2, C_3, and C_4, respectively, and substituting the results in equation (31) yields,

$$\frac{dM_3}{dt} = a_{3,2} M_2 + a_{3,3} M_3 + a_{3,4} M_4, \quad (32)$$

where

$$a_{2,3} = \frac{Q_{f1}^{ST}}{V_2(1 + B_2)}, \quad (33)$$

$$a_{3,3} = - \left(\frac{Q_{b1}^{ST} + Q_{b2}^{ST}}{V_3(1 + B_3)} + \lambda_3 \right), \quad (34)$$

$$a_{3,4} = \frac{Q_{f2}^{ST}}{V_4(1 + B_4)} \cdot \quad (35)$$

System of Equations

The remaining 19 mass balance equations with corresponding matrix elements were derived in a similar manner. The complete listing of all 24 mass balance equations is given in Appendix 1. The total chemical mass in each compartment is defined for i = 6,7,...22, by

$$M_i = (1 + B_i)\, V_i\, C_i. \quad (36)$$

The possibility of loss of mass due to volatilization from leaves is included by stating:

$$\text{rate of loss via volatilization} = \frac{D_{CH} A_{11}}{\Delta x_{11}} (H_C C_{18} - C_{air}) \quad (37)$$

where H_C is the dimensionless Henry law constant for the chemical compound being modeled, D_{CH} (cm^2/h) is the effective chemical diffusion coefficient of the compound in the boundary layer over the leaf surface, C_{air} (g/g) is the concentration of the chemical compound in the mixed air outside the boundary layer, Δx_{11} (cm) is the thickness of the boundary layer, and A_{11} (cm^2) is the effective area of volatilization. Rules, similar to equation (37), were also written for leaves 2 and 3. Equation (37) allows communication with the atmosphere and incorporation of atmospheric conditions such as wind speed, and air temperature, and relative humidity.

Solution Method

The complete system of 24 differential equations in 24 unknowns can be written in matrix form as

$$\frac{d\underset{\sim}{M}}{dt} = \underset{\sim}{A}\underset{\sim}{M} + \underset{\sim}{S}, \tag{38}$$

with initial conditions summarized as

$$\underset{\sim}{M}(o) = \underset{\sim}{M}_o , \tag{39}$$

where M is the 24 x 1 vector of unknown masses at time t, S is the 24 x 1 vector of sources which may have nonzero entries at positions 14, 17, and 20, A is the 24 by 24 irreducible transport transfer matrix, which is real, weakly diagonally dominant, has negative diagonal entries, and whose off diagonal entries are either positive or zero (Varga, 1962), and M_o is the 24 x 1 vector of initial chemical masses.

The system of equations given by equation (38) is linear and has constant coefficients, over the arbitrary slice T_L to T_U hours. As such this system has a unique continuous solution vector M(t) (Boyce and DiPrima, 1965). Each element $M_i(t)$ of M(t) is itself a linear combination of at most 24 elementary exponential functions. Because assignment of appropriate weighting factors is not practical with current knowledge, we chose to approximate the solution numerically. The method outlined below is now enjoying a renewed interest and usage due to the availability of microcomputers with large storage, high speed, and double precision arithmetic. It is a useful method for large, sparse, arrays with constant coefficients such as frequently arise in biological and control systems.

Define the matrix exponential function, sometimes called the fundamental solution matrix, to be

$$e^{At} = I + \sum_{\ell=1}^{\infty} \frac{(At)^{\ell}}{\ell!} . \tag{40}$$

This series serves as the basis for the numerical solution method, although it is useful for computing only for small values of time t (Boyce and DiPrima, 1965), where I is the identity matrix. Boyce and DiPrima (1965) prove many important properties about this matrix exponential function, such as

i) differentiation: $$\frac{d\, e^{At}}{dt} = A\, e^{At} \tag{41}$$

ii) commutation: $$Ae^{At} = e^{At}A \tag{42}$$

iii) commutation: $$A^{-1} e^{At} = e^{At} A^{-1} \tag{43}$$

Rewrite equation (38) as

$$\frac{d\underset{\sim}{M}}{dt} - A\underset{\sim}{M} = \underset{\sim}{S} \tag{44}$$

and matrix multiply left by e^{-At}, the inverse matrix of e^{At} (Boyce and DiPrima, 1965), and recast the system into the form

$$\frac{d(e^{-At}\underset{\sim}{M})}{dt} = e^{-At}\underset{\sim}{S} \tag{45}$$

Next, superimpose on the time line a lattice of points t_0, t_1, t_2,... so that $t_0 = 0$, $t_1 = \Delta t$, $t_2 = 2\Delta t$, $t_3 = 3\Delta t$,..., then multiply both sides of equation (45) by the differential dt, and integrate both sides between the two time points t_n, t_{n+1}, to obtain:

$$e^{-At_{n+1}} \underset{\sim}{M}(t_{n+1}) - e^{-At_n} \underset{\sim}{M}(t_n)$$

$$= -A^{-1} (e^{-At_{n+1}} - e^{-At_n}) \underset{\sim}{S} \tag{46}$$

Matrix multiply left both sides of equation (46) by $e^{At_{n+1}}$ to obtain the explicit recursion formula

$$\underset{\sim}{M}(t_{n+1}) = e^{A\Delta t} \underset{\sim}{M}(t_n) - A^{-1}(I - e^{A\Delta t}) \underset{\sim}{S} \tag{47}$$

Note that no approximation has as yet been made. Equation (47) is an exact solution of the original differential system, but the solution consists of M evaluated only on a discrete set of time points. Define the constant vector W via the formula

$$\underset{\sim}{W} = -A^{-1} (I - e^{A\Delta t}) \underset{\sim}{S} \tag{48}$$

Clearly, on the discrete set of time points $t_0, t_1, t_2 \ldots$

$$\underset{\sim}{M}(t_{n+1}) = e^{A\Delta t} \underset{\sim}{M}(t_n) + \underset{\sim}{W} \tag{49}$$

which is a 24-dimensional, first-order, nonhomogeneous, difference system (Varga, 1962; Jacquez, 1972).

Mathematical induction shows that the unique solution to system (49) is

$$\underset{\sim}{M}(t_n) = (e^{A\Delta t})^n \underset{\sim}{M}_o + (I - e^{A\Delta t})^{-1} (I - (e^{A\Delta t})^n) \underset{\sim}{W} \tag{50}$$

for $n = 1, 2, 3 \ldots$

Because $e^{A\Delta t}$ is a positive 24 x 24 array with a spectral radius (modulus of the maximum eigenvalue) less than 1, $e^{A\Delta t}$ is said to be a convergent array since, as $n \to \infty$, $(e^{A\Delta t})^n \to Z$, the array of zero elements (Varga, 1962). It can be shown that

$$\lim_{n\to\infty} \underset{\sim}{M}(t_n) = -A^{-1}\,\underset{\sim}{S}$$

which follows directly from equation (50).

Equation (49) is used for computational purposes. The approximation is made because $e^{A\Delta t}$ can only be computed to the double precision limits of the computer. A useful method for carrying out the computation is to observe that

$$e^{A\Delta t} = (e^{\frac{A\Delta t}{N}})^N = ((e^{\frac{-A\Delta t}{N}})^{-1})^N = [(e^{\frac{-A\Delta t}{N}})^{-1}]^N \qquad (51)$$

where N is chosen to be a power of 2, just large enough so that

$$\max_{1\le i\le 24}\left\{\left|\frac{-a_{ii}\Delta t}{N}\right|\right\} < 1 \qquad (52)$$

(Ward, 1977, Moler and Van Loan, 1978).

The key to computing $\exp[A\Delta t]$ to high precision is to first compute $\exp[-A\Delta t/N]$ using the matrix exponential function definition 40 to the double precision limits of the computer. Next, compute $(\exp[-A\Delta t/N])^{-1}$, the inverse-scaled exponential matrix function via the classical LU factorization method. Lastly, raise $\exp[-A\Delta t/N]^{-1}$ to the power N. Other scaling methods exist (Golub and Van Loan, 1983). Time matching scheme (49) is a stable scheme in that any small perturbation introduced into the data at some time $t_k > 0$, propagates in a bounded fashion as time exceeds t_k, arbitrarily large (Varga, 1962).

Effective Concentrations

In most experimental situations it is difficult, if not impossible, to sample the phloem, xylem, or storage compartments individually

to determine concentrations ($\mu g/cm^3$) at points in time. For example, when evaluating accumulation by leaves it is usually most convenient to harvest groups of leaves and obtain an average concentration (DPM/g) or ($\mu g/g$) for the group. An average or "effective tissue concentration" can then be obtained by dividing the chemical mass present by the wet mass of tissue ($\mu g/g$). An effective volume-based concentration ($\mu g/cm^3$) can be obtained when the density is known. Assuming that the density of most plant parts of young soybean plants is 1 g/cm^3, effective concentrations ($\mu g/cm^3$) are defined as below. In the definition, (t) indicates concentration at time t and OA indicates the overall average concentration for the indicated plant part:

i) in the roots,

$$C_{roots}(t) = \sum_{i=0}^{4} M_i / \sum_{i=0}^{4} V_i; \quad (53)$$

ii) in the individual stem parts

$$C_{stem\ b}(t) = \sum_{i=5}^{7} M_i / \sum_{i=5}^{7} V_i; \quad (54)$$

$$C_{stem\ m}(t) = \sum_{i=8}^{10} M_i / \sum_{i=8}^{10} V_i; \quad (55)$$

$$C_{stem\ t}(t) = \sum_{i=11}^{13} M_i / \sum_{i=11}^{13} V_i; \quad (56)$$

iii) in the stem,

$$C_{stem\ OA}(t) = \sum_{i=5}^{13} M_i / \sum_{i=5}^{13} V_i; \quad (57)$$

iv) in the individual leaf clusters,

$$C_{\text{leaf } 1}(t) = \sum_{i=14}^{16} M_i / \sum_{i=14}^{16} V_i; \quad (58)$$

$$C_{\text{leaf } 2}(t) = \sum_{i=17}^{19} M_i / \sum_{i=17}^{19} V_i; \quad (59)$$

$$C_{\text{leaf } 3}(t) = \sum_{i=20}^{22} M_i / \sum_{i=20}^{22} V_i; \quad (60)$$

v) in the leaves,

$$C_{\text{leaf OA}}(t) = \sum_{i=14}^{22} M_i / \sum_{i=14}^{22} V_i. \quad (61)$$

APPLICATION TO EXPERIMENTS

Introduction

This part of the manuscript describes the application of the model to previously obtained experimental data on uptake of the herbicide Bromacil® by soybean plants (Glycine max) (McFarlane and Pfleeger, 1987). The purpose of this exercise was to calibrate the model.

Calibration of mathematical models generally consists of using the model in a parameter estimation or system identification mode for application to a set of experimentally obtained data sets. Convergence on the values of parameters is guided by some measure or criterion of "goodness of fit," e.g. mean square error or mean square deviation. Several different system driving variables may be involved (Godfrey and diSteffano, 1987). Ideally, the model is developed first, then experiments are designed and carried out to test the assumptions on which the model is based (Box et al., 1978). The lack of fit between model prediction and experimental measurement is assessed and the model may be changed to obtain improved matching between model prediction and experiment. Additional sets of experiments are then designed for testing the model. In the present case, previously obtained data were used and the model was adapted to allow for peculiar experimental differences. Results of seven uptake experiments involving three bromacil concentrations and three transpiration rates were available.

Experimental Procedures

Soybean [Glycine max (L.) Merr. dwarf cultivar Fiskeby v] plants were grown in a hydroponic nursery (McFarlane and Pfleeger, 1986) in a greenhouse until leaves at the eleventh or twelfth node were just

starting to develop. All lateral stems were removed as they initiated. The nutrient solution was a modified, half-strength, Hoagland solution (Berry, 1978) with a pH of 6.0 and electrical conductivity of 1.2 dS/m. Plants of similar size were transferred to the exposure chambers described by McFarlane and Pfleeger (1987). Plants were acclimated for three days to the conditions of the controlled environment prior to adding ^{14}C-labeled bromacil (U-$^{14}C_6H_{13}BrN_2O_2$) to the nutrient solution. The specific activity of the treatment stock was $6.76*10^6$ Bq/mmole bromacil as measured by liquid scintillation analysis and gas/liquid chromatography. The treatment was started by the addition of the amount of bromacil stock solution needed to obtain the desired concentration in each plant exposure chamber. The concentrations used in each of the three experiments are in Table 4. In addition to other environmental parameters, root exposure was monitored by periodically sampling the hydroponic solution and analyzing for ^{14}C activity. Each sample was analyzed in triplicate and the analytical variation in counting replicate samples was never larger than 3 percent of the mean.

The solution volume was maintained automatically at 6.5 liters by replacing transpired water with nutrient solution but without bromacil. Since bromacil uptake was approximately proportional to the transpiration rate, chemical was lost at a faster rate from the solution with a high transpiration rate than from one with a low transpiration rate.

Bromacil uptake was measured by periodically removing plants from each chamber for determination of ^{14}C concentration of the plant parts. The stems were cut at the crown, the leaves removed, and fresh weights were determined for leaves, stems, and roots. The tissues were freeze dried. Roots and leaf tissues were ground to a powder, then subsamples

Table 4. Environmental parameters and plant functions during uptake test (BROM3).

Parameter	Units	Value			CV%
		BROM1	BROM3	BROM5	
Photosynthetic Photon flux (PPF)*	μmol/s m^2	350	350	350	5
Air Temperature	C	23	23	23	2
Specific humidity	g/m^3			20	1
(low tr.)				16	
(medium tr.)				12	
(high tr.)					
Windspeed	m/s			0.6	15
CO^2	$mmol/m^3$			15.6	5
Transpiration					
(low)	cm^3/h plant	---	4.6	1.2	10
(medium)		---	7.6	5.7	
(high)		7.0	9.5	7.3	
Bromacil concentration of bathing solution	$\mu g/cm^3$	0.328	0.180	0.058	

*Light cycle on/off was 24/0 hours.

were obtained and burned in a Packard 306 sample oxidizer. The CO_2 was collected and analyzed for ^{14}C activity by liquid scintillation counting. Stem material was not easily ground because of its fibrous nature, therefore segments were selected from the lower, middle, and top portions of each plant and oxidized without powdering. Attention was given to the possibility of chemical loss during drying and as a result of incomplete combustion in the oxidation step. Quality assurance tests confirmed that less than 1 percent was lost in either procedure.

Transformation of bromacil was tested by evaluation of thin-layer chromatographs made from plant extracts and from the hydroponic solution. Only bromacil was found in the nutrient solution and roots, but about 5 percent of the ^{14}C activity in the leaves was determined to be associated with another chemical. This result was also found in other studies (McFarlane et al., 1987). Since this was a small contribution to the total ^{14}C activity, and since all the bromacil was accounted for in this study, it was assumed that the results presented on the basis of DPM are an accurate description of the movement patterns of bromacil in the test plants.

Three experiments with bromacil uptake were conducted, each with some different aspect in timing, dosing concentration or experimental conditions (Table 4). The knowledge gained from the first experiment (BROM1) led to the design of the second (BROM3) which included three exposure chambers, each with a different transpiration rate. In the final experiment (BROM5) bromacil was periodically added to each chamber so that the concentration in the nutrient solutions remained approximately constant throughout the exposure. In the first two tests, individual leaves, stems, and root segments were analyzed. In the last test, samples were pooled and subsamples representing plant regions were analyzed.

Since two types of experiments were conducted, namely, one with decreasing bromacil concentration and one with constant bromacil concentration, the mathematical model was formulated in a manner which allowed either condition to exist in the simulation.

Results of the three experiments include measurements of transpiration rates, leaf areas, wet mass of harvested plant parts (Table 5),

Table 5. Measured transpiration rates, leaf areas, and wet masses of roots, stems, and leaves for three experiments with different bromacil concentrations. The data shown are averages of several measurements obtained during an experimental period of 220 hrs for BROM5, 55 hrs for BROM3, and 72 hrs for BROM1. Number in parenthesis following leaf area and mass of wet plant material is estimated standard error (ese).

Experiment	Leaf area	Transp rate	Wet mass of plant parts		
			Roots	Stems	Leaves
	cm^2	cm^3/cm^2 hr	g	g	g
BROM5	765 (103)	2.61×10^{-3}	24.7 (3.5)	4.5 (0.8)	16.7 (2.9)
	725 (122)	7.82×10^{-3}	31.1 (9.3)	6.5 (1.4)	17.3 (4.0)
	825 (116)	8.85×10^{-3}	31.5 (6.0)	6.6 (1.1)	19.9 (3.7)
			Stems plus leaves		
BROM3	1578 (250)	2.77×10^{-3}	45.5 (6.1)	71.2 (7.8)	
	1761 (261)	4.32×10^{-3}	56.5 (9.2)	91.4 (9.9)	
	1794 (160)	5.26×10^{-3}	47.9 (4.8)	77.0 (8.2)	
BROM1	845 (110)	8.65×10^{-3}	30.0 (6.3)	6.1 (0.6)	21.3 (2.1)

and concentrations of radio-labeled bromacil in the separately harvested plant parts as a function of exposure time (Table 6). The transpiration rates shown in Table 6 were obtained by measuring the volume of water lost during measurement intervals. Table 5 indicates that the plants of the BROM3 experiment were about twice as large as those of BROM1 and BROM5.

The BROM5 experiment had the lowest bromacil concentration. The measured concentration of radio-labeled bromacil in the tank was 3250 DPM/cm^3, which corresponds to 0.058 μg bromacil/cm^3 solution (Table 4). The BROM3 experiment used an initial bromacil concentration which was 3.1 times higher (0.180 $\mu g/cm^3$) and BROM1 used an initial bromacil concentration which was 9.1 times higher (0.528 $\mu g/cm^3$).

Table 5 lists the average biomass of plant parts present during each experiment. The question of growth was of concern with these experiments, particularly with BROM5 which lasted eight days. Measurement showed that there was not a systematic increase in biomass during the time of the experiments. This was confirmed by means and estimated standard errors (ese) of leaf areas and wet masses which were calculated for each measurement sequence. The decision was made that all experiments could be treated as steady-state experiments with respect to plant growth.

Measurements of radioactivity in each harvested plant part in DPM per unit of wet mass (Table 6) show the increase in radio labeled bromacil with time. The C^{14}-labeled bromacil was counted and reported as DPM per whole tissue region. This is an aggregate value for a region and does not give the concentration of the individual leaf or stem compartments.

The model was designed to allow evaluation of three separate stem and leaf compartments in each plant and simulations were run in this mode. For output the compartments were summed, because measurements were made in this manner. The effective bromacil concentration of the wet tissue in DPM/g was defined to be the total DPM measured in the wet tissue divided by the wet mass of this tissue in grams. This assumes that the mass of wet tissue can be equated to the volume of that tissue, i.e. the density of wet tissue, excluding air spaces, is 1 g/cm^3. The definitions follow from equations (53-61). Measurements of DPM concentration can be converted into mg per cm^3 by using the conversion factor of 1.82×10^{-5} mg of bromacil per DPM. The factor

Table 6. Bromacil concentrations in DPM per gram wet biomass.

BROM5

Time	Low			Medium			High		
	Roots	Stems	Leaves	Roots	Stems	Leaves	Roots	Stems	Leaves
(hr)	DPM/g wet mass								
8	5,149	3,654	507	5,537	9,495	2,079	5,763	5,233	3,472
26	7,058	11,864	3,473	6,767	9,565	10,221	7,065	10,12	14,9[illegible]
50	8,315	18,634	7,262		22,303	22,883	8,239	25,086	2[illegible]1
122		36,793	26,293	12,521	33,252	49,[illegible]99	10,485	32,684	[illegible],247
145	16,094	35,815	30,148	15,039	30,124	61,[illegible]17	13,950	38,093	106,952
169	18,041	36,512	35,009	18,652	38,244	71,081	16,993	31,52[illegible]	122,381
193	19,876	60,609	33,155	19,139	32,377	67,277	16,253	[illegible]7,6[illegible]9	133,190
218		51,010	42,686		41,4[illegible]7		21,234	[illegible],715	140,209

BROM3

Time	Low		Medium		High	
	Roots	Shoots	Roots	Shoots	Roots	Shoots
(hr)	DPM/g wet mass					
3.0	12,616	536	15,042	[illegible],031	12,521	1,792
7.0	15,651	2,725	14,641	[illegible],978	13,237	6,060
15.0	14,550	6,0[illegible]	17,779	7,587	13,926	14,119
23.0	16,218	10,23[illegible]	21,452	13,162	15,683	18,236
31.0	16,614	14,7[illegible]0	21,731	15,803	17,046	29,237
39.0	20,542	26,926	19,0[illegible]7	19,661	16,876	32,068
47.0	21,382	25,527	26,2[illegible]1	21,601	21,085	27,770
55.0	17,7[illegible]	29,81[illegible]	**	33,074	18,006	36,435

BROM1

Time	Tank	Roots	Stems			Leaves		
			Bottom	Mid	Top	Bottom	Mid	Top
(hr)	DPM/g wet mass							
0.0	31,625	0.0	0.0	0.0	0.0	0.0	0.0	0.0
1.0	29,186	24,737	11,158	7,002	4,667	904	1,171	837
4.0	27,8[illegible]	33,009	32,563	29,252	17,878	14,817	12,808	14,929
8.0	26,38[illegible]	32,007	47,592	42,421	31,172	43,027	40,659	58,762
24.0	25,[illegible]30	40,982	62,247	64,403	48,477	128,911	107,338	81,505
48.0	24,200	44,497	86,676	86,590	90,527	259,725	254,319	414,127
72.0	22,175	52,554	85,225	81,675	88,982	370,528	368,820	628,669

follows from:

$0.05834\ (\mu g/cm^3)/3200\ (DPM/cm^3) = 1.82 \times 10^{-5}\ (mg/DPM)$.

Qualitative Overview of Results

An initially very rapid increase in concentration occurred in the roots (Figure 3) with all experiments, followed by a slower rate of increase which remained nearly constant with time. The rapid increase during the first few hours of exposure was attributed to the filling of the free space of the root cortex with the bathing solution, with a concurrent rapid entry of solute into the cortex cells. The rapid permeation occurred as the transpiration stream drew in the bathing solution immediately upon exposure to the solution. This rapid increase indicates a large value for the storage coefficient during the early part of the uptake process with smaller values during the time following the initial loading.

Concentrations of the stem compartments of the BROM5 and BROM3 experiments (Figure 4) did not show the rapid initial increase that was found in the root compartments. However, a rapid increase in concentration did occur with the BROM1 experiment, with plants exposed to the high concentration of bromacil in the bathing solution (Table 4). The increase in stem concentrations was nearly linear for all three experiments during the first 50 hours of exposure. Concentrations in the stem compartments were higher than in the root compartments, suggesting that storage coefficients for the stem compartments were higher than for the root compartments and that the ratio of forward storage coefficient (Q_b) to backward storage coefficient (Q_f) was higher.

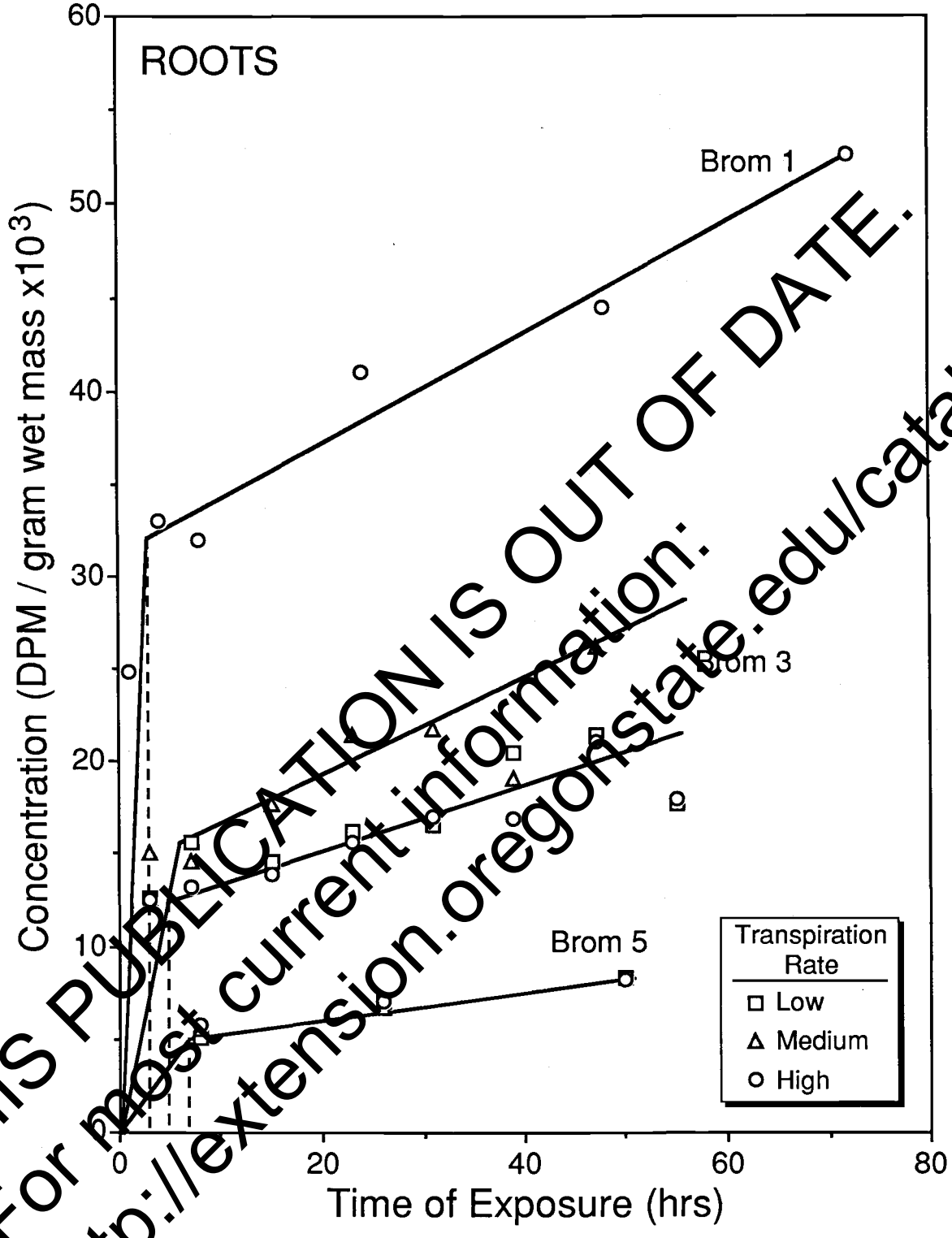

Figure 3. Measured bromacil concentrations in the root compartments. Details of the experimental procedures are in the text. The curves shown were drawn by hand to emphasize trends in increase in concentration. The graphs show an initial rapid rise in concentration, followed by a linear increase with time.

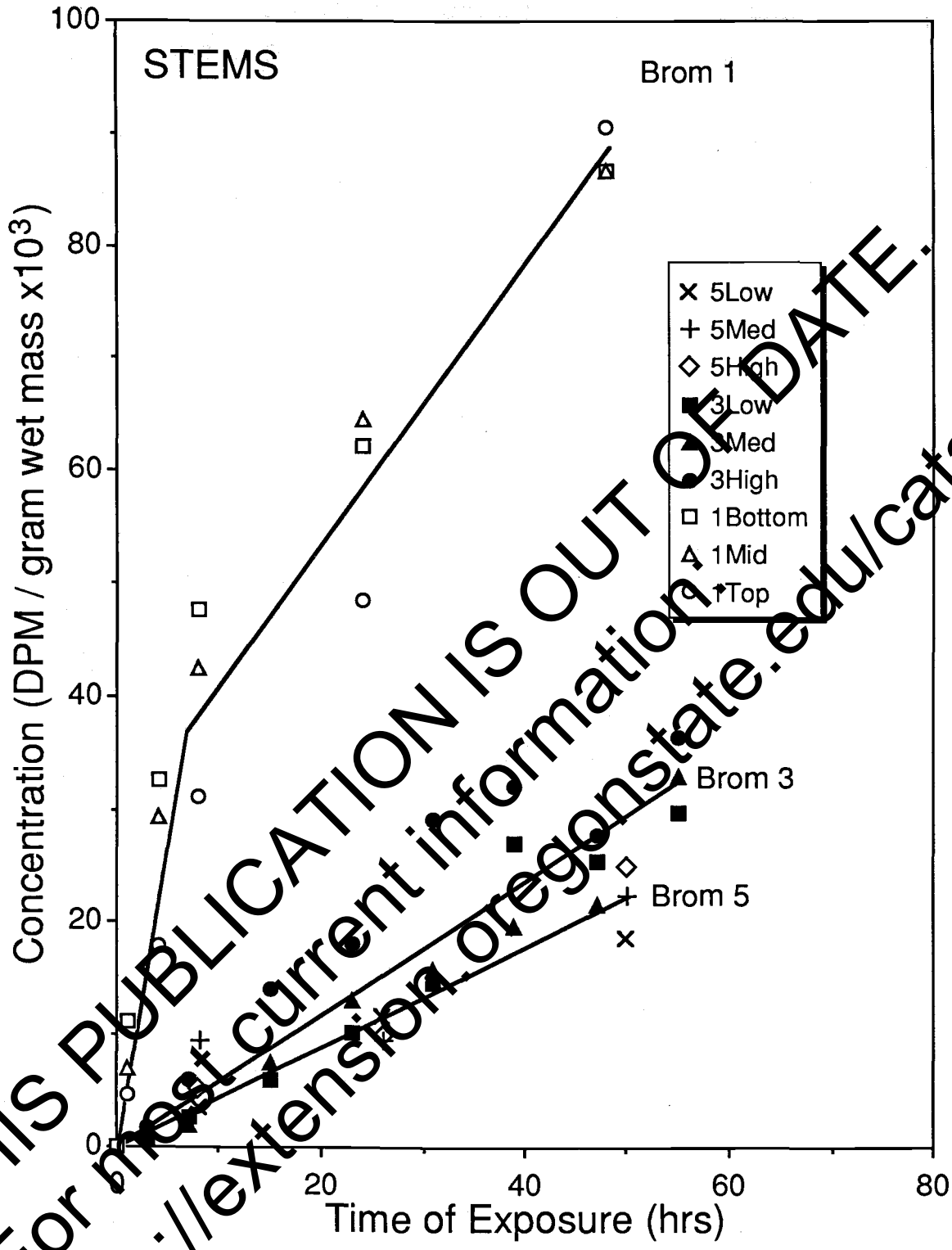

Figure 1. Measured bromacil concentrations in the stem compartments. Details of the experimental procedures are in the text. Curves were drawn by hand to emphasize trends in increase in concentrations. The graphs show a linear increase in concentration during the exposure period.

Results for the leaf compartments show a delayed arrival of the bromacil when compared to the root and stem compartments (Figure 5). Results for the BROM3 experiment are not shown because stems and leaves were analyzed together. Concentrations in the leaf compartments were still low after 10 hours of exposure. Storage in the leaf compartments continued in an apparent linear manner. This linear increase persisted over the entire 200-hour exposure period of the BROM5 experiment.

Concentrations at the end of 50 hours of exposure plotted as functions of solution concentrations (Figure 6) show that concentration effects may occur with bromacil uptake. The concentrations increased in a nonlinear manner with increasing exposure concentration for all three plant parts. The relationship had a weakly negative exponent for roots and stems, but a strong positive exponent for leaves.

Calibration

The purpose of the modeling exercise was to develop procedures for describing, by means of mathematical models, plant uptake of organic chemicals or more specifically, bromacil uptake by soybean seedlings. Uptake behavior is embedded in the storage and mobilization coefficients and the calibration of the model was therefore with respect to these coefficients.

Calibration of mathematical models ideally consists of using the model in a parameter estimation mode. Numerical procedures are used to find the parameter values which provide simulation results closely approximating experimental results. Convergence on the values of the parameters is guided by some measure or criterion of "goodness of fit," e.g. mean square error or mean square deviation. For this study the

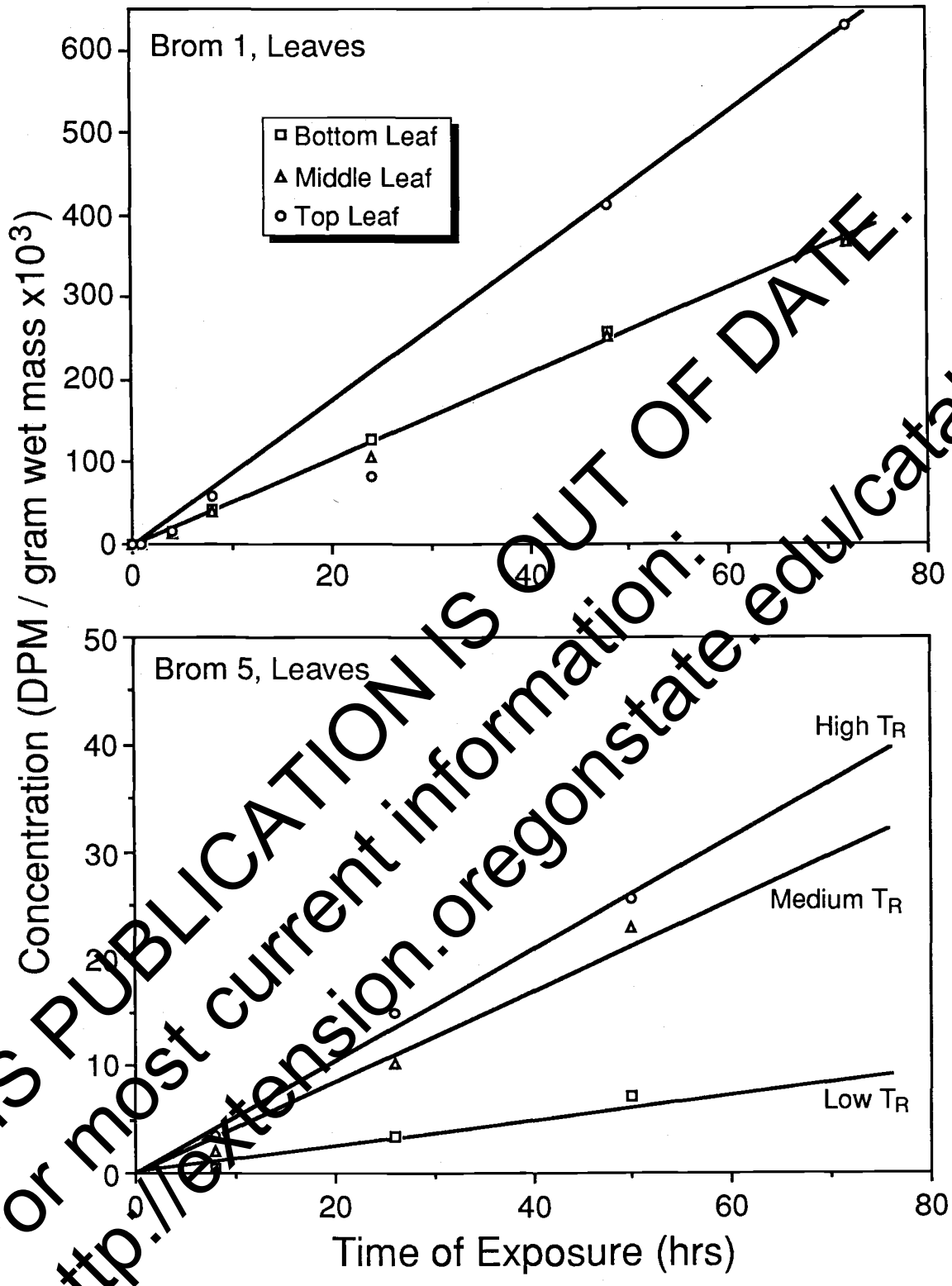

Figure 5. Measured bromacil concentrations in the leaf compartments for the BROM1 and BROM5 experiments. Curves were drawn by hand to emphasize trends. Results suggest a linear rate of uptake in these experiments with constant transpiration rates.

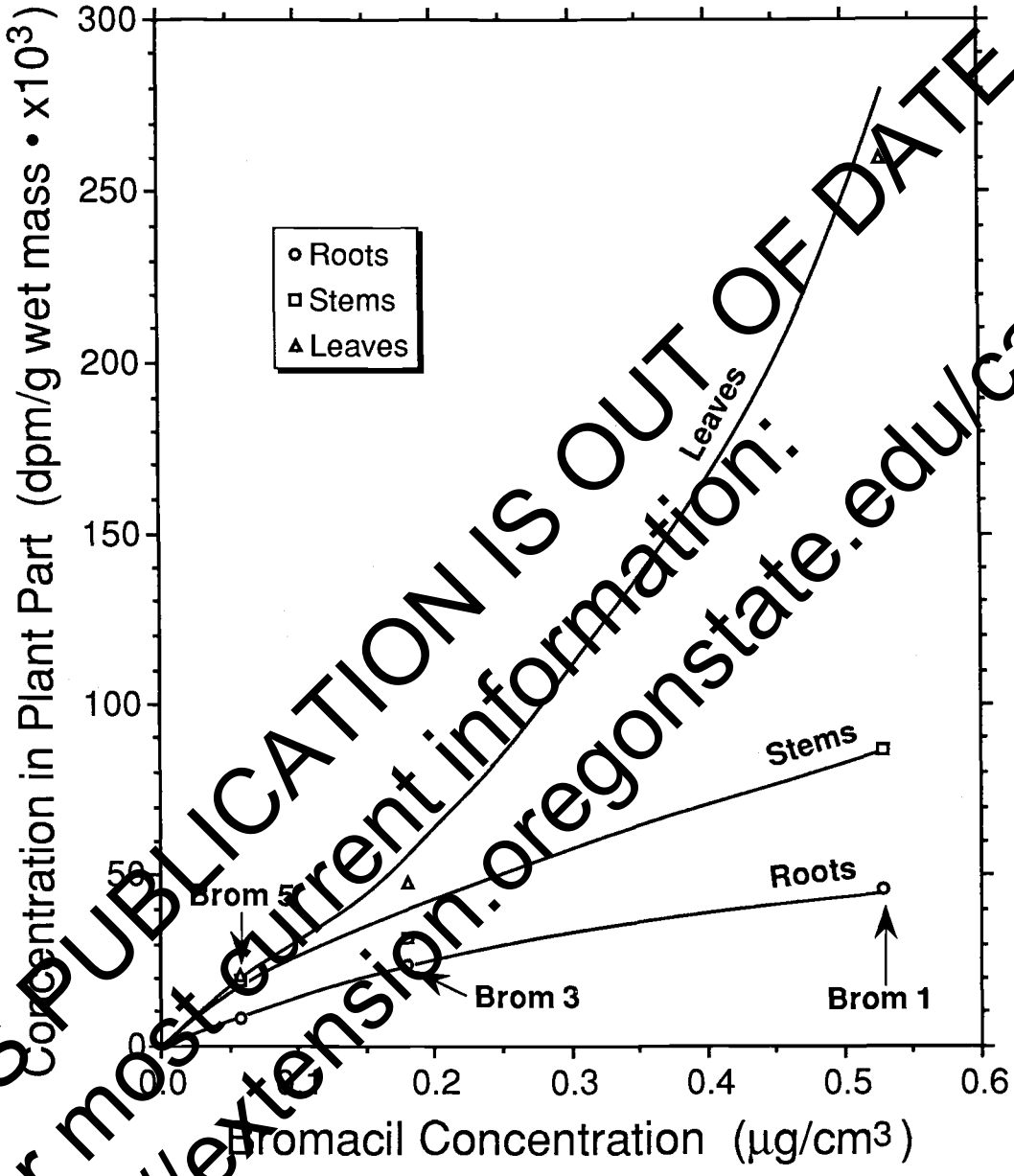

Figure 1. Concentration at 50 hrs of exposure as a function of solution concentration.

number of data points was not sufficient to follow this ideal procedure. Since model development is a recent activity, this circumstance is not unusual. Godfrey and diSteffano (1987) recently addressed the problem and describe procedures for finding parameters using incomplete data sets.

According to recommended procedures, the data of the uptake experiments were first used to gain insight into the process to be modeled. This was initiated earlier in the manuscript with a qualitative analysis of the experimental results. This analysis was also used to set initial values of the parameters. Thus an iterative procedure, guided at each step by comparison of simulation and experimental data, was used to systematically adjust Q_{fi} and Q_{bi} values until agreement between simulation and measured results was obtained. About 50 sets of simulations were needed to arrive at the set of storage coefficients which gave acceptable agreement with experimental results. Providing mathematical proof that the storage coefficients obtained in this manner are unique is not possible. Another set of values, different from those shown which would give an equally good fit to the data, may exist.

UTAB (1) is a medium-resolution model. As such, it requires values for a large number of geometric and physiologic parameters which must be obtained before calibration with respect to storage coefficients can begin. Values of the parameters were chosen on the basis of a "normalized" plant with a total leaf area of 1000 cm^2 and then scaled according to measured plant sizes. Leaf areas were in the range 800 to 1,800 cm^2 (Table 2). This approach was used in earlier reports

(Boersma et al., 1988a,b,c) and values for anatomical features of soybean plants were derived from these reports.

Volumes of Compartments

Literature data and experimental results indicated that the generic soybean plant with a leaf area of 1,000 cm^2 would have a root volume of 25 cm^3, a stem volume of 6 cm^3, and a leaf volume of 25 cm^3 (Boersma, 1988a). The experimental plants corresponded approximately to these values in terms of ratios and absolute values (Table 5). The next step in setting up the data base for simulation was to obtain volumes of all compartments of the model for each experiment. The procedure for doing so is detailed by Table 7. The example shown in Table 7 is for BROM5, medium transpiration rate. The first step was to change from wet mass to volume, based on the assumption of a tissue density excluding air spaces equal to 1 g/cm^3. The first column in Table 7 shows the aggregate volume for each plant part of the normalized plant, i.e. 25 cm^3 for the roots, 6 cm^3 for the stems, and 25 cm^3 for the leaves. The second column shows the percent of each of these volumes occupied by subcompartments. These percentages were chosen from literature reports. The root was divided into the region outside the endodermis (cortex) and the region inside the endodermis (xylem + phloem + storage). Seventy-five percent was allocated to the cortex and 25 percent to the stele. Then volumes of cortex and stele were further subdivided. Of the cortex volume, 85 percent was allocated to cell volume and 15 percent to apparent free space. The stele was subdivided into 4 percent xylem, 93 percent storage, and 3 percent phloem.

Table 7. Basis for calculating the compartment volumes of the experimental plants. The example shown is BROM5, medium transpiration rate.

Compartment name and number	Base volume	Fraction to compartment		Base volumes	Volumes BROM5 (med.)
	cm^3			cm^3	cm^3
ROOT	25				
Root apparent free space (0)		0.75	0.15	2.813	3.499
Root cortex cells (1)			0.83	15.938	19.826
Root xylem (2)		0.25	0.04	0.250	0.311
Root storage (3)			0.93	5.813	7.231
Root phloem (4)			0.03	0.188	0.233
				25.000	31.160
STEM	6				
Bottom stem xylem (5)		0.735	0.04	0.176	0.191
Bottom stem storage (6)			0.93	4.101	4.443
Bottom stem phloem (7)			0.03	0.132	0.143
Mid stem xylem (8)		0.182	0.04	0.044	0.047
Mid stem storage (9)			0.93	1.016	1.100
Mid stem phloem (10)			0.03	0.033	0.035
Top stem xylem (11)		0.083	0.04	0.020	0.0217
Top stem storage (12)			0.93	0.463	0.5047
Top stem phloem (13)			0.03	0.015	0.0162
				6.000	6.500
LEAF	25				
Leaf cluster 1 xylem (14)		0.5	0.01	0.125	0.087
Leaf cluster 1 storage (15)			0.98	12.250	8.477
Leaf cluster 1 phloem (16)			0.01	0.125	0.087
Leaf cluster 2 xylem (17)		0.3	0.01	0.075	0.052
Leaf cluster 2 storage (18)			0.98	7.350	5.086
Leaf cluster 2 phloem (19)			0.01	0.075	0.052
Leaf cluster 3 xylem (20)		0.2	0.01	0.050	0.035
Leaf cluster 3 storage (21)			0.98	4.900	3.391
Leaf cluster 3 phloem (22)			0.01	0.050	0.035
				25.000	17.300

Stem volume was allocated as follows: 73.5 percent to bottom stem segment, 18.2 percent to middle stem segment, and 8.3 percent to upper stem segment. The volume of each stem segment was divided into 3 percent for phloem, 4 percent for xylem, and 93 percent for storage. Total leaf volume was divided into 50 percent, 30 percent, and 20 percent to lower, middle, and upper leaf, respectively. Each of these volumes was divided into 1 percent phloem, 1 percent xylem, and 95 percent storage.

The volumes used for simulation were then calculated by scaling the base values from Table 7 in proportion to volumes derived from measured plant mass (Table 5) using linear scaling. For example, with the medium transpiration rate of BROM5 the mean root mass was 31.1 g (Table 5). The volumes of root compartments (labeled 0 through 4) were obtained by multiplication of the base volume of root compartment shown in Table 7 by the quotient (31.1/25.0 = 1.244). This yielded the root compartment volumes shown in the last column in Table 4. The sum of these volumes should be 31.1 cm^2. The scale factor for the stem compartments was (6.5/6.0 = 1.083), and (17.3/25 = 0.692) for the leaf compartments. The same procedure was used to obtain volumes for the other experiments. Table 8 summarizes the other geometric parameters used in the UTAB 1.0 simulation runs.

Chemical and Physical Parameters

Information available for bromacil suggested setting sorption parameters, first-order irreversible loss process parameters, and reflection coefficients all equal to zero. This information must be

Table 8. Values of parameters used in UTAB 4.6 for geometric and chemical properties for each compartmental boundary and fluid flow rate.

Index	Regions connected	Area	Thickness	Diffusion coeff.	Fluid flow* rate
		(cm^2)	(cm)	(cm^2/h)	(cm^3/h)
0	Soil/apparent free space	6,350	0.00375	0.0036	5.671
1	Soil/root xylem	3,180	0.0001	1.8×10^{-7}	5.671
2	Root xylem/bottom stem xylem	0.00784	0.5	0.0036	6.975
3	Bottom stem phloem/root phloem	0.0056	0.5	0.0036	1.304
4	Root phloem/root xylem	1.0	0.001	3.6×10^{-5}	1.304
5	Bottom stem xylem/mid stem xylem	0.00504	1.0	0.0036	3.29
6	Mid stem phloem/ bottom stem phloem	0.00360	1.0	0.0036	0.4537
7	Mid stem xylem/top stem xylem	0.00284	1.0	0.0036	1.249
8	Top stem phloem/mid stem phloem	0.00203	1.0	0.0036	0.1135
9	Bottom stem xylem/leaf 1 xylem	0.00784	10.0	0.0036	5.686
10	Leaf 1 xylem/leaf 1 phloem	5.0	0.001	3.6×10^{-5}	0.8505
11	Leaf 1 xylem/atmosphere	10.0	1.0	0.0036	2.835
12	Leaf 1 phloem/bottom stem phloem	0.0056	10.0	0.0036	0.8505
13	Mid stem xylem/leaf 2 xylem	0.00504	8.0	0.0036	2.041
14	Leaf 2 xylem/leaf 2 phloem	3.0	0.001	3.6×10^{-5}	0.3402
15	Leaf 2 xylem/atmosphere	6.0	1.0	0.0036	1.701
16	Leaf 2 phloem/mid stem phloem	0.0028	8.0	0.0036	0.3402
17	Top stem xylem/leaf 3 xylem	0.00284	5.0	0.0036	1.249
18	Leaf 3 xylem/leaf 3 phloem	2.0	0.001	3.6×10^{-5}	0.1135
19	Leaf 3 xylem/atmosphere	4.0	1.0	0.0036	1.135
20	Leaf 3 phloem/top stem phloem	0.00203	5.0	0.0036	0.1135

*Fluid flow rates were calculated using formulas in Table 3, with $f_1 = 0.3$, $f_2 = 0.2$, and $f_3 = 0.1$, $Q_{TR} = 5.67$ cm^3/hr/plant.

secured outside of the model. Initial concentrations of bromacil were zero in all compartments except in the "soil compartment."

Phloem Transport

The model contains a parameter for the ratio of xylem flow to phloem flow. In order to run the model, it was necessary to choose this ratio for each leaf. The rate of water transport in xylem and phloem depends on environmental conditions and vigor of growth. Under

the constant environmental conditions of the experimental chambers the xylem and phloem flow rates could be assumed to remain constant. The ratio of xylem to phloem flow has been measured in many experiments (Noble, 1983). Based on these reports the ratio was set highest in the oldest leaf and smallest in the youngest leaf, as follows: $f_1 = 0.3$, $f_2 = 0.2$, and $f_3 = 0.1$, respectively.

Concentration of Bromacil in Bathing Solution

In the BROM3 experiment the concentration of bromacil in the bathing solution was maintained to be approximately constant. This condition was simulated in the model by setting the volume of the soil compartment very large (1.0×10^{10} cm^3). The initial mass of bromacil set at 3.2×10^{13} DPM so that the initial concentration was 3,200 DPM/cm^3 which is equal to the experimental condition of 0.058 $\mu g/cm^3$. The amount of bromacil taken up by plants during the 200-hour simulation time was negligible relative to the mass of bromacil remaining in the soil compartment. For BROM3 and BROM1 the soil volume was set equal to 6,400 cm^3, which was the volume of the root chambers, and the initial concentrations were those of the experiments (Table 4).

Transpiration Rate

The total rate of transpiration measured experimentally (Table 5). Measured rates were allocated to the three leaves in approximate proportion to leaf area, i.e. 50 percent to leaf 1, 30 percent to leaf 2, and 20 percent to leaf 3.

Storage Coefficients

The objective of the calibration procedure was to find plausible values of the storage coefficients. Important qualitative observations may be derived from Figures 3 through 5 and from literature reports. The value of storage coefficients for molecules such as glycine may be approximated from the relationship $Q = (DKA/\Delta x)$ (equation 2 with $\sigma = 0$). For such molecules $D \cong 0.036$ cm^2/hr. Assuming $\sigma = 0$, $\Delta x = 0.1$ cm and $A = 1.0$ cm^2 obtains $Q \cong 0.360$ cm^3/hr for a surface area of 1 cm^2. There are many uncertainties with this estimate. The value for D is for a dilute solution. Furthermore, only part of the surfaces of cells are available for diffusion, making Q smaller than shown. Diffusion may be limited by partitioning at the membrane surfaces. In the experiments, the surface area of compartments could be much larger than 1 cm^2. However, the value of $Q \cong 0.360$ cm^3/hr provides a useful estimate for the initial simulation.

In the leaves the rate of increase in bromacil concentration at the medium transpiration rate and low-exposure concentration (BROM5) was approximately 0.100×10^3 DPM/g-hr (Figure 5). This corresponds to $(0.100 \times 10^3$ DPM/g-hr $\times 1.82 \times 10^{-5})$ μg/DPM $= 1.82 \times 10^{-3}$ μg/g-hr $=$ 0.00182 μg/g-hr. This is the rate that would apply to 1 cm^3 of storage volume. For a storage volume of 10 cm^3 the rate would be 0.0182 μg/hr. The increase in concentration is the consequence of Q_f and Q_b, thus with $Q_b = 0.5\ Q_f$ the necessary Q_f should be 0.036 cm^3/hr. Based on these considerations, the initial guesses of $Q_f = 0.10$ cm^3/hr and $Q_b = 0.05$ cm^3/hr were used for stems and leaves.

Other considerations were that bromacil moves readily from transport vessels to surrounding tissues as indicated by the rapid increase

in concentrations in roots and stems following exposure. Storage coefficients for phloem and xylem may therefore be assumed to be equal to each other for a given tissue. Finally, we assumed that the storage and mobilization coefficients are proportional to storage volume. This proportionality derives from the volume to surface area relationship indicated in equation 1.

DISCUSSION

Introduction

Simulations rapidly achieved the condition where the correct total mass of chemical was stored in the plant as a function of time, indicating that the overall process was correctly described and that physical and chemical parameters were correct. However, the measured distribution between the three plant parts was not immediately simulated. This distribution is determined by storage coefficients. Progress with obtaining agreement between simulations and experiments was judged from tabulation of the ratio of simulated concentration (C_s) divided by experimentally measured concentration (C_{exp}, Table 9).

The quotients shown in Table 9 are those of the final run in the "eyeball" curve-fitting calibration procedure. The storage coefficients which resulted from the calibration procedure are in Table 10.

Figures 7 through 13 show simulated (solid lines) and measured (data points) concentrations for BROM5 (Figures 7, 8, and 9 for low, medium, and high transpiration rates, respectively), BROM3 (Figures 10, 11, and 12), and BROM1 (Figure 13). Ratios of simulated concentrations divided by measured concentrations (Table 9), indicate that experimental results of all experiments were simulated with equal success. The model simulated all the important features of the uptake behavior revealed by the experiments.

An additional step in the analysis was the effort to find structure in the storage coefficients found by the calibration procedure. Important considerations were to look for the relationship between storage coefficients and size of compartments, possible effects of concentration and/or transpiration rates, and differences, if any,

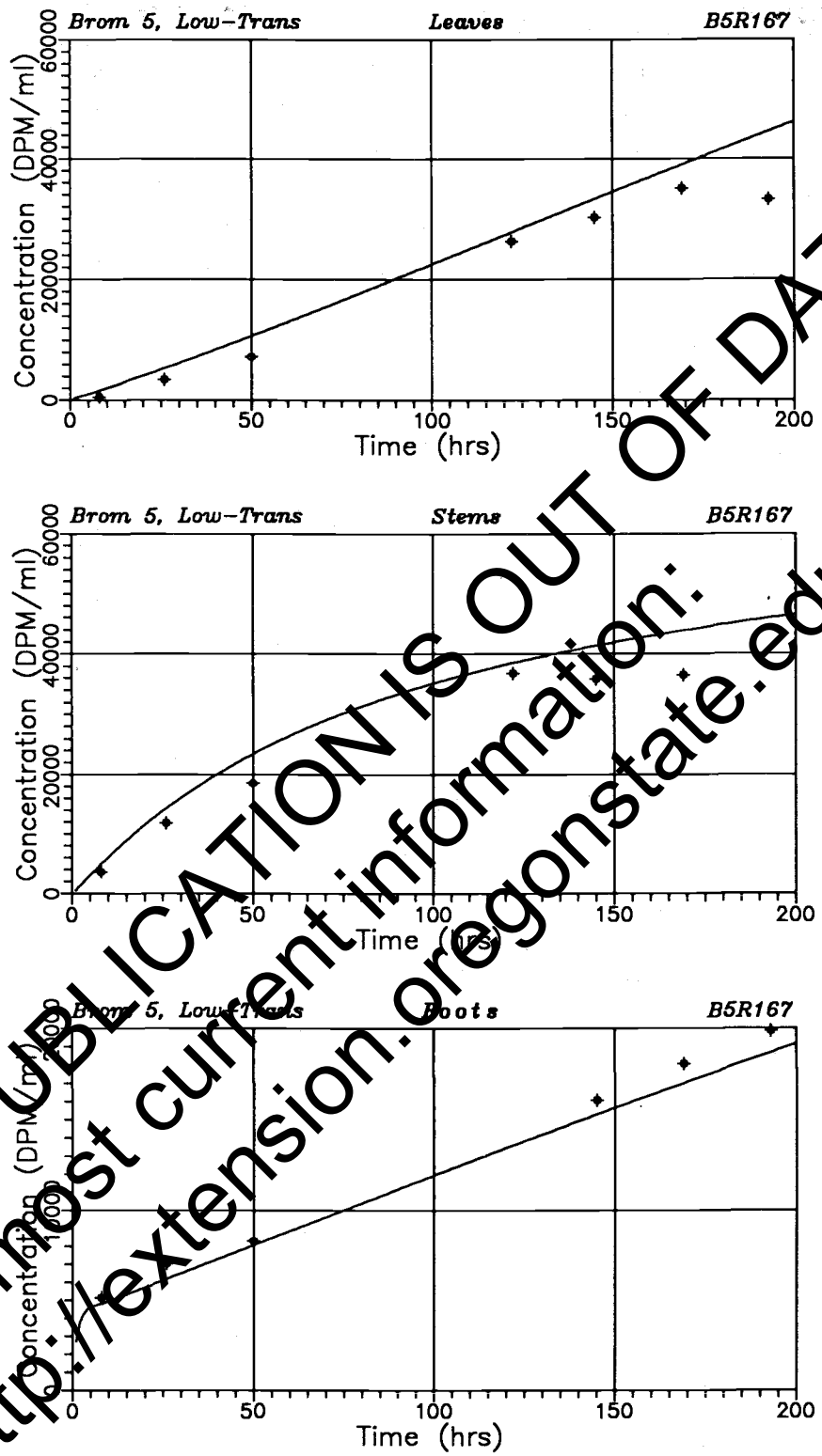

Figure 7. Concentrations in roots, stems, and leaves as a function of time for BROM5, low transpiration rate.

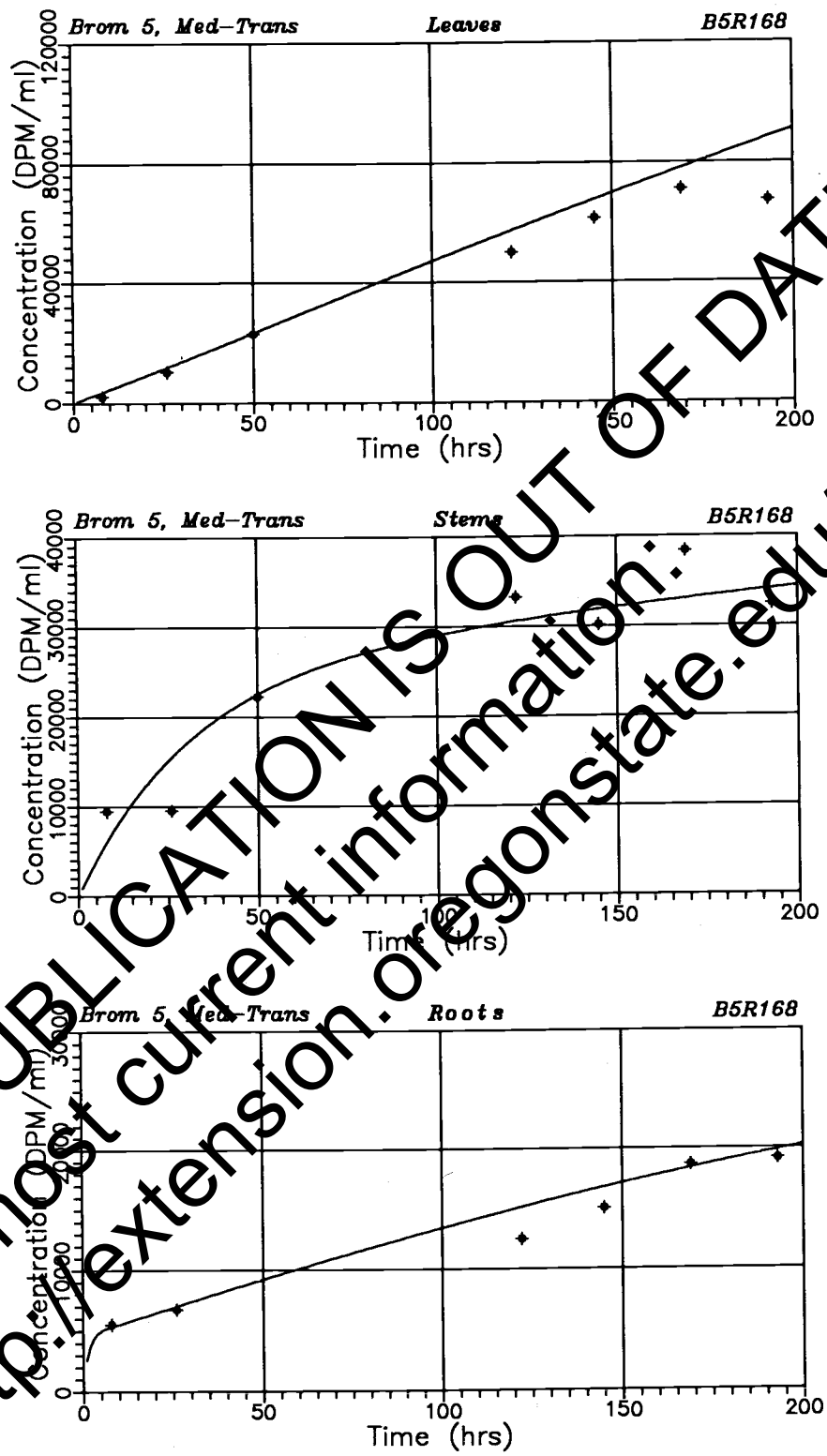

Figure 8. Concentrations in roots, stems, and leaves as a function of time for BROM5, medium transpiration rate.

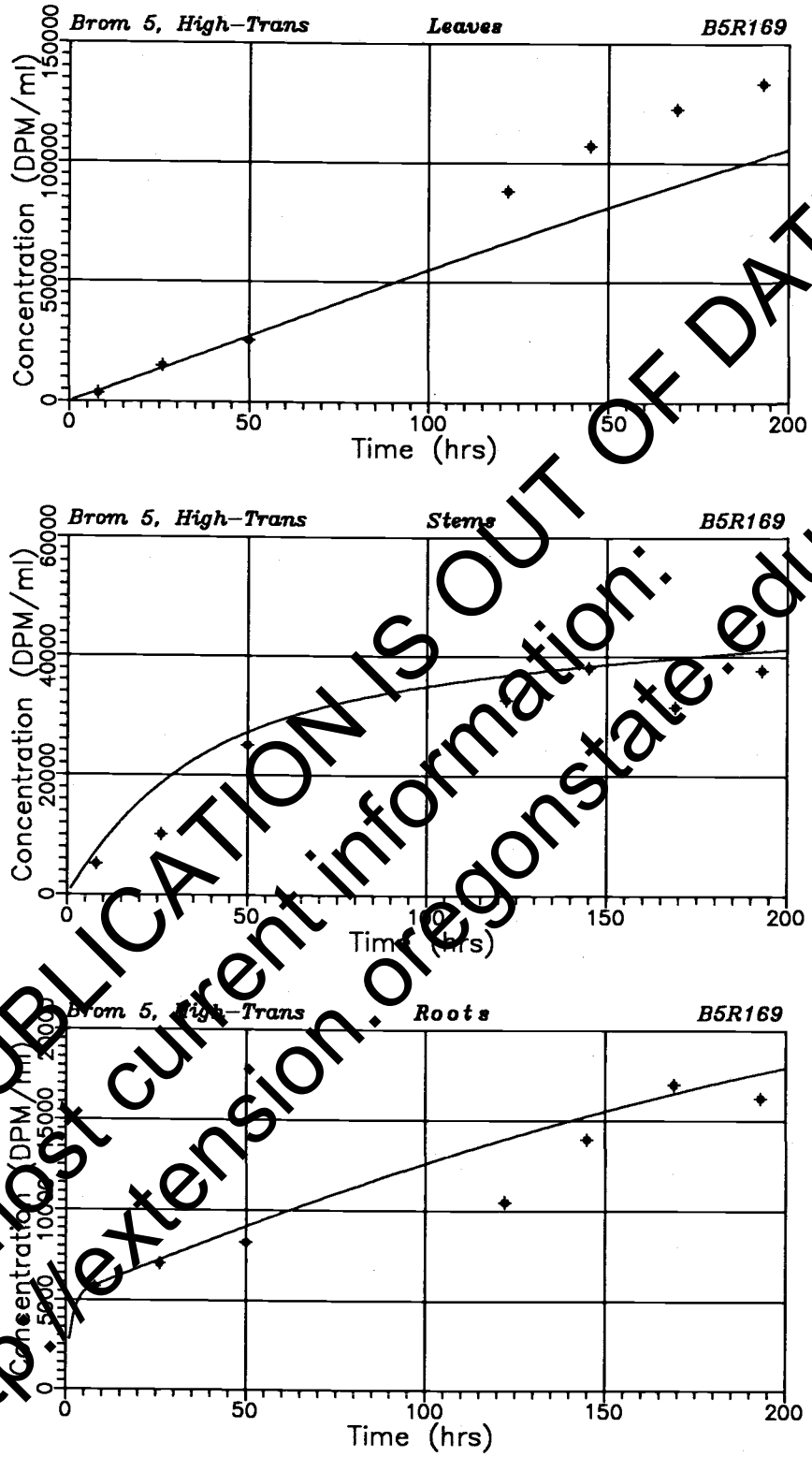

Figure 9. Concentrations in roots, stems, and leaves as a function of time for BROM5, high transpiration rate.

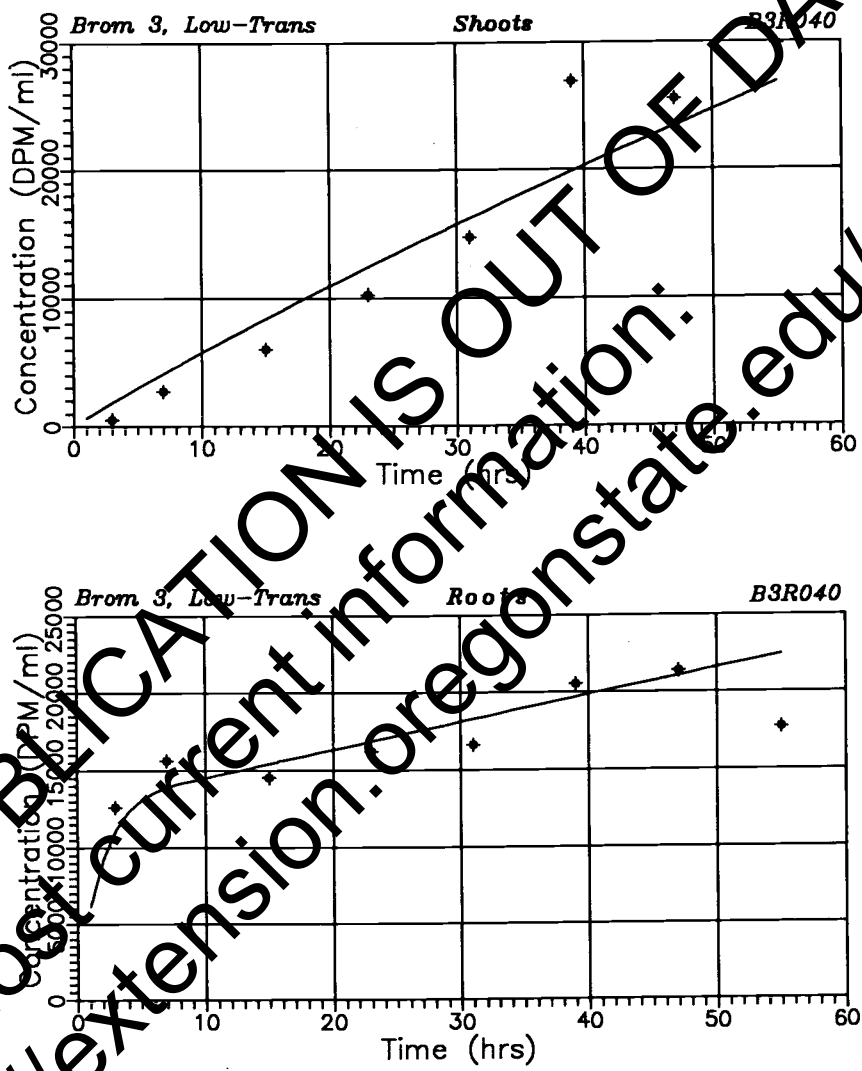

Figure 10. Concentrations in roots, stems, and leaves as a function of time for BROM3, low transpiration rate.

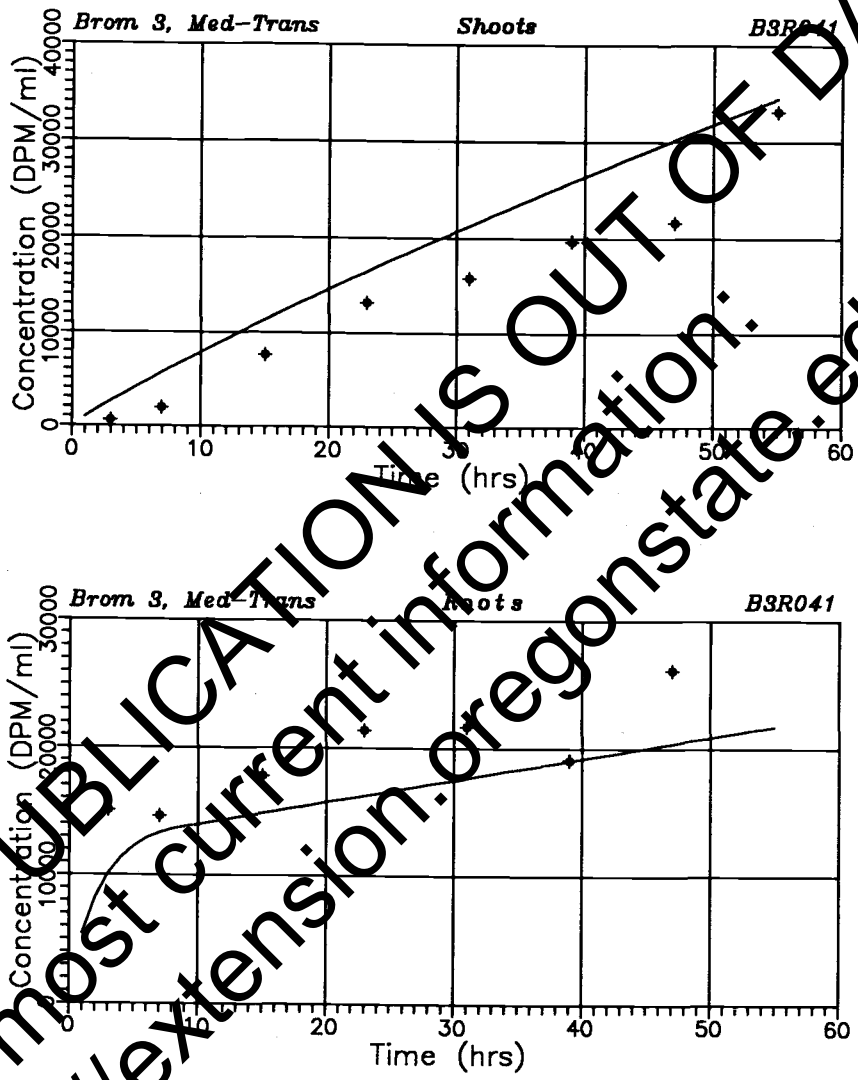

Figure 11. Concentrations in roots, stems, and leaves as a function of time for BROM3, medium transpiration rate.

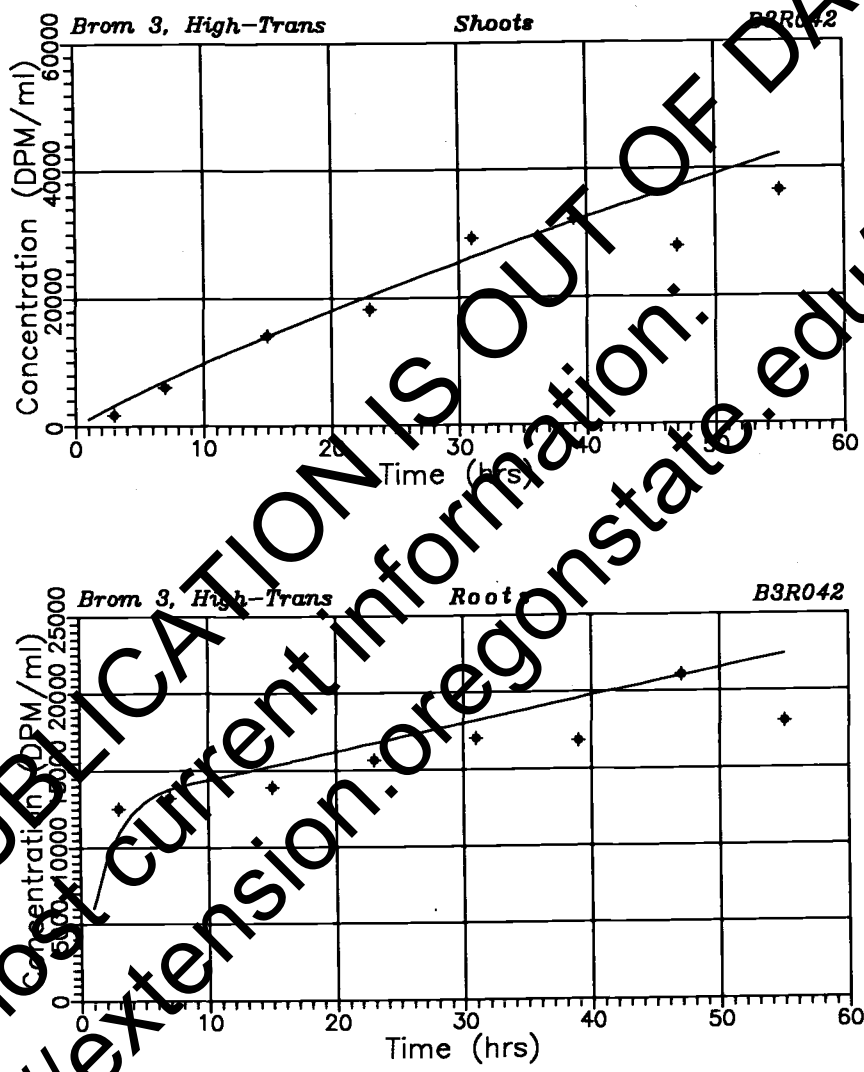

Figure 12. Concentrations in roots, stems, and leaves as a function of time for BROM3, high transpiration rate.

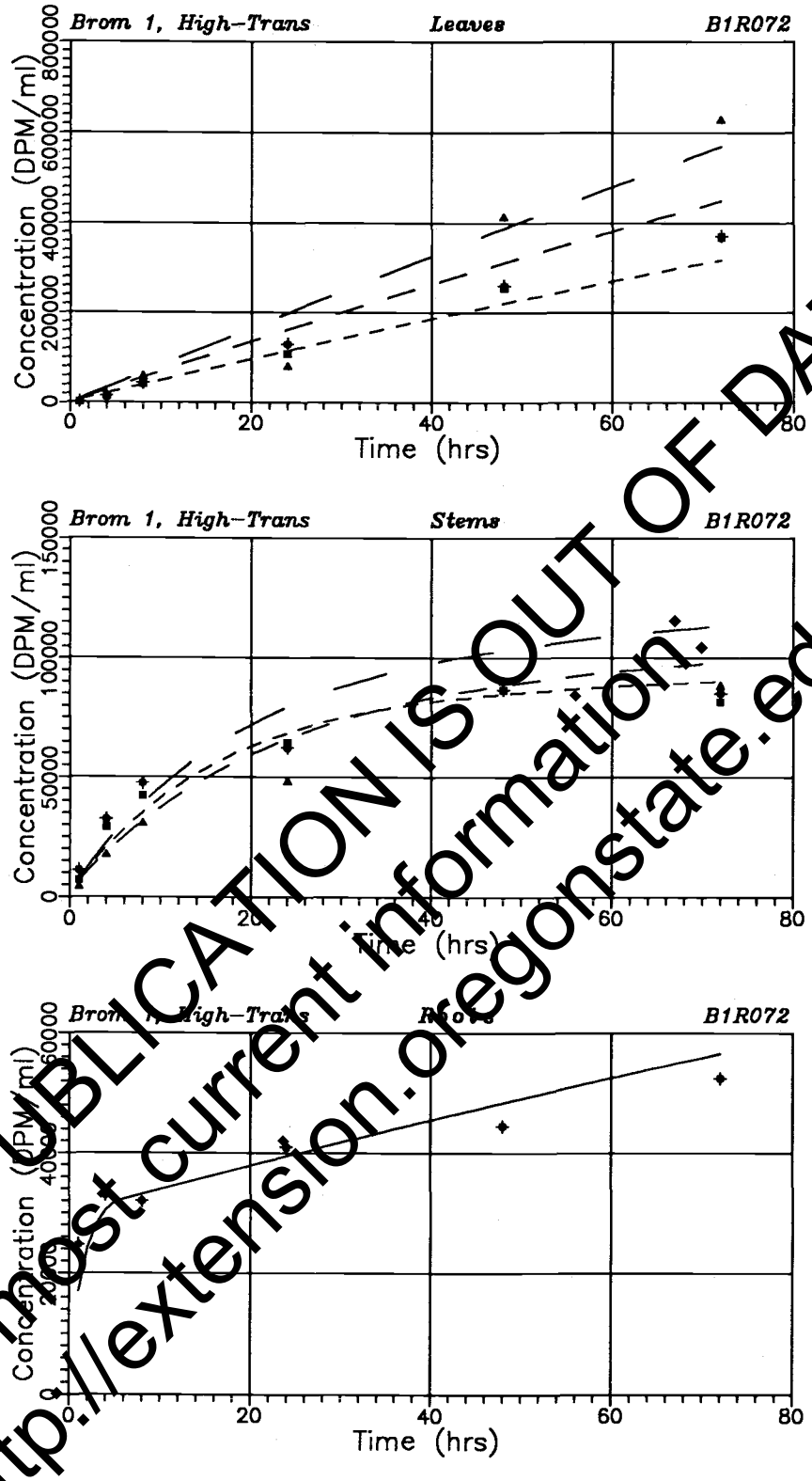

Figure 13. Concentrations in roots, stems, and leaves as a function of time for BROM1.

Table 9. Simulated concentrations (C_s) divided by measured concentrations (C_{exp}) at three transpiration rates.

BROM5

Time	Low			Medium			High		
	Roots	Stems	Leaves	Roots	Stems	Leaves	Roots	Stems	Leaves
(hr)	Ratio C_s/C_{exp}								
8	-0.93	1.37	3.15	-0.97	-0.64	1.71	1.01	1.40	1.43
26	-0.88	1.21	1.54	1.04	1.62	1.15	1.03	1.84	-0.92
50	-0.97	1.26	1.47	0.00	1.01	1.02	1.11	1.08	1.06
122	0.00	1.05	1.06	1.21	-0.92	1.14	1.33	1.13	-0.76
145	-0.95	1.15	1.10	1.12	1.06	1.10	1.09	1.01	-0.73
169	-0.94	1.20	1.11	-0.98	-0.86	1.10	-0.97	1.26	-0.74
193	-0.94	0.00	1.34	1.04	1.05	1.31	1.09	1.09	-0.77

BROM3

Time	Low		Medium		High	
	Roots	Shoots	Roots	Shoots	Roots	Shoots
(hr)	Ratio C_s/C_{exp}					
3.0	-0.88	3.49	-0.67	4.13	-0.87	1.82
7.0	-0.89	1.51	-0.91	2.87	1.04	1.17
15.0	1.06	1.39	-0.84	1.49	1.10	-0.99
23.0	1.04	1.21	-0.76	1.25	1.07	1.12
31.0	1.10	1.10	-0.81	1.35	1.07	-0.90
39.0	-0.96	-0.74	-1.00	1.31	1.16	-0.99
47.0	-0.99	-0.91	-0.78	1.40	-1.00	1.33
55.0	1.27	-0.90	0.00	1.04	1.24	1.16

BROM1

Time	Roots	Stem			Leaves		
		Bottom	Mid	Top	Bottom	Mid	Top
(hr)	Ratio C_s/C_{exp}						
0	-0.69	-0.64	-0.96	1.56	6.24	5.96	9.44
4.0	-0.92	-0.64	-0.63	1.26	1.37	2.16	2.20
8.0	-1.03	-0.74	-0.75	1.25	-0.92	1.35	1.12
24.0	-0.96	1.10	1.02	1.63	-0.89	1.50	2.42
48.0	1.09	-0.98	1.02	1.14	-0.85	1.22	-0.94
72.0	1.08	1.06	1.20	1.28	-0.86	1.22	-0.91

Table 10. Values of storage (forward) and mobilization (backward) transfer coefficient determined by the calibration procedure used in the text.

Compartment	Volume	Q-f	Q-b	Ratio Qf/Qb
	cm^3	cm^3/hr	cm^3/hr	
BROM5-low				
Root cortex	15.75	26.000	13.000	2.0
		0.290	0.018	16.1
Root storage	5.743	0.190	0.009	21.1
Stem bottom	3.076	0.405	0.050	8.1
Stem middle	0.762	0.100	0.015	6.7
Stem top	0.347	0.045	0.006	7.5
Leaf bottom	8.183	0.104	0.013	8.0
Leaf middle	4.910	0.070	0.009	7.8
Leaf top	3.273	0.048	0.006	8.0
BROM5-medium				
Root cortex	19.83	28.000	13.000	2.2
		0.270	0.030	9.0
Root storage	7.231	0.175	0.023	7.6
Stem bottom	4.443	0.268	0.099	2.7
Stem middle	1.100	0.068	0.027	2.5
Stem top	0.502	0.030	0.012	1.5
Leaf bottom	8.477	0.108	0.013	8.3
Leaf middle	5.086	0.071	0.009	7.9
Leaf top	3.391	0.049	0.006	8.2
BROM5-high				
Root cortex	20.08	31.000	13.000	2.4
		0.200	0.038	5.3
Root storage	7.324	0.130	0.025	5.2
Stem bottom	4.511	0.250	0.095	2.6
Stem middle	1.115	0.065	0.0215	2.6
Stem top	0.510	0.028	0.011	2.6
Leaf bottom	8.751	0.118	0.015	7.9
Leaf middle	5.851	0.0880	0.010	8.0
Leaf top	3.900	0.055	0.007	7.9
BROM3-low				
Root cortex	29.01	25.000	13.000	1.9
		0.375	0.031	12.1
Root storage	10.579	0.270	0.027	10.0
Stem bottom	9.440	0.577	0.264	2.2
Stem middle	2.338	0.146	0.074	2.0
Stem top	1.066	0.065	0.032	2.0
Leaf bottom	28.155	0.217	0.027	8.0
Leaf middle	16.893	0.168	0.021	8.0
Leaf top	11.262	0.130	0.016	8.1

Table 10. Continued.

Compartment	Volume	Q-f	Q-b	Ratio Q_f/Q_b
	cm^3	cm^3/hr	cm^3/hr	
BROM3-medium				
Root cortex	36.02	25.000	13.000	1.9
		0.320	0.021	15.2
Root storage	13.136	0.270	0.020	13.5
Stem bottom	10.793	0.657	0.328	2.0
Stem middle	2.673	0.167	0.084	2.0
Stem top	1.219	0.077	0.036	2.1
Leaf bottom	32.188	0.230	0.029	7.9
Leaf middle	19.313	0.179	0.022	8.1
Leaf top	12.875	0.140	0.018	7.8
BROM3-high				
Root cortex	30.54	215.000	13.000	1.9
		0.260	0.020	13.0
Root storage	11.137	0.200	0.020	10.0
Stem bottom	10.212	0.621	0.310	2.0
Stem middle	2.529	0.158	0.080	2.0
Stem top	1.153	0.070	0.036	1.9
Leaf bottom	30.449	0.225	0.028	8.0
Leaf middle	18.269	0.174	0.022	7.9
Leaf top	12.179	0.138	0.017	8.1
BROM1				
Root cortex	19.11	18.000	11.000	1.5
		0.120	0.027	4.4
Root storage	6.975	0.085	0.018	4.7
Stem bottom	4.170	0.168	0.140	1.2
Stem middle	1.032	0.032	0.027	1.2
Stem top	0.471	0.017	0.015	1.1
Leaf bottom	10.437	0.220	0.020	11.0
Leaf middle	6.262	0.170	0.017	10.0
Leaf top	4.175	0.100	0.010	10.0

between the three plant parts. To prepare for this analysis the ratios Q_f/Q_b shown in Table 10 were reordered as shown in Table 11.

Roots

Root concentrations increased rapidly during the first hours of exposure (Figures 7 through 13). The duration of this period of rapid uptake decreased with increasing concentration of the bathing solution. This uptake pattern was reproduced by the model by using large storage coefficients during this initial period. The large storage coefficients were changed to lower values after 10 hours of simulation for BROM5, 8 hours for BROM3, and 6 hours for BROM1. The uptake behavior reflected the rapid uptake which occurred upon the initial entry of solution into the root-free space. The medium transpiration rate for BROM5 was 5.7 cm^3/hr per plant; the root volume was 23.3 cm^3, consisting of 3.5 cm^3 apparent free space and 19.8 cm^3 cortex volume. At the indicated transpiration rate the water in the 3.5 cm^3 of apparent free space would be flushed out in 0.6 hour. Uptake after that time represents rapid storage in the cortex cells.

The instantaneous exposure would not occur under field conditions, except where a spill of contaminant occurred so that contaminated water would reach the root zone over a short period of time. For such conditions, the model should be run as done here. More likely is the scenario with low-level, chronic exposure such as occurs where plants are growing in contaminant soil water. The chronic exposure should be modeled using the smaller storage coefficients. Following the rapid initial uptake, storage continued in the root cortex and storage compartment of the root stele at a lower rate.

Table 11. Ratios Q_f/Q_b for individual plant parts. The transpiration rate for each experiment is listed at the top of each data column in the units of 10^{-3} cm^3/cm^2 hr.

Compartment		BROM5 (2.61)	BROM5 (7.82)	BROM5 (8.85)	BROM3 (2.77)	BROM3 (4.32)	BROM3 (5.26)	BROM1 (8.65)
Roots cortex		16.1	9.0	5.3	12.1	15.20	11.0	4.4
Roots storage		21.1	7.6	5.2	10.0	13.5	10.0	4.7
Stems	bottom	8.1	2.7	2.6	2.2	2.0	2.0	1.2
	middle	6.7	2.5	2.6	2.0	2.0	2.0	1.2
	top	7.5	2.5	2.6	2.0	2.1	1.9	1.1
Leaves	bottom	8.0	8.3	7.9	8.0	7.9	8.0	11.0
	middle	7.8	7.9	8.0	8.0	8.1	9	10.0
	top	8.0	8.2	7.9	8.1	7.8	1	10.0

A relationship between storage coefficients of the root cortex and the root storage compartments was not apparent. The storage coefficients decreased with transpiration rate for the BROM5 and BROM3 experiments, but a clear relationship was not found. However, when the ratio of Q_f/Q_b was evaluated as a function of transpiration rate (Figure 14) a relationship was found. This ratio is a measure of storage rate, a higher ratio indicating more rapid storage. A similar transpiration rate dependency was not found with the storage coefficients of stem or leaf compartments (Table 11). These results indicate that the rate of storage was higher at the low transpiration rate. While the number of data points is small, the decreasing rate of storage with increasing rate of transpiration was observed with all experiments where the comparison could be made. Reasons for this relationship are not clear to us at this time. Other reports have suggested that uptake is independent of transpiration rate.

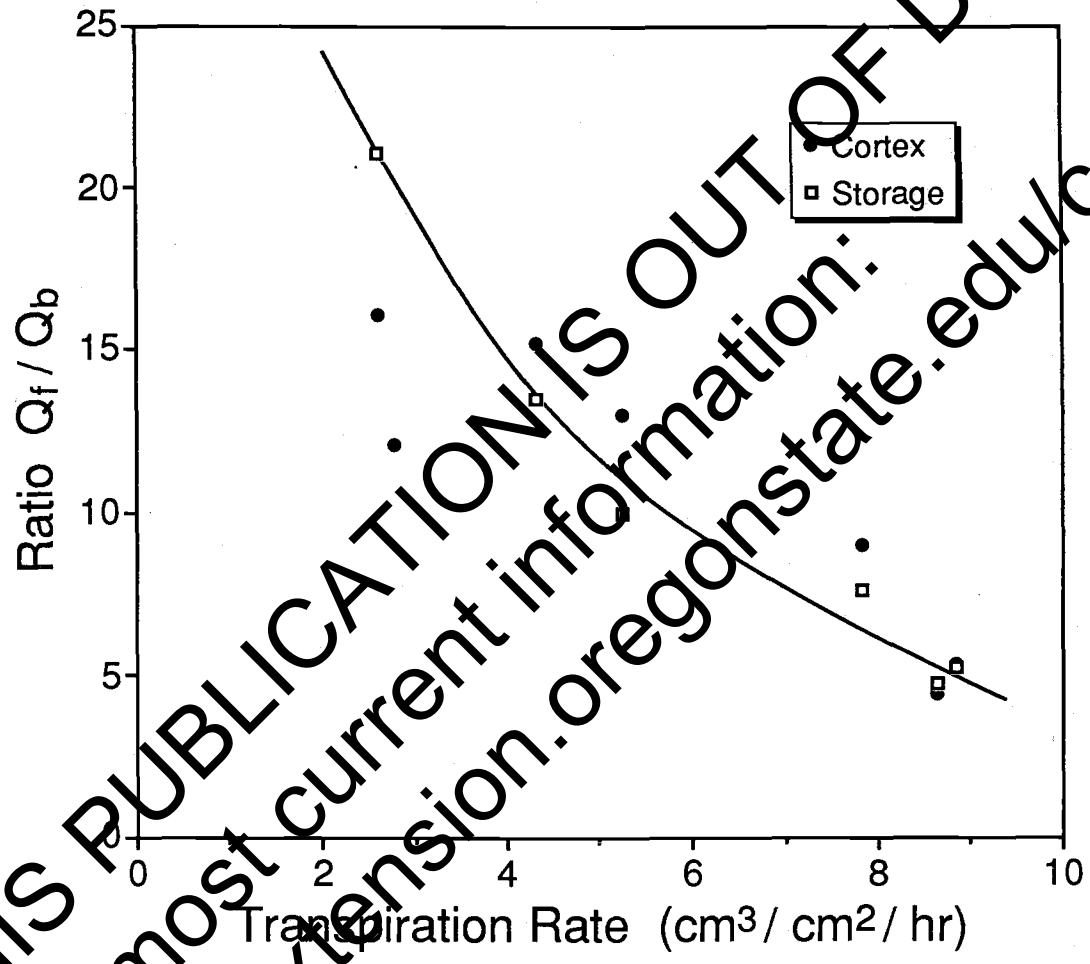

Figure 14. Ratio Q_f/Q_b for the root cortex and for root storage compartments as a function of transpiration rate.

Stems

The relationship between storage coefficients and stem volumes was found to be linear (Figure 15). The same relationship applied to all experiments except BROM5, low transpiration rate. The proportionality in the absence of a transpiration or concentration effect reflects the proportionality of storage with surface area, as was previously discussed.

Leaves

Storage coefficients of leaves were related to leaf volume in an exponential manner (Figure 16). The relationship was the same for BROM5 and BROM3 experiments, but had a higher exponent for the BROM1 experiment. The difference between the BROM1 and the other two experiments may indicate a concentration effect. Storage coefficients did not increase with the increase of concentration from BROM5 to BROM3, but increased about 50 percent by increasing the concentration from BROM3 to BROM1. This concentration effect may result from an affect of bromacil on plant tissue which occurs at the much higher concentrations in the leaf with the BROM1 experiment. This effect was also shown earlier in Figure 6.

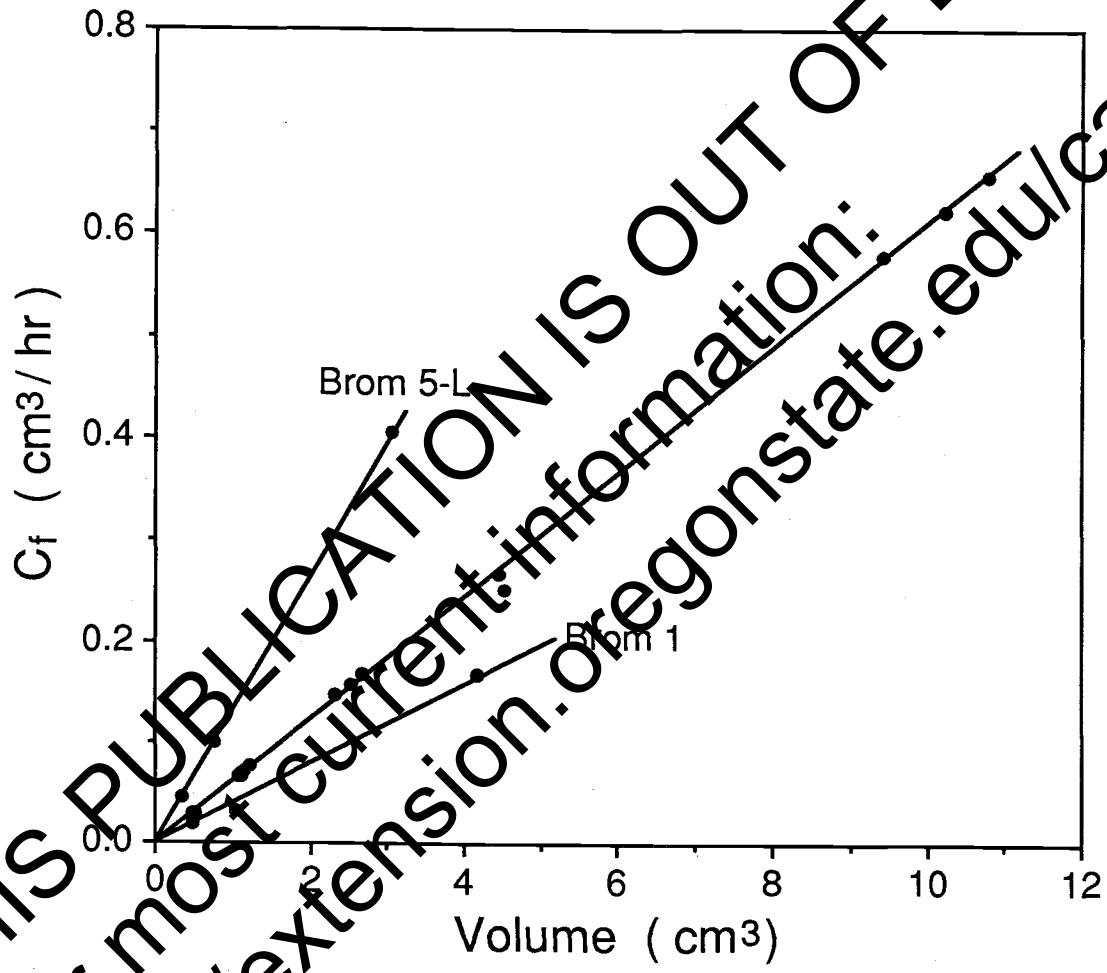

Figure 18. Forward storage coefficients for stem compartments plotted as a function of volumes of stem storage compartments.

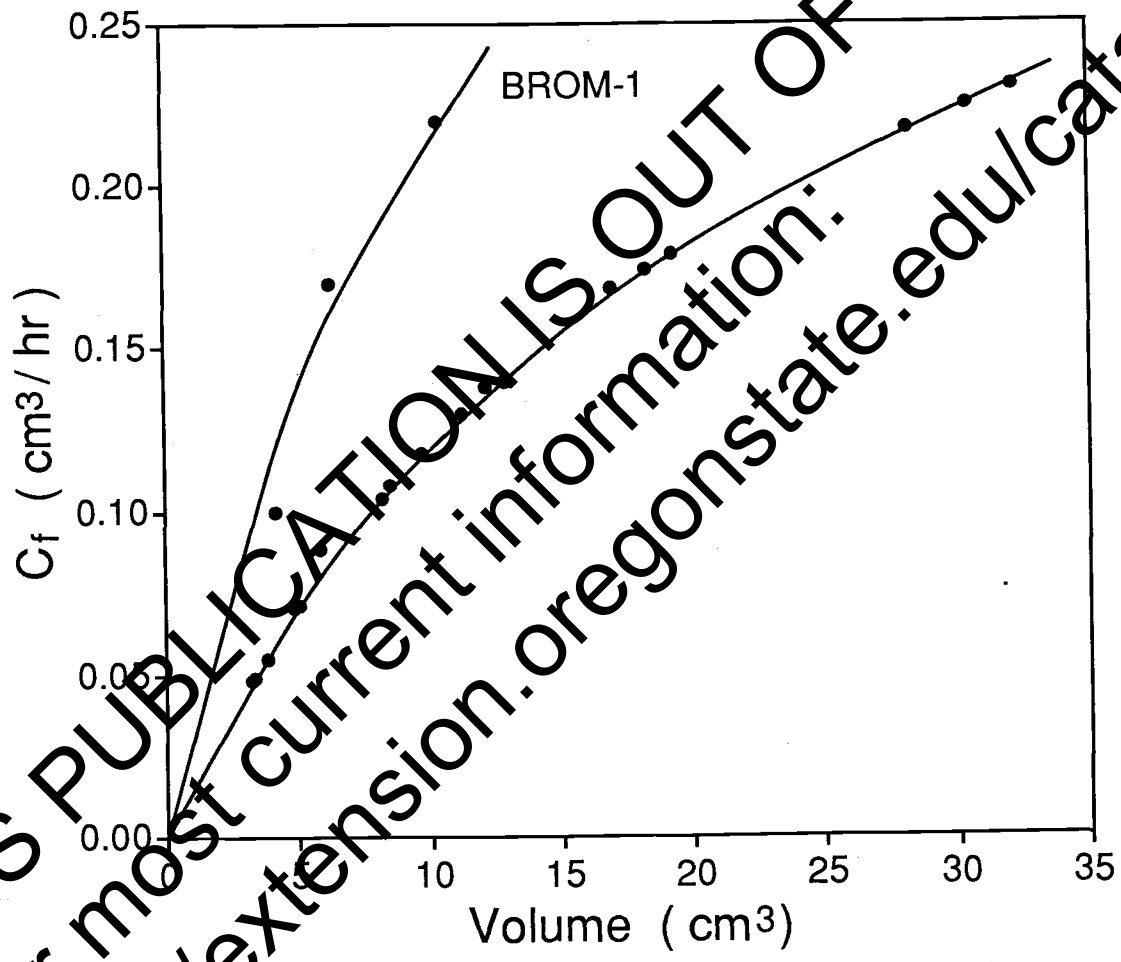

Figure 16. Forward storage coefficients for leaf compartments plotted as a function of volumes of leaf storage compartments.

SENSITIVITY ANALYSIS

Introduction

One of the best methods for choosing the parameters in a sensitivity study of a mathematical model is the factorial design (Box et al., 1978). This "experimental design" is practical when the number of independent parameters is less than or equal to 10. However, UTAB 4.6 contains more than 200 independent parameters. It is therefore not practical to choose a factorial design for varying the parameters. It is also nearly impossible to set up and solve, in closed form, a set of sensitivity equations as described by Bard (1974). For purposes of this report only some of the individual parameters which are important to the uptake, accumulation, and translocation processes were varied. The results of changing these parameters are compared with BROM5 medium transpiration rate as the reference simulation. Nineteen sets of simulations were made. The parameters which were evaluated and their values are in Table 12. Results are shown in Figures 17 through 27.

Transpiration Rate

The transpiration rate used for the reference simulation was that of the BROM5 medium transpiration rate (Table 12). The curves labeled Ref in Figure 17 correspond to this transpiration value. The curve labeled A corresponds to the simulation with the low transpiration rate, while the curve labeled B corresponds to the simulation with the high transpiration rate. Simulations show an increase in concentration in all three plant parts as a result of increasing the transpiration rate and a decrease in all three plant parts as a result of decreasing the transpiration rates. On a relative basis, the effect of increasing

Table 12. Values of parameters used in the sensitivity simulations. The data base for BROM5 medium transpiration rate was the reference level for these simulations.

Parameter changed	Curve	Values used
Transpiration rate	Ref	BROM5 Med Trans (2.61 x 10^{-3} cm^3/cm^2 hr)
	A	BROM5 Low Trans (7.82 x 10^{-4} cm^3/cm^2 hr)
	B	BROM5 High Trans (8.85 x 10^{-3} cm^3/cm^2 hr)
Ratio (phloem/xylem)	Ref	f_1=0.3, f_2=0.2, f_3=0.1
	A	f_1=0.15, f_2=0.15, f_3=0.1
	B	f_1=0, f_2=0, f_3=0
Diffusion coefficient across Casparian strip	Ref	DIFFU[1] = 1.8 x $.10^{-7}$ cm^2/hr
	A	DIFFU[1] = 1.8 x 10^{-6} Gm^2/hr
	B	DIFFU[1] = 1.8 x 10^{-6} Gm^2/hr
Reflection coefficient for Casparian strip	Ref	SIGMA[1] = 0.0
	A	SIGMA[1] = 0.2
	B	SIGMA[1] = 0.7
Reflection coefficient of leaf membrane separating phloem and xylem	Ref	SIGMA[10;14;18] = 0.0
	A	SIGMA[10;14;18] = 0.2
	B	SIGMA[10;14;18] = 0.7
Constant (Q_f/Q_b) ratio	Ref	All Q_f's and Q_b's as in Table 8
	A	All Q_f's and Q_b's ÷ by 2
	B	All Q_f's and Q_b's times 2
Variable (Q_f/Q_b) ratio	Ref	All Q_f's and Q_b's as in Table 8
	A	All Q_f's and Q_b's ÷ by 2
	B	All Q_f's and Q_b's times 2
Sorption Coefficients in root compartments	Ref	All B's = 0.0
	A	B(1)=B(3)=0.5
	B	B(1)=B(3)=1.0
First-order loss rates	Ref	All λ's = 0.0 (1/hr)
	A	λ_{15}=0.0016, λ_{18}=0.00175, λ_{21}=0.0018
	B	λ_{15}=0.0032, λ_{18}=0.0035, λ_{21}=0.0036
	C	λ_{15}=0.0064, λ_{18}=0.0070, λ_{21}=0.0072

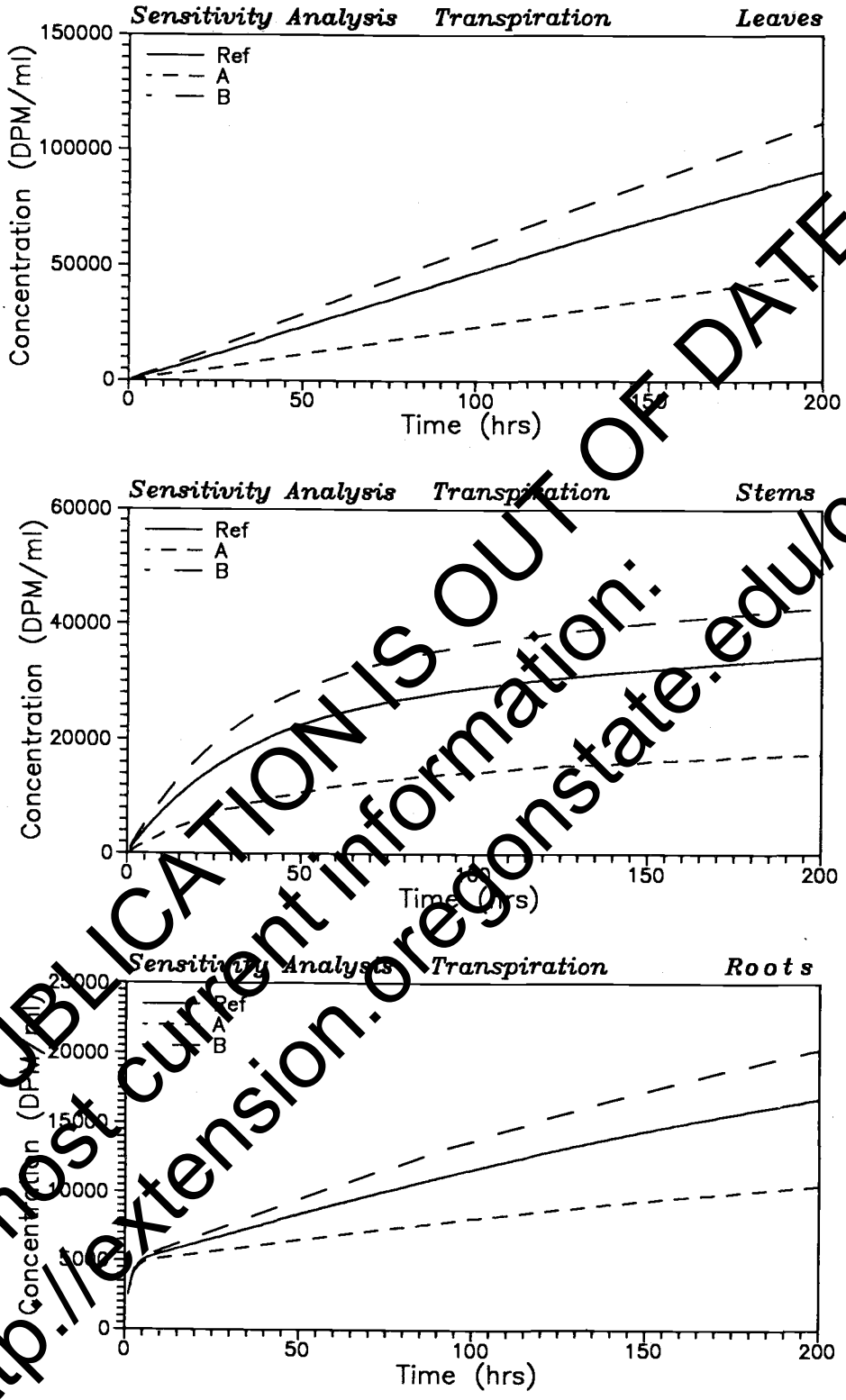

Figure 17. Simulations showing the effect of changing the transpiration rate. Reference simulation was with BROM5 medium transpiration rate, Tr = 5.67 cm^3/hr. Comparisons are with low transpiration rate Tr = 2.00 cm^3/hr (curves A) and high transpiration rate, Tr = 7.80 cm^3/hr (curves B).

the transpiration rate was much smaller than the effect of decreasing the transpiration rate. The decrease in the transpiration rate by 67 percent decreased the concentration at 200 hours in the leaves (curve A) from 1.57×10^6 to 8.09×10^5 dpm/gm, in the stems from 2.23×10^5 to 1.14×10^5 dpm/gm, and in the roots from 5.21×10^5 to 3.26×10^5 dpm/gm. On the other hand, increasing the transpiration rate by 13 percent (curve B) produced a corresponding increase in the concentrations of the three plant regions. The increases in concentrations were from 1.57×10^6 to 1.93×10^6 dpm/g in the leaves, from 2.23×10^5 to 2.78×10^5 dpm/g in the stems, and from 5.21×10^5 to 6.31×10^5 dpm/g in the roots. These simulations show that the effects of increasing transpiration rates are not linear. The increase in concentrations diminishes as concentrations become higher.

Ratio: Phloem Transport Rate/Xylem Transport Rate

The ratio (phloem transport rate/xylem transport rate) is a measure of the mobility of the chemical in the plant. A higher ratio means that chemical accumulating in the leaves readily enters the phloem pathway through which it is transported back to the roots. The expectation is that a low ratio increases the concentrations in the leaves and decrease concentrations in stems and roots, whereas a high ratio decreases the concentrations in the leaves and increases concentrations in stems and roots. Results agreed with these expectations (Figure 18). Simulation with the ratios equal to zero (curve A), i.e. no phloem transport, showed the expected increase in concentrations in the leaves and decrease in stems and roots. The decrease in concentrations in stems and roots were large, namely from 2.23×10^5 to $5.12 \times$

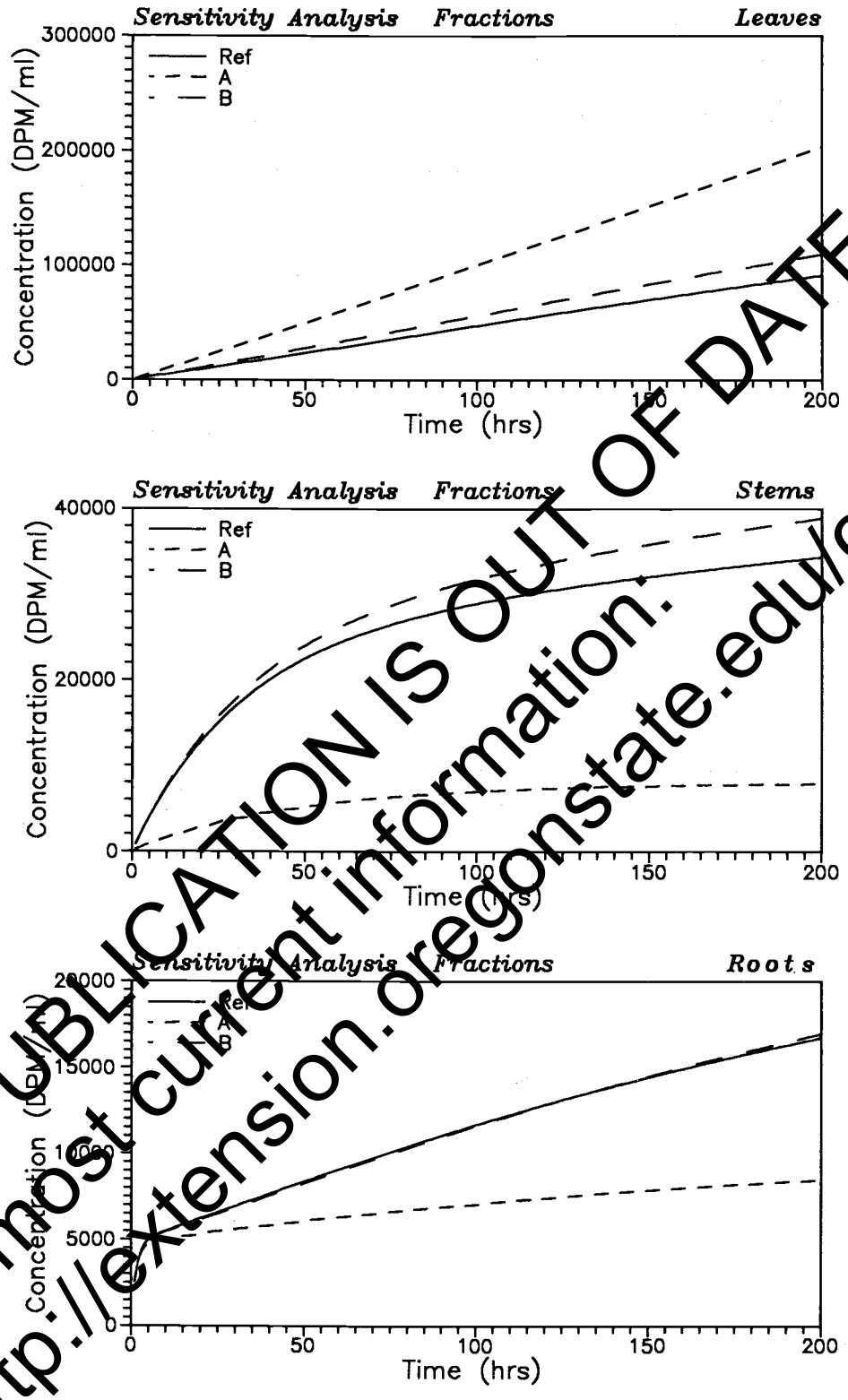

Figure 18. Simulations showing the effects of changing the ratios of phloem transport rate divided by xylem transport rate. Reference simulation was with the fractions set to f_1 = 0.3; f_2 = 0.2, f_3 = 0.1. Simulation A: f_1 = 0.0; f_2 = 0.0, f_3 = 0.0, and Simulation B: f_1 = 0.15; f_2 = 0.15, and f_3 = 0.1.

10^4 dpm/g in the stems and from 5.21 x 10^5 to 2.63 x 10^5 dpm/g in the roots. The increase in the leaves was dramatic, namely from 1.57 x 10^6 to 3.52 x 10^6 dpm/g. Simulation with the phloem/xylem ratio greater than zero showed the expected increase in the stems, namely from 2.23 x 10^5 to 2.52 x 10^5 dpm/g, but there was no change in the concentrations in the roots when compared with the reference simulation. Concentration in the leaves were lowest with the reference simulation. The fact that for ratios greater than 0.1 the concentration in the roots did not respond to the further increases indicates that this process is no longer a rate-limiting process. Compound is being recycled sufficiently fast so that storage is the rate limiting process. The small increase in concentrations in the leaves relative to the reference curve, namely from 1.57 x 10^6 to 1.80 x 10^6 dpm/g, is attributed to the fact that the slower recycling results in a longer residence time in the leaves which therefore increases the leaf storage of bromacil.

Diffusion Coefficient of the Casparian Strip

For this simulation the diffusion coefficient of the Casparian strip was changed. This coefficient determines the rate at which diffusion across the Casparian strip can occur. The value of this coefficient is important with respect to diffusion from the root xylem and phloem compartments back to the root cortex. The role played by this coefficient can be learned from the mass balance equations, specifically equations (9) and (21). The expectation was that a decrease in the diffusion coefficient would increase the amount of chemical in the plant and therefore increase the concentrations in all compartments. Similarly, an increase in the diffusion coefficient at the

Casparian strip was expected to decrease the total amount of chemical in the plant and therefore produce a decrease in the concentrations in all plant compartments. These expectations were borne out by the simulations shown in Figure 19. The effects were not linear, however. The effect of increasing the diffusion coefficient by a factor of 10 was somewhat larger than that of decreasing it by the same factor. Increasing the coefficient decreased the concentrations at 200 hours in the leaves from 1.57×10^6 to 1.18×10^6 dpm/gm, in the stems from 2.23×10^5 to 1.60×10^5 dpm/gm, and in the roots from 5.21×10^5 to 4.25×10^5 dpm/gm. Increasing the diffusion coefficient increased the concentrations in the leaves from 1.57×10^6 to 2.33×10^6 dpm/gm, in the stems from 2.23×10^5 to 3.54×10^5 dpm/gm, and in the roots from 5.21×10^5 to 7.07×10^5 dpm/gm.

Reflection Coefficient of the Casparian Strip

The reflection coefficient is a measure of the ease of passing across the Casparian strip. A reflection coefficient equal to zero allows the chemical to pass unimpeded, a reflection coefficient equal to one does not allow any chemical to pass this barrier. All plant parts were expected to be influenced equally by changes in the reflection coefficient of the Casparian strip. This expectation was confirmed by the results (Figure 20). With the reflection coefficient equal to 0.3, concentrations in leaves decreased from 1.57×10^6 to 1.49×10^6 dpm/gm, in the stems from 2.23×10^5 to 2.01×10^5 dpm/gm, and in the roots from 5.21×10^5 to 4.83×10^5 dpm/gm. Setting the reflection equal to 0.7 further decreased concentrations, namely from 1.57×10^6 to 1.03×10^6 dpm/gm in the leaves, from 2.23×10^5 to

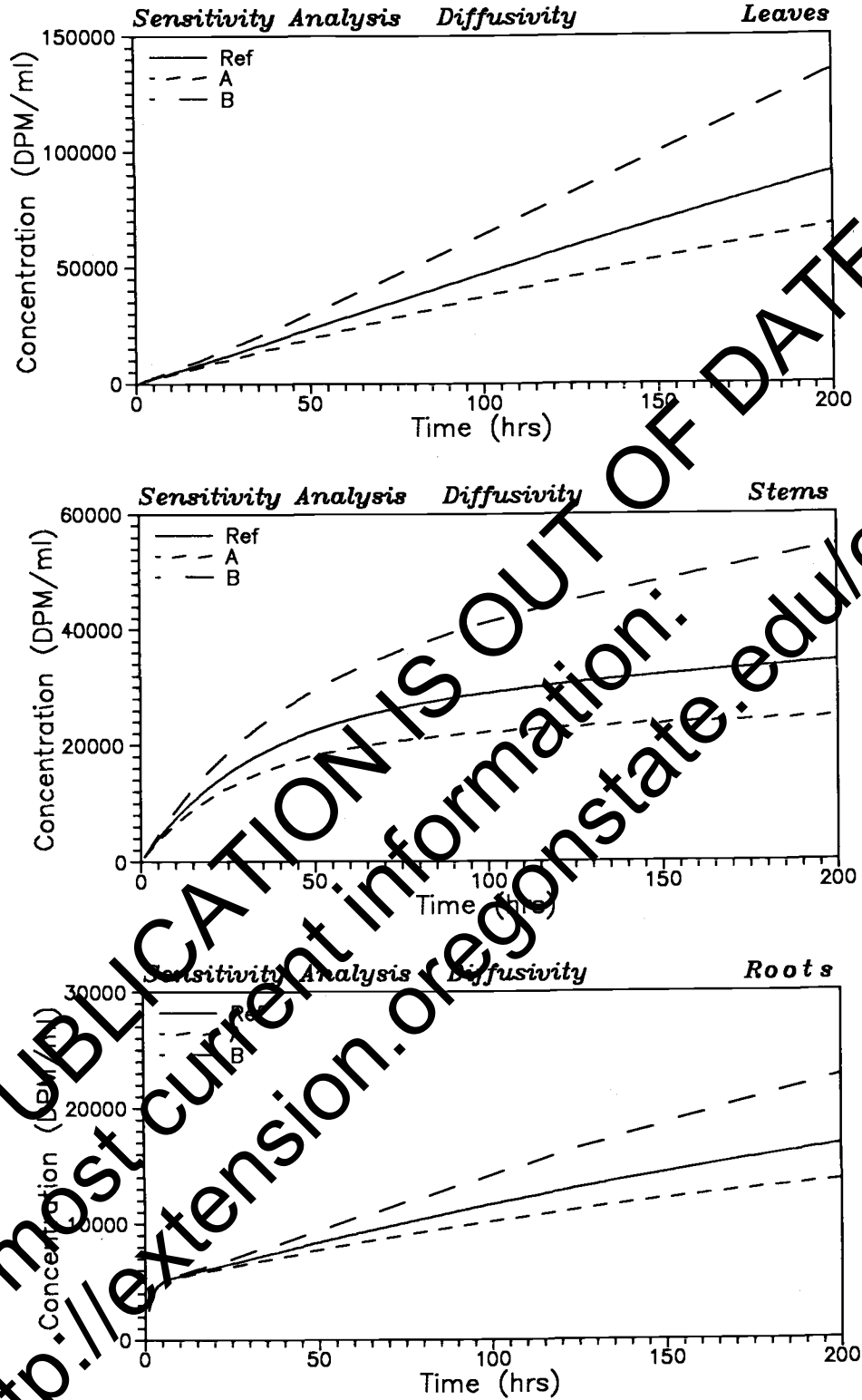

Figure 19. Simulations showing the effects of changing the diffusion coefficient of the boundary representing the Casparian strip. Reference simulation was with D = 1.8 x 0.10^{-7} cm^2/hr. Simulation A: D = 1.8 x 10^{-6} cm^2/hr, simulation B: D = 1.8 x 10^{-8} cm^2/hr.

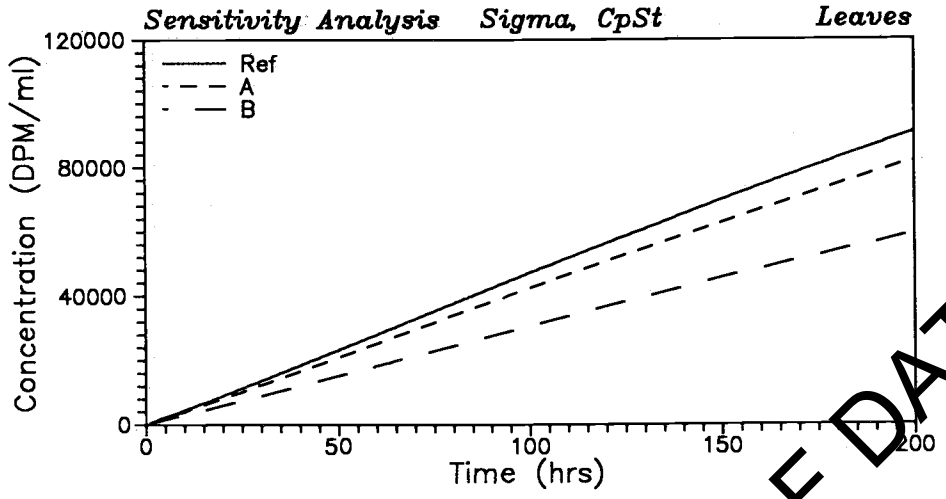

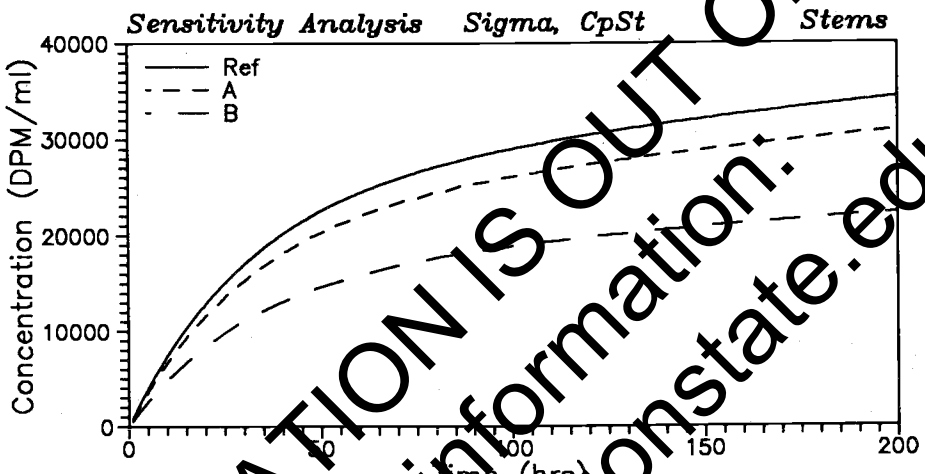

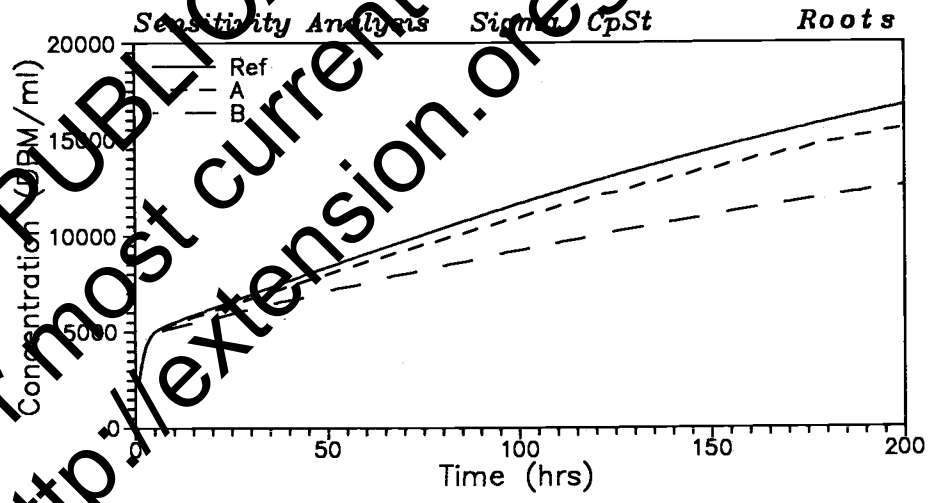

Figure 20. Simulation showing effects of changing the reflection coefficient of the boundary representing the Casparian strip. Reference simulation was with $\sigma = 0.0$. Simulation A: $\alpha = 0.2$; simulation B: $\sigma = 0.7$.

1.46 x 10^5 dpm/gm in the stems, and from 5.21 x 10^5 to 3.91 x 10^5 dpm/gm in the roots.

Reflection Coefficients in the Leaf Membranes Separating Xylem and Phloem Pathway

The reflection coefficient of the membrane separating xylem and phloem pathways is a measure of the ease with which the chemical can enter the phloem pathway. An increase in this reflection coefficient in the leaves was expected to increase concentrations in the leaf despite the "choking-off" effect an increasing σ has. The concentrations in the leaf xylem increased under these conditions, thereby driving more compound into storage. Concentration in stems and roots were expected to decrease as the entry into the phloem system was decreased by the increasing reflection coefficients. These expectations were confirmed by the simulations. Figure 21 shows that concentrations increased in the leaves and decreased in stems and roots. Changes from the reference level with the reflection coefficient equal to zero to the simulation with σ = 0.2 were small. A larger change occurred with the reflection coefficient σ = 0.7. With these simulations the total amount of chemical in the plant was the same so that increases in leaf concentrations corresponded to decreases in stem and root concentrations.

Storage Coefficients

The role played by the storage and mobilization coefficients was discussed in detail in the text of this report. The values of the storage coefficients, Q_f's, and the mobilization coefficients, Q_b's,

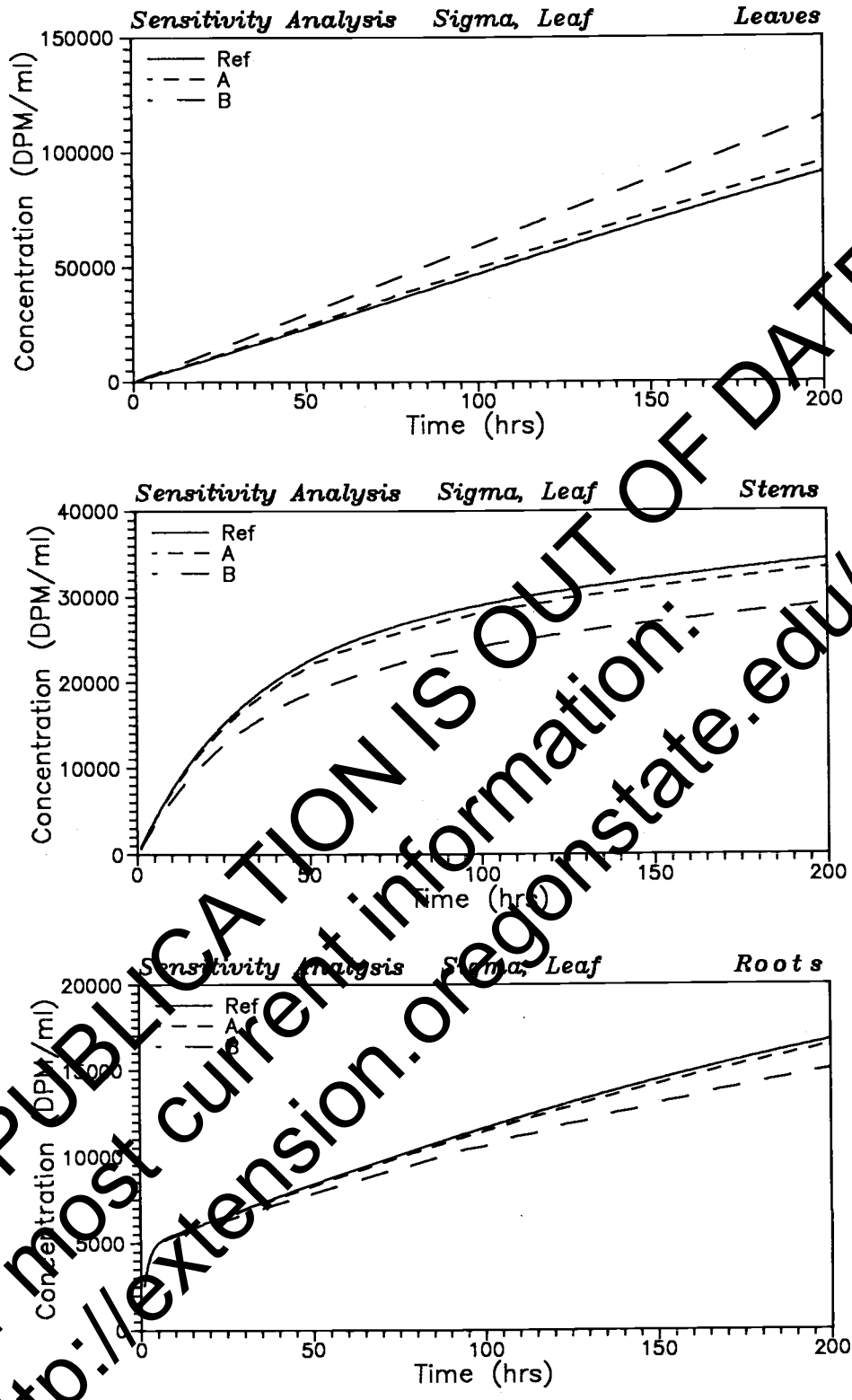

Figure 21. Simulations showing the effects of changing the reflection coefficients of the membranes in the leaves which separate phloem from xylem (σ_{10}, σ_{14}, and σ_{18}). Reference simulation was with the three coefficients equal to zero. Simulation A, σ's equal to 0.2; Simulation B, σ's equal to 0.7.

were increased by a factor of 2 (curves B) in one simulation and decreased by a factor of 2 (curves A) in the second simulation. With these changes the ratios Q_f/Q_b remained the same. Figure 22 shows that the simultaneous increase of Q_f's and Q_b's by a factor of 2 increased the concentrations in leaves, while decreasing concentrations in the stems and increasing concentrations in the roots. The increases in the leaves was from 1.57×10^6 to 2.07×10^6 dpm/gm, the decrease in the stems was from 2.23×10^5 to 1.94×10^5 dpm/gm, and the increase in the roots was from 5.21×10^5 to 5.45×10^5 dpm/gm. The ratio (Q_f/Q_b) of the leaves was higher than for the other two plant parts, so that an increase by a factor of 2 resulted in increased storage. Since more of the chemical taken up by the plant was stored in the leaves, less remained available for storage in stems and roots. In the competition for chemical to be stored, the stems were the most strongly effected, with little change in the roots.

When values of (Q_f/Q_b) were decreased by a factor of 2, uptake in the leaf decreased, as did the uptake in the roots; however, uptake by the stems increased. The simulation resulted in a lower concentrations in the leaves, as expected. Reasons for the increases in stems and decreases in roots are not clear. Since the ratios were not changed the final concentrations at very long time values are the same for all simulations. However, the rate at which equilibrium concentrations are achieved depends on the ratio (Q_f/Q_b).

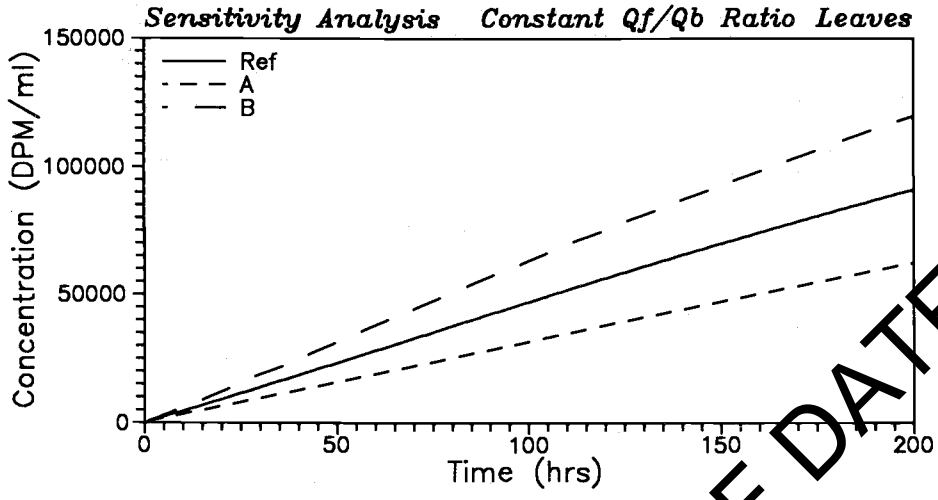

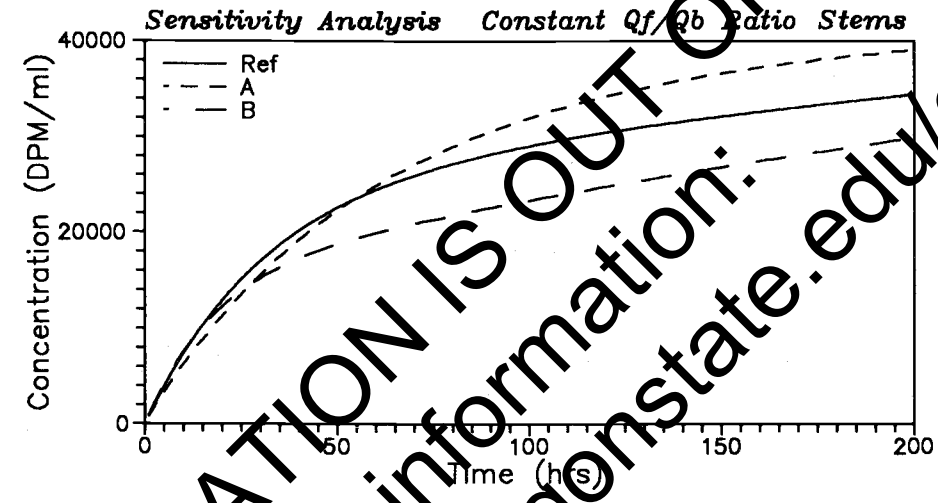

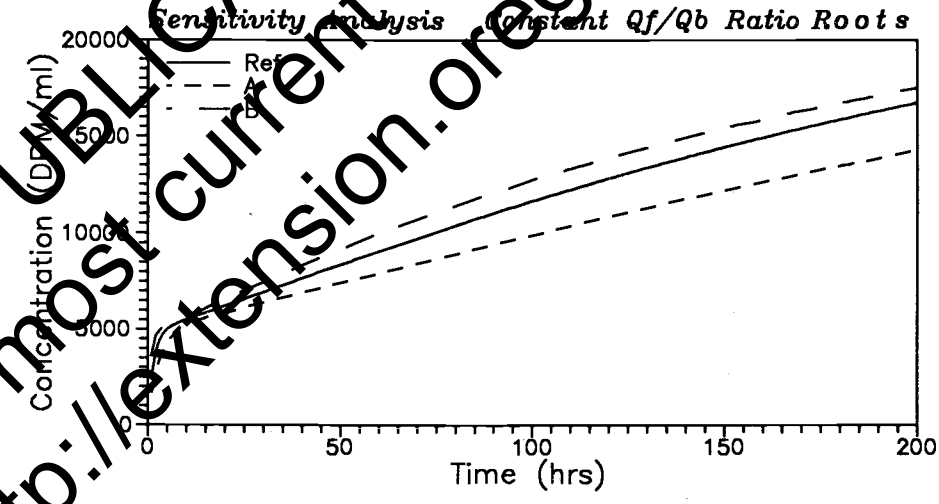

Figure 22. Simulations showing the effect of increasing or decreasing values of the forward (Q_b) and backward (Q_b) coefficients while maintaining the same ratio Q_f/Q_b. The reference simulation was with all Q_f's and Q_b's as in Table 8. For Simulation A, all coefficients were divided by two; for Simulation B, all storage coefficients were multiplied by two.

Change in the Ratio Q_f/Q_b

When the ratio Q_f/Q_b was changed, equilibrium concentrations, as well as rates of approach to equilibrium, changed in each plant part. With the ratio increased by a factor of 2 (curves B), storage increased and the increases were similar for all three plant parts. Figure 23 shows that the increases were from 1.57×10^6 to 2.18×10^6 dpm/gm for leaves, from 2.23×10^5 to 3.00×10^5 dpm/gm for stems, and from 5.21×10^5 to 7.78×10^5 dpm/gm for roots. Concentrations decreased in all plant parts by decreasing the Q_f/Q_b (curves A) ratios, and the decreases were about the same for each plant part. The decreases were from 1.57×10^6 to 1.00×10^6 dpm/gm for leaves, from 2.23×10^5 to 1.46×10^5 dpm/gm for stems, and from 5.21×10^5 to 3.23×10^5 dpm/gm for roots.

Sorption Coefficients in the Root Storage Compartments

The sorption coefficients allow linear equilibrium sorption to occur. The effect is equivalent to that of increasing the volume of a compartment in which sorption occurs. Figure 24 shows simulations with the sorption coefficients of the root storage compartments set equal to 0.5 and 1.0. Results (Figure 24) indicate that these changes did not change the concentrations of the leaves and stems, but concentrations in the root compartments increased, as was expected. The increase was from 5.21×10^5 to 6.47×10^5 dpm/gm for $B_1 = B_3 = 0.5$, and from 5.21×10^5 to 7.50×10^5 dpm/gm for $B_1 = B_3 = 1.0$.

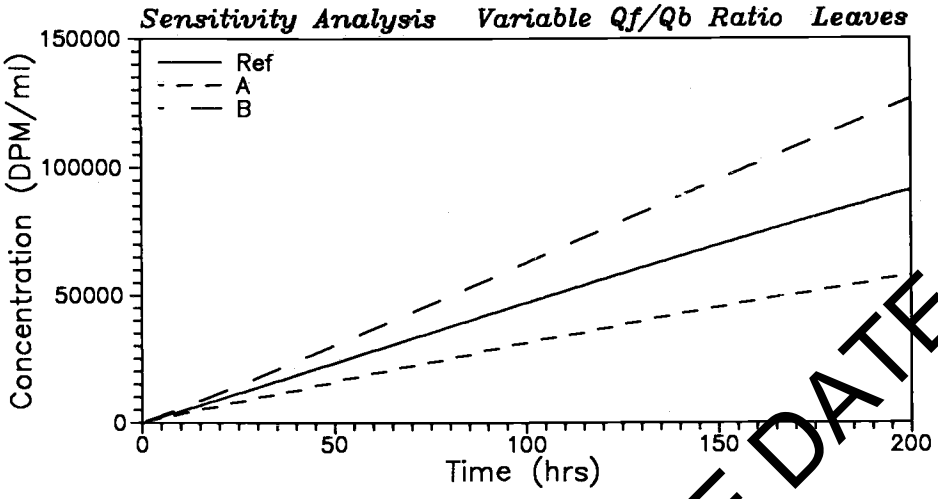

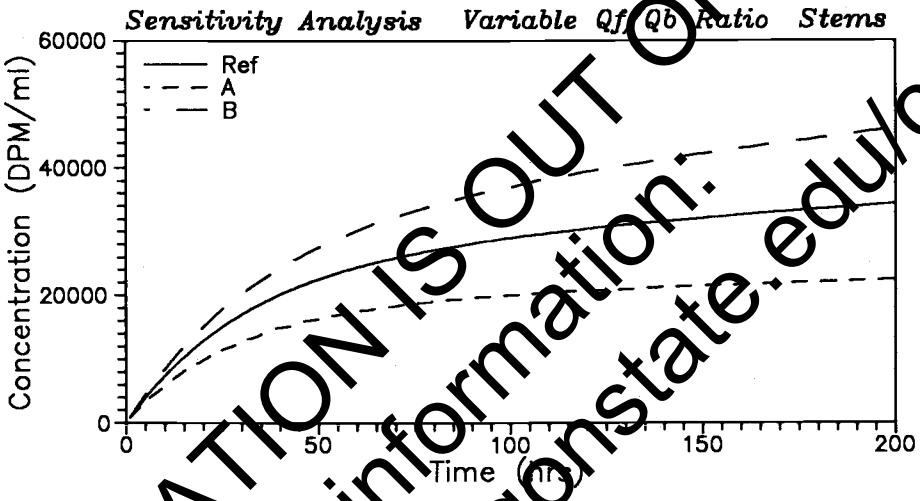

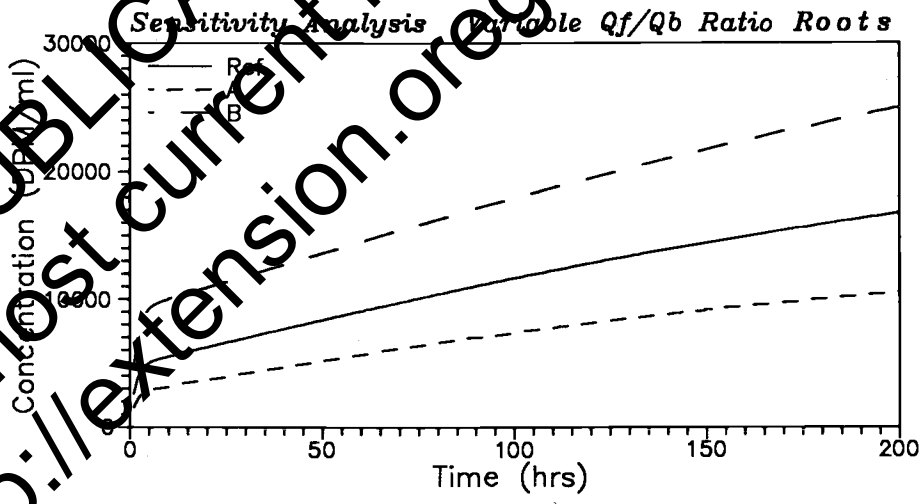

Figure 28. Simulations showing the effects of changing the ratios of forward storage coefficients to the backward storage coefficients. Reference simulation was with all storage coefficients as shown in Table 8. For Simulation A, all forward storage coefficients (Q_f) were divided by two while leaving the Q_b the same; for Simulation B, all forward storage coefficients were multiplied by two, while leaving the Q_b's the same.

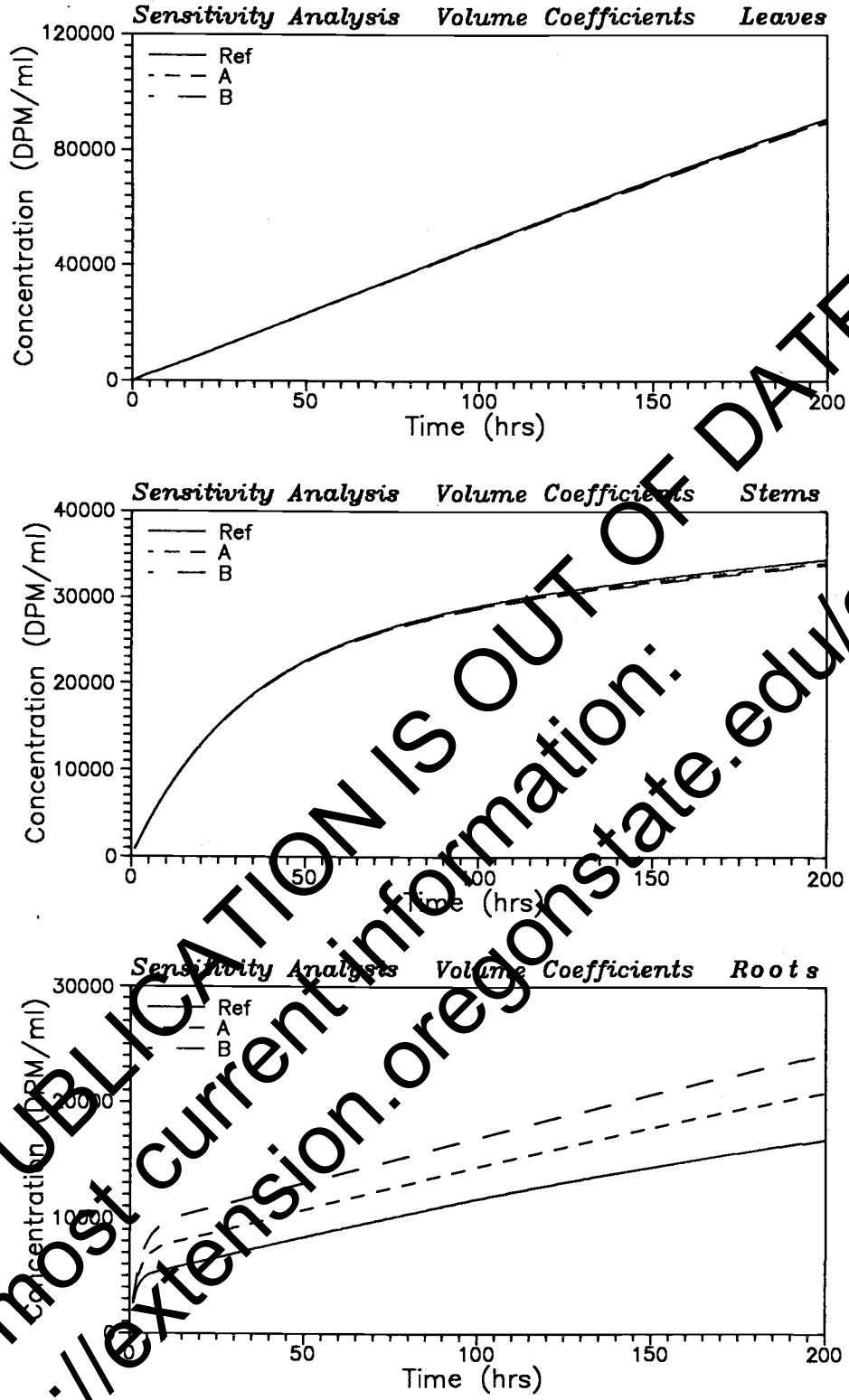

Figure 2[illegible]. Simulations showing the effects of changing the sorption coefficients (B's) in the root compartments. These coefficients immobilize chemical so that the coefficient has an effect that is similar to that of increasing or decreasing the volume of the compartment. Reference simulation was with values of the sorption coefficients B = 0. Simulation A, sorption coefficients of the two root compartments, $B_1 = B_3 = 0.5$; Simulation B, sorption coefficient of the two root compartments, $B_1 = B_3 = 1.0$.

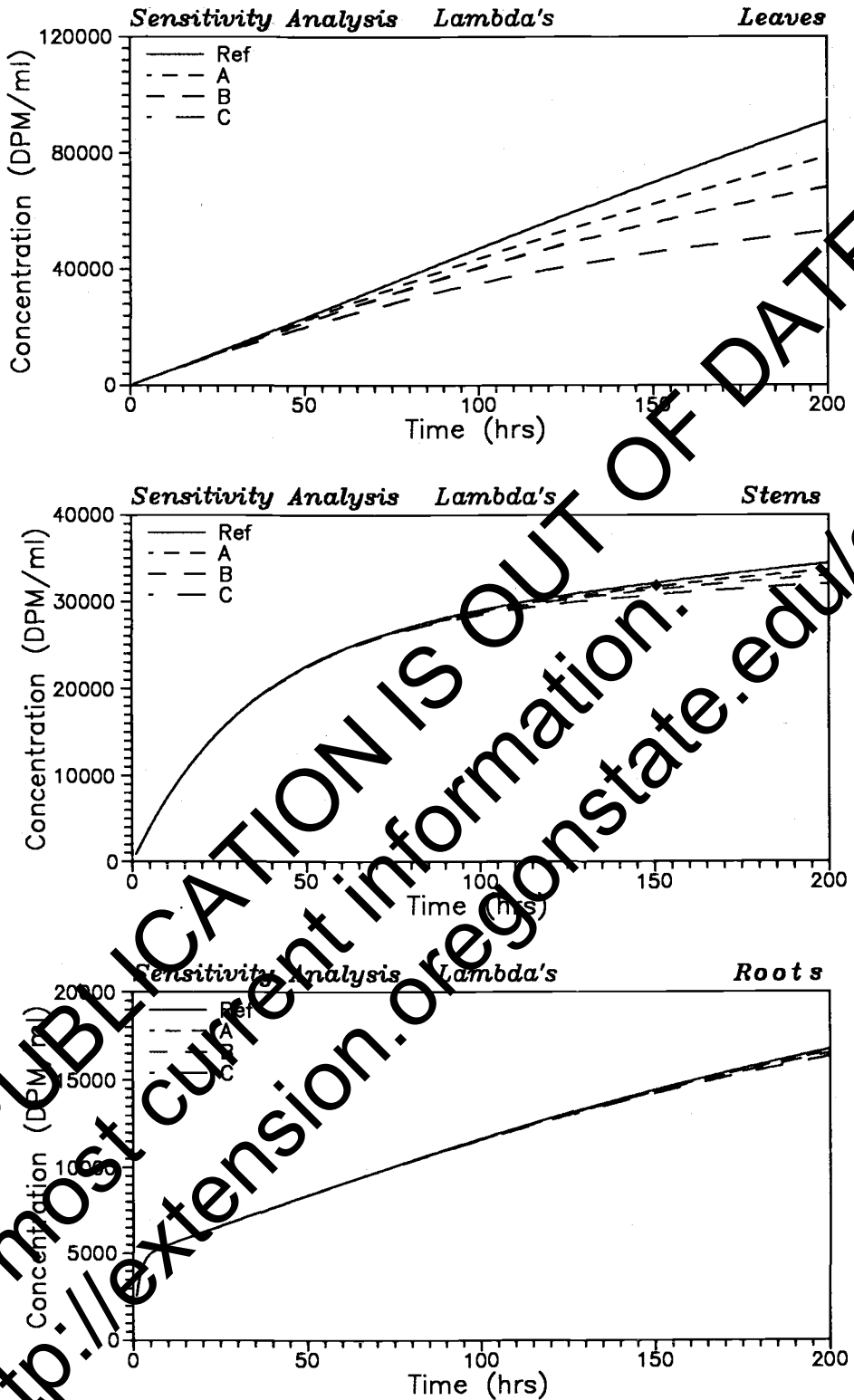

Figure 25. Simulations showing effects of changing the rates of first-order loss (λ) in the leaves. Reference simulation was with all λ's equal to zero. Simulation A: $\lambda_{15} = 0.0016$, $\lambda_{18} = 0.00175$, $\lambda_{21} = 0.0018$; simulation B: $\lambda_{15} = 0.0032$, $\lambda_{18} = 0.0035$, $\lambda_{21} = 0.0036$; simulation C: $\lambda_{15} = 0.0064$, $\lambda_{18} = 0.0070$, $\lambda_{21} = 0.0072$.

Rate of First Order Losses

This simulation shows the result of allowing first-order loss processes to operate. In the reference simulation, the rate of first-order loss were zero in all compartments. For the simulation shown in Figure 25, values of the coefficient, λ, were as shown in Table 12. Appendix I, equations (15), (18), and (21), indicate the role played by this coefficient. The effects were most pronounced in the leaves, which was expected since values were not changed in stem and root compartments. An increase in the value of λ has the effect of decreasing the concentration. As there is less and less chemical available in the leaves, the redistribution of the chemical by the phloem pathway is affected so that, increasingly, the concentration in the stem compartments shows a decrease. Concentrations in the root compartments started to show a decrease as well.

Combined Effects

In conclusion of the limited set of sensitivity simulations, two simulations were done in which several parameters were changed from the reference data set at the same time. The sets of parameters for each of these two simulations are in Table 13. Results are in Figures 26 and 27. The simulation in Figure 26 is labelled "combined high" and the simulation in Figure 27 is labelled "combined low." This terminology derived from the high concentrations with the simulation in Figure 27 and the low concentrations with the simulations in Figure 27.

The most influential parameter in these simulations was clearly the diffusion coefficient at the Casparian strip. The diffusion coefficient of the simulation labelled "combined high" was the lower of the two

simulations and that was two orders of magnitude lower than with the simulation referred to as "combined low." The diffusion coefficient at the Casparian strip determines the rate of diffusion back to the bathing solution of the root medium. With the high diffusion coefficient, the rate of backward diffusion was high. This rate increased as the concentration of the nutrient solution decreased. The concentrations in all three plant parts approached a steady state with the "combined low" simulation, whereas the concentrations of the reference simulation and the "combined high" simulation continued to increase. The lower rate of increase in the concentrations with the "combined low" simulations was also in part caused by high value of first-order loss rate in the leaves. The high concentrations in the roots with the "combined high" simulations derived in part from high value of the sorption coefficients in the root compartments. The very low concentration in the stems of the "combined low" simulations resulted from the very low value of the phloem/xylem transport rate and the high reflection coefficient at the root surface.

Table 13. Values of the parameters used for simulations in which several parameters were changed for an evaluation of combined effects.

Parameter	Value of parameters	
	Simulation in Fig. 26	Simulation in Fig. 27
Transpiration ($cm^3/cm^2/hr$)	$Tr = 8.85 \times 10^{-3}$	$Tr = 7.82 \times 10^{-3}$
Phloem/xylem transport rate	f_1=0.30; f_2=0.20; f=0.10	$f_1=f_2=f_3$=0.0
Diffusion coefficient (cm^2/hr)	$D_1 = 1.8 \times 10^{-8}$	1.8×10^{-6}
Reflection coefficient, root	$\sigma_1 = 0.2$	$\sigma_1 = 0.7$
Reflection coefficient, leaf	$\sigma_{10}=\sigma_{14}=\sigma_{18}=0.7$	$\sigma_{10}=\sigma_{14}=\sigma_{18}=0.2$
Ratio: Q_f/Q_b	Q_f/Q_b = 2 times reference	Q_f/Q_b=0.50 times reference
Sorption coefficient, root	$B_1 = B_3 = 1.0$	$B_1 = B_3 = 0.5$
First order loss rate, leaves	$\lambda_{15} = 0.00160$ $\lambda_{18} = 0.00175$ $\lambda_{21} = 0.00180$	$\lambda_{15} = 0.00640$ $\lambda_{18} = 0.00700$ $\lambda_{21} = 0.00720$

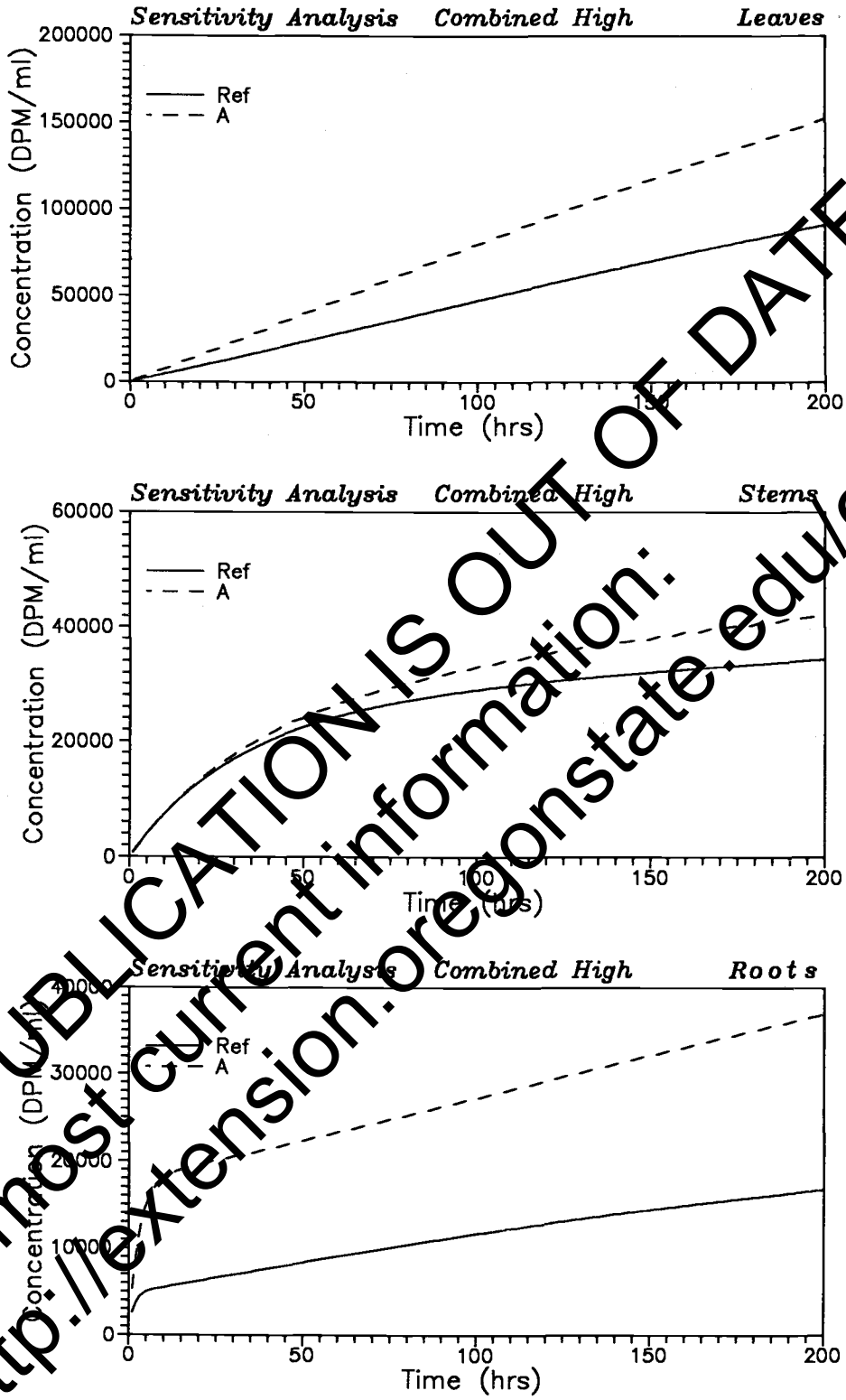

Figure 26. Simulations showing the combined effects of changing several parameters at the same time. Reference simulation was with data set for BROM5 medium transportation rate (Table 8). Values of parameters used for this simulation are in Table 13.

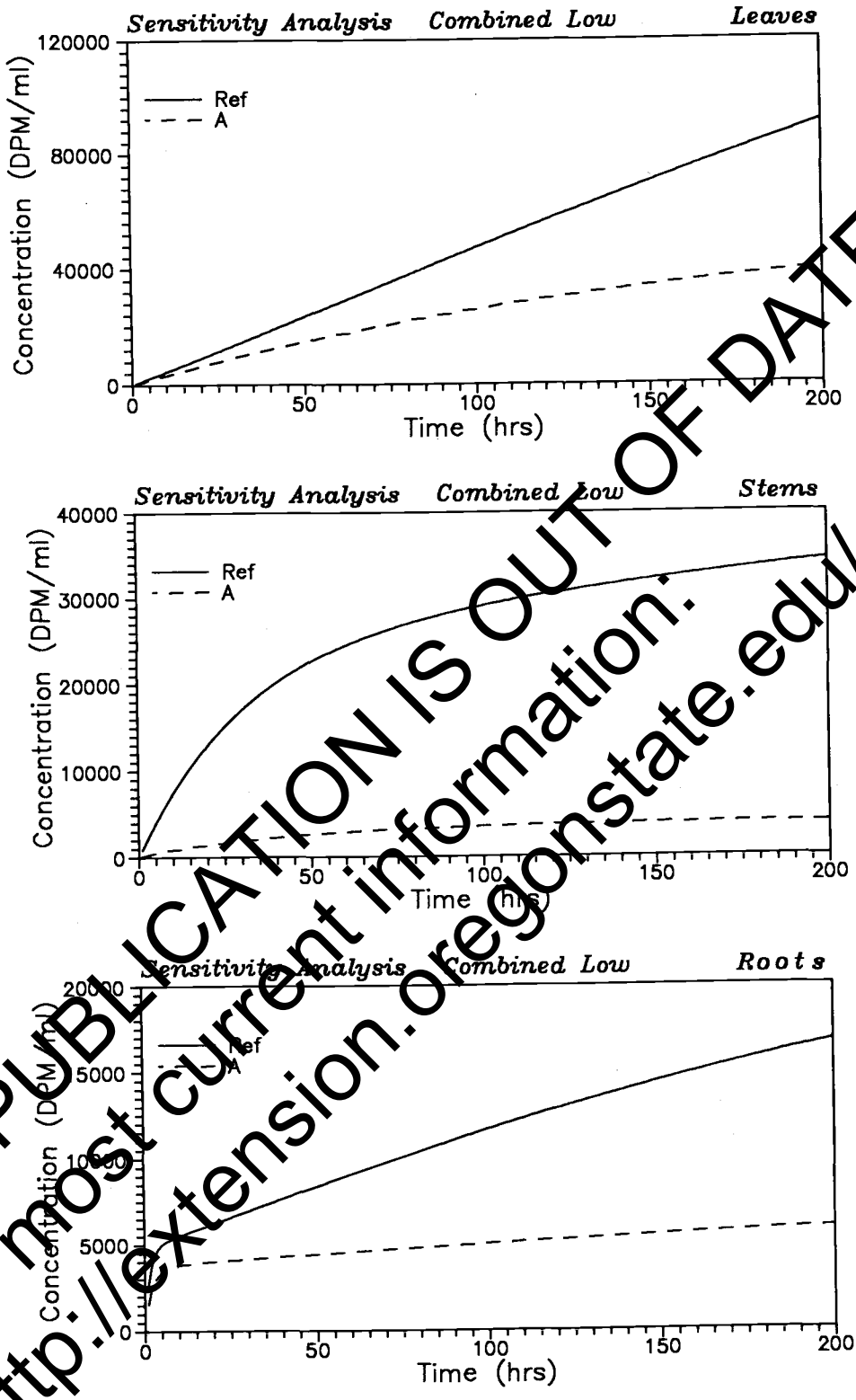

Figure 27. Simulation showing the combined effects of changing several parameters. Reference simulation was with data set for BROM5 medium transpiration rate (Table 8). Values of parameters used for this simulation are in Table 13.

CONCLUSIONS

The model satisfactorily predicted the observed uptake and distribution patterns for bromacil in soybean plants at the stage of growth and under the environmental conditions used in the experiments involving a range of transpiration rates. This indicates that the model provides an accurate representation of uptake and the influence of transpiration rate on the uptake and translocation of this chemical. Parameter values used in the model for compartment size were selected from literature and experimental observation. They functioned well in these simulations and they are appropriately applied in the model. The chemical parameters for storage, mobilization, and diffusion when used in the model also yielded satisfactory results, suggesting that they are also appropriately applied. Finally, the calibration, although of limited scope, showed that the model equations yielded an accurate picture of the actual UTAB patterns for bromacil in soybeans used in these experiments. The theoretical exercise of compiling the model is shown to be a constructive step in learning how to predict the fate of xenobiotic contamination in plants.

The model shows excellent promise for future use. However, additional testing and validation are needed. Mathematical models can be used productively in combination with experimental results to obtain values of the unknown coefficients. Unfortunately, the parameters which characterize compartments usually cannot be estimated uniquely from "pulsed" or "wash-out" type of experimental data when the number of compartments exceeds two (Godfrey and diSteffano, 1987). When using large system models for determination of unknown coefficients, experiments must be carefully designed so that input/output information

(variables) can be measured over time for fixed environmental conditions. The input/output information so obtained would best be used in an optimization scheme based on a nonlinear least squares or minimum residual square error criterion to identify as many as possible of the characterizing parameters. An optimization scheme could not be used here because the data set was of the "lumped" type. Data requirements must be firmly kept in mind when contemplating use of models.

LITERATURE CITED

Bard, Y. 1974. Nonlinear Parameter Estimation. Academic Press, New York. 341 pp.

Berry, W. L. 1978. Nutrition, containers, and media. In: R. W. Langhans, ed., A Growth Chamber Manual, Environmental Control for Plants. Cornell University Press, Ithaca, NY. pp. 117-135.

Boersma, L., F. T. Lindstrom, C. McFarlane, and E. L. McCoy. 1988a. Model of coupled transport of water and solutes in plants. Spec. Report No. 818. Agric. Exp. Sta., Oregon State Univ., Corvallis. 109 p.

Boersma, L., F. T. Lindstrom, C. McFarlane, and E. L. McCoy. 1988b. Uptake of organic chemicals by plants: A theoretical model. Soil Science 146:403-417.

Boersma, L., F. T. Lindstrom, C. McFarlane, and K. P. Suen. 1988c. User Guide: Uptake and transport of chemical by plants; thee leaf model. Spec. Report No. 819. Agric. Exp. Sta., Oregon State Univ., Corvallis. 19 p.

Box, G. E. P., W. G. Hunter, and J. S. Hunter. 1978. Statistics for Experiments: An Introduction to Design, Data Analysis, and Model Building. Wiley, New York. 633 pp.

Boyce, W. E. and R. C. DiPrima. 1965. Elementary Differential Equations and Boundary Value Problems. John Wiley and Sons, New York. 485 pp.

Christy, A. L. and J. M. Ferrier. 1973. A mathematical treatment of Münch's pressure-flow hypothesis of phloem translocation. Plant Physiol. 52:531-538.

Eschich, W., R. F. Evert, and J. H. Young. 1972. Solution Flow in Tubular Semipermeable Membranes. Planta 107:279-300.

Ferrier, J. M. and A. L. Christy. 1975. Time-dependent behavior of a mathematical model of Münch translocation. Plant Physiol. 55:511-514.

Godfrey, K. R. and J. J. diSteffano, III. 1987. Identifiability of model parameters. In: E. Walter, ed., Identifiability of Parametric Models. Pergamon Press, Oxford. 119 pp.

Goeschl, J. D., C. E. Magnuson, D. W. DeMichele, and P. J. H. Sharpe. 1976. Concentration-dependent unloading as a necessary assumption for a closed form mathematical model of osmotically driven pressure flow in phloem. Plant Physiol. 58:556-562.

Golub, G. H. and C. F. Van Loan. 1983. Matrix Computations. Johns Hopkins University Press, Baltimore. 476 p.

Jachetta, J. J., A. P. Appleby, and L. Boersma. 1986a. Use of the pressure vessel to measure concentrations of solutes in apoplastic and membrane-filtered symplastic sap in sunflower leaves. Plant Physiol. 82:995-999.

Jachetta, J. J., A. P. Appleby, and L. Boersma. 1986b. Apoplastic and symplastic pathways of atrazine and glyphosate transport in shoots of seedling sunflower. Plant Physiol. 82:1000-1007.

Jacquez, J. A. 1972. Compartmental Analysis in Biology and Medicine. Elsevier, Amsterdam. 237 p.

McGrady, J. K., C. McFarlane, and F. T. Lindstrom. 1987. The transport and affinity of substituted benzenes in soybeans. J. Expt. Bot. 38:1875-1890.

McFarlane, J. C. and T. Pfleeger. 1986. Plant exposure laboratory and chambers, Vol. 1. EPA-600/3-86-007a. USEPA, Corvallis, OR.

McFarlane, J. C. and T. Pfleeger. 1987. Plant exposure chambers for study of toxic chemical-plant interactions. J. Environ. Qual. 16(4):361-371.

McFarlane, C., C. Nolt, C. Wickliff, T. Pfleeger, R. Shimabuku, and M. McDowell. 1987. The uptake, distribution and metabolism of four organic chemicals by soybean plants and barley roots. Environ. Tox. and Chem. 6:847-856.

Moler, C. B. and C. F. Van Loan. 1978. Nineteen dubious ways to compute the exponential of a matrix. SIAM Review 20:801-836.

Nobel, P. S. 1983. Biophysical Plant Physiology and Ecology. W. H. Freeman and Company, New York, NY. 608 pp.

Seagrave, R. C. 1971. Biomedical Applications of Heat and Mass Transfer. Iowa State Univ. Press, Ames, Iowa. 175 pp.

Tyree, M. T., C. A. Peterson, and L. W. Edgington. 1979. A simple theory regarding immobility of xenobiotics with special reference to the nematicide, oxamyl. Plant Physiol. 63:367-374.

Varga, R. S. 1962. Matrix Iterative Analysis. Prentice-Hall, Englewood Cliffs, NJ. 322 p.

Ward, R. C. 1977. Numerical Computation of the matrix exponential with accuracy estimates. SIAM J. Num. Anal. 14:600-614.

Weir, G. J. 1981. Analysis of Münch theory. Math. Biosci. 56:141-

APPENDIX 1

DEFINITIONS OF THE NON-ZERO COEFFICIENTS, a_{ij}.

-1) Soil compartment

$$\frac{dM_{-1}}{dt} = a_{-1,-1} M_{-1} + a_{-1,0} M_0$$

$$a_{-1,-1} = -\left[\frac{\frac{D_0 A_0}{\Delta x_0} + Q_0}{\epsilon V_{-1}(1 + B_{-1})} + \lambda_{-1}\right]; \qquad a_{-1,0} = \frac{\frac{D_0 A_0}{\Delta x_0}}{V_0(1 + B_0)}$$

0) Root free space compartment

$$\frac{dM_0}{dt} = a_{0,-1} M_{-1} + a_{0,0} M_0 + a_{0,1} M_1 + a_{0,2} M_2$$

$$a_{0,-1} = \frac{\frac{D_0 A_0}{\Delta x_0} + Q_0}{\epsilon(1 + B_{-1}) V_{-1}}$$

$$a_{0,0} = -\left[\frac{\frac{D_0 A_0}{\Delta x_0} + \frac{D_1 A_1}{\Delta x_1} + Q^{ST}_{f0} + Q_0(1 - \sigma)}{V_0(1 + B_0)} + \lambda_0\right]$$

$$a_{0,1} = \frac{Q^{ST}_{b0}}{V_1(1 + B_1)}; \qquad a_{0,2} = \frac{D_1 A_1}{V_2(1 + B_2)}$$

1) Root exterior cells compartment

$$\frac{dM_1}{dt} = a_{1,0} M_0 + a_{1,1} M_1$$

$$a_{1,0} = \frac{Q^{ST}_{f0}}{V_0(1 + B_0)}; \qquad a_{1,1} = -\left(\frac{Q^{ST}_{b0}}{V_1(1 + B_1)} + \lambda_1\right)$$

2) Root xylem compartment

$$\frac{dM_2}{dt} = a_{2,0} M_0 + a_{2,2} M_2 + a_{2,3} M_3 + a_{2,4} M_4 + A_{2,5} M_5$$

$$a_{2,0} = \frac{\frac{D_1 A_1}{\Delta x_1} + Q_1(1 - \sigma_1)}{V_0(1 + B_0)}$$

$$a_{2,2} = -\left[\frac{\frac{D_1 A_1}{\Delta x_1} + \frac{D_4 A_4}{\Delta x_4} + \frac{D_2 A_2}{\Delta x_2} + Q_2(1 - \sigma_2) + Q_{f1}^{ST}}{V_2(1 + B_2)} + \lambda_2\right]$$

$$a_{2,3} = \frac{Q_{b1}^{ST}}{V_3(1 + B_3)}; \qquad a_{2,4} = \frac{\frac{D_4 A_4}{\Delta x_4} + Q_4(1 - \sigma_4)}{V_4(1 + B_4)},$$

$$a_{2,5} = \frac{\frac{D_2 A_2}{\Delta_2}}{V_5(1 + B_5)}$$

3) Root storage compartment

$$\frac{dM_3}{dt} = a_{3,2} M_2 + a_{3,3} M_3 + a_{3,4} M_4$$

$$a_{3,2} = \frac{Q_{f1}^{ST}}{V_2(1 + B_2)}; \qquad a_{3,3} = -\left[\frac{Q_{b1}^{ST} + Q_{b2}^{ST}}{V_3(1 + B_3)} + \lambda_3\right],$$

$$a_{3,4} = \frac{Q_{f2}^{ST}}{V_4(1 + B_4)}$$

4) Root phloem lumen compartment

$$\frac{dM_4}{dt} = a_{4,2} M_2 + a_{4,3} M_3 + a_{4,4} M_4 + a_{4,7} M_7$$

$$a_{4,2} = \frac{\frac{D_4 A_4}{\Delta x_4}}{V_2(1 + B_2)} \quad ; \qquad a_{4,3} = \frac{Q_{b2}^{ST}}{V_3(1 + B_3)}$$

$$a_{4,4} = - \left(\frac{\frac{D_4 A_4}{\Delta x_4} + Q_4(1 - \sigma_4) + \frac{D_3 A_3}{\Delta x_3} + Q_{f2}^{ST}}{V_4(1 + B_4)} + \lambda_4 \right)$$

$$a_{4,7} = \frac{\frac{D_3 A_3}{\Delta x_1} + Q_3(1 - \sigma_3)}{V_7(1 + B_7)}$$

5) Bottom stem xylem compartment

$$\frac{dM_5}{dt} = a_{5,2} M_2 + a_{5,5} M_5 + a_{5,6} M_6 + a_{5,8} M_8 + a_{5,14} M_{14}$$

$$a_{5,2} = \frac{\frac{D_2 A_2}{\Delta x_2} + Q_2(1 - \sigma_2)}{V_2(1 + B_2)}$$

$$a_{5,5} = - \left(\frac{\frac{D_2 A_2}{\Delta x_2} + \frac{D_5 A_5}{\Delta x_5} + Q_5(1 - \sigma_5) + \frac{D_9 A_9}{\Delta x_9} + Q_9(1 - \sigma_9) + Q_{f3}^{ST}}{V_5(1 + B_5)} + \lambda_5 \right)$$

$$a_{5,6} = \frac{Q_{b3}^{ST}}{V_6(1 + B_6)} \qquad a_{5,8} = - \frac{\frac{D_5 A_5}{\Delta x_5}}{V_8(1 + B_8)}$$

$$a_{5,14} = \frac{\frac{D_9 A_9}{\Delta x_9}}{V_{14}(1 + B_{14})}$$

6) Bottom stem storage compartment

$$\frac{dM_6}{dt} = a_{6,5} M_5 + a_{6,6} M_6 + a_{6,7} M_7$$

$$a_{6,5} = \frac{Q_{f3}^{ST}}{V_5(1 + B_5)}; \qquad a_{6,6} = -\left[\frac{Q_{b3}^{ST} + Q_{b4}^{ST}}{V_6(1 + B_6)} + \lambda_6\right]$$

$$a_{6,7} = \frac{Q_{f4}^{ST}}{V_7(1 + B_7)}$$

7) Bottom stem phloem compartment

$$\frac{dM_7}{dt} = a_{7,4} M_4 + a_{7,6} M_6 + a_{7,7} M_7 + a_{7,10} M_{10} + a_{7,16} M_{16}$$

$$a_{7,4} = \frac{\frac{D_3 A_3}{\Delta x_3}}{V_4(1 + B_4)}; \qquad a_{7,6} = \frac{Q_{b4}^{ST}}{V_6(1 + B_6)}$$

$$a_{7,7} = -\left[\frac{\frac{D_3 A_3}{\Delta x_3} + Q_3(1 - \sigma_3) + \frac{D_6 A_6}{\Delta x_6} + \frac{D_{12} A_{12}}{\Delta x_{12}} + Q_{f4}^{ST}}{V_7(1 + B_7)} + \lambda_7\right]$$

$$a_{7,10} = \frac{\frac{D_6 A_6}{\Delta x_6} + Q_6(1 - \sigma_6)}{V_{10}(1 + B_{10})}; \qquad a_{7,16} = \frac{\frac{D_{12} A_{12}}{\Delta x_{12}} + Q_{12}(1 - \sigma_{12})}{V_{16}(1 + B_{16})}$$

8) Mid stem xylem lumen compartment

$$\frac{dM_8}{dt} = a_{8,5} M_5 + a_{8,8} M_8 + a_{8,9} M_9 + a_{8,11} M_{11} + a_{8,17} M_{17}$$

$$a_{8,5} = \frac{\frac{D_5 A_5}{\Delta x_5} + Q_5(1 - \sigma_5)}{V_5(1 + B_5)}$$

$$a_{8,8} = -\left\{\frac{\frac{D_3 A_3}{\Delta x_3} + \frac{D_7 A_7}{\Delta x_7} + Q_7(1-\sigma_7) + \frac{D_{13} A_{13}}{\Delta x_{13}} + Q_{13}(1-\sigma_{13}) + Q_{f5}^{ST}}{V_8(1 + B_8)} + \lambda_8\right\}$$

$$a_{8,9} = \frac{Q_{b5}^{ST}}{V_9(1 + B_9)} ; \qquad a_{8,11} = \frac{\frac{D_7 A_7}{\Delta x_7}}{V_{11}(1 + B_{11})}$$

$$a_{8,17} = \frac{\frac{D_{13} A_{13}}{\Delta x_{13}}}{V_{17}(1 + B_{17})}$$

9) Mid stem storage compartment

$$\frac{dM_9}{dt} = a_{9,8} M_8 + a_{9,9} M_9 + a_{9,10} M_{10}$$

$$a_{9,8} = \frac{Q_{f5}^{ST}}{V_8(1 + B_8)} \qquad a_{9,9} = -\left\{\frac{Q_{b5}^{ST} + Q_{b6}^{ST}}{V_9(1 + B_9)} + \lambda_9\right\}$$

$$a_{9,10} = \frac{Q_{f6}^{ST}}{V_{10}(1 + B_{10})}$$

10) Mid stem phloem lumen compartment

$$\frac{dM_{10}}{dt} = a_{10,7}\,M_7 + a_{10,9}\,M_9 + a_{10,10}\,M_{10} + a_{10,13}\,M_{13} + a_{10,19}\,M_{19}$$

$$a_{10,7} = \frac{\frac{D_6\,A_6}{\Delta x_6}}{V_7(1 + B_7)} \quad ; \qquad a_{10,9} = \frac{Q_{b6}^{ST}}{V_9(1 + B_9)}$$

$$a_{10,10} = -\left(\frac{\frac{D_8\,A_8}{\Delta x_8} + \frac{D_6\,A_6}{\Delta x_6} + Q_6(1 - \sigma_6) + \frac{D_{16}\,A_{16}}{\Delta x_{16}} + Q_{16}^{ST}}{V_{10}(1 + B_{10})} + \lambda_{10}\right)$$

$$a_{10,13} = \frac{\frac{D_8\,A_8}{\Delta x_8} + Q_8(1 - \sigma_8)}{V_{13}(1 + B_{13})}; \qquad a_{10,19} = \frac{\frac{D_{16}\,A_{16}}{\Delta x_{16}} + Q_{16}(1 - \sigma_{16})}{V_{16}(1 + B_{16})}$$

11) Top stem xylem lumen compartment

$$\frac{dM_{11}}{dt} = a_{11,8}\,M_8 + a_{11,11}\,M_{11} + a_{11,12}\,M_{12} + a_{11,20}\,M_{20}$$

$$a_{11,8} = \frac{\frac{D_7\,A_7}{\Delta x_7} + Q_7(1 - \sigma_7)}{V_8(1 + B_8)}$$

$$a_{11,11} = -\left(\frac{\frac{D_7\,A_7}{\Delta x_7} + \frac{D_{17}\,A_{17}}{\Delta x_{17}} + Q_{17}(1 - \sigma_{17}) + Q_{f7}^{ST}}{V_{11}(1 + B_{11})} + \lambda_{11}\right)$$

$$a_{11,12} = \frac{Q_{b7}^{ST}}{V_{12}(1 + B_{12})}; \qquad a_{11,20} = \frac{\frac{D_{17}\,A_{17}}{\Delta x_{17}}}{V_{20}(1 + B_{20})}$$

12) Top stem storage compartment

$$\frac{dM_{12}}{dt} = a_{12,11} M_{11} + a_{12,12} M_{12} + a_{12,13} M_{13}$$

$$a_{12,11} = \frac{Q_{f7}^{ST}}{V_{11}(1 + B_{11})} ; \qquad a_{12,12} = -\left(\frac{Q_{b7}^{ST} + Q_{b8}^{ST}}{V_{12}(1 + B_{12})} + \lambda_{12} \right) ,$$

$$a_{12,13} = \frac{Q_{f8}^{ST}}{V_{13}(1 + B_{13})}$$

13) Top stem phloem lumen compartment

$$\frac{dM_{13}}{dt} = a_{13,10} M_{10} + a_{13,12} M_{12} + a_{13,13} M_{13} + a_{13,22} M_{22}$$

$$a_{13,10} = \frac{\frac{D_8 A_8}{\Delta x_8}}{V_{10}(1 + B_{10})} ; \qquad a_{13,12} = \frac{Q_{b8}^{ST}}{V_{12}(1 + B_{12})}$$

$$a_{13,13} = -\left(\frac{\frac{D_8 A_8}{\Delta x_8} + Q_8(1 - \sigma_8) + \frac{D_{20} A_{20}}{\Delta x_{20}} + Q_{f8}^{ST}}{V_{13}(1 + B_{13})} + \lambda_{13} \right)$$

$$a_{13,22} = \frac{\frac{D_{20} A_{20}}{\Delta x_{20}}}{V_{22}(1 + B_{22})}$$

14) Leaf cluster 1 xylem lumen compartment

$$\frac{dM_{14}}{dt} = a_{14,5} M_5 + a_{14,14} M_{14} + a_{14,15} M_{15} + a_{14,16} M_{16} + S_{16}$$

$$a_{14,5} = \frac{\frac{D_9 A_9}{\Delta x_9} + Q_9(1 - \sigma_9)}{V_5(1 + B_5)} ;$$

$$a_{14,14} = -\left[\frac{\frac{D_9 A_9}{\Delta x_9} + \frac{D_{10} A_{10}}{\Delta x_{10}} + Q_{10}(1 - \sigma_{10}) + \frac{D_{CH} A_{11} H_c}{\Delta x_{11}} + Q_{f9}^{ST}}{V_{14}(1 + B_{14})} + \lambda_{14}\right]$$

$$a_{14,15} = \frac{Q_{b9}^{ST}}{V_{15}(1 + B_{15})}; \qquad a_{14,16} = \frac{\frac{D_{10} A_{10}}{\Delta x_{10}}}{V_{16}(1 + B_{16})}$$

$$S_{14} = \frac{D_{CH} A_{11} C_{air}}{\Delta x_{11}}$$

15) Leaf cluster 1 storage compartment

$$\frac{dM_{15}}{dt} = a_{15,14} M_{14} + a_{15,15} M_{15} + a_{15,16} M_{16}$$

$$a_{15,14} = \frac{Q_{f9}^{ST}}{V_{14}(1 + B_{14})}; \qquad a_{15,15} = -\left[\frac{Q_{b9}^{ST} + Q_{b10}^{ST}}{V_{15}(1 + B_{15})} + \lambda_{15}\right],$$

$$a_{15,16} = \frac{Q_{f10}^{ST}}{V_{16}(1 + B_{16})}$$

16) Leaf cluster 1 phloem-lumen compartment

$$\frac{dM_{16}}{dt} = a_{16,7} M_7 + a_{16,14} M_{14} + a_{16,15} M_{15} + a_{16,16} M_{16}$$

$$a_{16,7} = \frac{\frac{D_{12} A_{12}}{\Delta x_{12}}}{V_7(1 + B_7)}; \qquad a_{16,14} = \frac{\frac{D_{10} A_{10}}{\Delta x_{10}} + Q_{10}(1 - \sigma_{10})}{V_{14}(1 + B_{14})}$$

$$a_{16,15} = \frac{Q_{b10}^{ST}}{V_{15}(1 + B_{15})}$$

$$a_{16,16} = -\left[\frac{\frac{D_{10}\,A_{10}}{\Delta x_{10}} + \frac{D_{12}\,A_{12}}{\Delta x_{12}} + Q_{12}(1 - \sigma_{12}) + Q_{f10}^{ST}}{V_{16}(1 + B_{16})} + \lambda_{16}\right]$$

17) Leaf 2 cluster xylem lumen compartment

$$\frac{dM_{17}}{dt} = a_{17,8}\,M_8 + a_{17,17}\,M_{17} + a_{17,18}\,M_{18} + a_{17,19}\,M_{19} + S_{17}$$

$$a_{17,8} = \frac{\frac{D_{13}\,A_{13}}{\Delta x_{13}} + Q_{13}(1 - \sigma_{13})}{V_8(1 + B_8)};$$

$$a_{17,17} = -\left[\frac{\frac{D_{13}\,A_{13}}{\Delta x_{13}} + \frac{D_{14}\,A_{14}}{\Delta x_{14}} + Q_{14}(1 - \sigma_{14}) + \frac{D_{CH_2O}\,A_{15}}{\Delta x_{15}} + Q_{f11}^{ST}}{V_{17}(1 + B_{17})} + \lambda_{17}\right]$$

$$a_{17,18} = \frac{Q_{b11}^{ST}}{V_{18}(1 + B_{18})}; \qquad a_{17,19} = \frac{\frac{D_{14}\,A_{14}}{\Delta x_{14}}}{V_{19}(1 + B_{19})}$$

$$S_{17} = \frac{D_{CH_2O}\,A_{15}\,C_{air}}{\Delta x_{15}}$$

18) Leaf 2 cluster storage compartment

$$\frac{dM_{18}}{dt} = a_{18,17}\,M_{17} + a_{18,18}\,M_{18} + a_{18,19}\,M_{19}$$

$$a_{18,17} = \frac{Q_{f11}^{ST}}{V_{17}(1 + B_{17})}; \qquad a_{18,18} = -\left[\frac{Q_{b11}^{ST} + Q_{b12}^{ST}}{V_{18}(1 + B_{18})} + \lambda_{18}\right],$$

$$a_{18,19} = \frac{Q_{f12}^{ST}}{V_{19}(1 + B_{19})}$$

19) Leaf 2 cluster phloem lumen compartment

$$\frac{dM_{19}}{dt} = a_{19,10} M_{10} + a_{19,17} M_{17} + a_{19,18} M_{18} + a_{19,19} M_{19}$$

$$a_{19,10} = \frac{\frac{D_{16} A_{16}}{\Delta x_{16}}}{V_{10}(1 + B_{10})}; \qquad a_{19,17} = \frac{\frac{D_{14} A_{14}}{\Delta x_{14}} + Q_{14}(1 - \sigma_{14})}{V_{17}(1 + B_{17})}$$

$$a_{19,18} = \frac{Q^{ST}_{f12}}{V_{18}(1 + B_{18})}$$

$$a_{19,19} = -\left[\frac{\frac{D_{16} A_{16}}{\Delta x_{16}} + Q_{16}(1 - \sigma_{16}) + \frac{D_{14} A_{14}}{\Delta x_{14}} + Q^{ST}_{f12}}{V_{19}(1 + B_{19})} + \lambda_{19}\right]$$

20) Leaf 3 cluster xylem lumen compartment

$$\frac{dM_{20}}{dt} = a_{20,11} M_{11} + a_{20,20} M_{20} + a_{20,21} M_{21} + a_{20,22} M_{22} + S_{20}$$

$$a_{20,11} = \frac{\frac{D_{17} A_{17}}{\Delta x_{17}} + Q_{17}(1 - \sigma_{17})}{V_{11}(1 + B_{11})}$$

$$a_{20,20} = -\left[\frac{\frac{D_{17} A_{17}}{\Delta x_{17}} + \frac{D_{18} A_{18}}{\Delta x_{18}} + Q_{18}(1 - \sigma_{18}) + \frac{D_{CH} H_c A_{19}}{\Delta x_{19}} + Q^{ST}_{f13}}{V_{20}(1 + B_{20})} + \lambda_{20}\right]$$

$$a_{20,21} = \frac{Q^{ST}_{b13}}{V_{21}(1 + B_{21})}; \qquad a_{20,22} = \frac{\frac{D_{18} A_{18}}{\Delta x_{18}}}{V_{22}(1 + B_{22})}$$

$$S_{20} = \frac{D_{CH} A_{19} C_{air}}{\Delta x_{19}}$$

21) Leaf 3 cluster storage compartment

$$\frac{dM_{21}}{dt} = a_{21,20} M_{20} + a_{21,21} M_{21} + a_{21,22} M_{22}$$

$$a_{21,20} = \frac{Q_{f13}^{ST}}{V_{20}(1 + B_{20})} ; \qquad a_{21,21} = -\left\{ \frac{Q_{b13}^{ST} + Q_{b14}^{ST}}{V_{21}(1 + B_{21})} + \lambda_{21} \right\}$$

$$a_{21,22} = \frac{Q_{f14}^{ST}}{V_{22}(1 + B_{22})}$$

22) Leaf 3 cluster phloem lumen compartment

$$\frac{dM_{22}}{dt} = a_{22,13} M_{13} + a_{22,20} M_{20} + a_{22,21} M_{21} + a_{22,22} M_{22}$$

$$a_{22,13} = \frac{\frac{D_{20} A_{20}}{\Delta x_{20}}}{V_{13}(1 + B_{13})} \qquad a_{22,20} = \frac{\frac{D_{18} A_{18}}{\Delta x_{18}} + Q_{f18}(1 - \sigma_{18})}{V_{20}(1 + B_{20})}$$

$$a_{22,21} = \frac{Q_{b14}^{ST}}{V_{21}(1 + B_{21})}$$

$$a_{22,22} = -\left[\frac{\frac{D_{20} A_{20}}{\Delta x_{20}} + Q_{20}(1 - \sigma_{20}) + \frac{D_{18} A_{18}}{\Delta x_{18}} + Q_{f14}^{ST}}{V_{22}(1 + B_{22})} + \lambda_{22} \right]$$